6-1986

Predictive Model for the Pulse Pressure in a Pulse-Jet Fabric Filter

Satoru Mitsutomi
University of Tennessee - Knoxville

To the Graduate Council:

I am submitting herewith a dissertation written by Satoru Mitsutomi entitled "Predictive Model for the Pulse Pressure in a Pulse-Jet Fabric Filter." I have examined the final electronic copy of this dissertation for form and content and recommend that it be accepted in partial fulfillment of the requirements for the degree of Doctor of Philosophy, with a major in Civil Engineering.

Wayne T. Davis, Major Professor

We have read this dissertation and recommend its acceptance:

Joe Wilkerson, Gregory Reed, Dennis Weeter

Accepted for the Council:

Carolyn R. Hodges

Vice Provost and Dean of the Graduate School

(Original signatures are on file with official student records.)

To the Graduate Council:

I am submitting herewith a dissertation written by Satoru Mitsutomi entitled "Predictive Model for the Pulse Pressure in a Pulse-Jet Fabric Filter." I have examined the final copy of this dissertation for form and content and recommend that it be accepted in partial fullfillment of the requirements for the degree of Doctor of Philosophy, with a major in Civil Engineering.

Wayne T. Davis, Major Professor

We have read this dissertation and recommended its acceptance:

Accepted for the Council:

Vice Provost
and Dean of The Graduate School

PREDICTIVE MODEL FOR THE PULSE PRESSURE IN A PULSE-JET FABRIC FILTER

A Dissertation

Presented for the

Doctor of Philosophy

Degree

The University of Tennessee, Knoxville

Satoru Mitsutomi

June 1986

ACKNOWLEDGMENTS

In the course of dissertation research, a number of scholars have assisted me generously. In particular I am indebted to Professors Wayne Davis, Joe Wilkerson, Gregory Reed, and Dennis Weeter, who served as my director and committee respectively. With their consultation, criticism, and encouragement, I was able to achieve results otherwise impossible. Whatever errors remain in my work, however, are solely my responsibility.

I especially wish to express my sincere appreciation to Dr. Wayne T. Davis for his invaluable advice, guidance and patience throughout my graduate education program.

Appreciation is also expressed to my fellow graduate students for helping my English grammer.

Special thanks is due my wife, Masumi, and my parents, Shyuich and Shie Jyozaki for their support, encouragement and understanding throughout the course of dissertation research.

ABSTRACT

Pulse-jet cleaned fabric filters are being utilized to filter dust from particulate laden gas streams. The pulse-jet fabric filter consists of a reservoir, a solenoid valve, a lateral pipe and a venturi/bag. The compressed air is released periodically through a solenoid valve and fills the lateral pipe. Then high velocity air is ejected from a series of orifices on the lateral pipe. As a result, the bag is rapidly inflated and dust is dislodged from the bag.

A predictive model for the pulse pressure in a pulse-jet fabric filter has been developed. Two types of models are presented: Simplified Static Model and Dynamic Model.

The Simplified Static Model treats the system as a series of spherical tanks in which the pressure develops uniformly throughout each tank. Each tank in series is connected by a valve. The mass balance equation is applied for the system and solved numerically. Sensitivity analysis has been conducted to evaluate the effect of configurations and operating parameters.

The dynamic model is developed to predict the local pressure developed in the system. The reservoir/lateral system is considered as a simple shock tube and the theory of a simple shock tube is applied to the system to predict the maximum pressure developed in the lateral. The maximum

pressure developed at the entry of the bag is predicted based on the velocity of injected air. The pressure developed at the top of the bag dissipates along the bag due to the permeation of air mass through the bag surface. The mass balance equation is applied to the mass of air traveling along the bag. Empirical corrections are applied to the dynamic model due to the complexity of the theoretical treatment. The empirical correction factors introduced are the friction coefficient in the lateral, pressure losses at the bag entrance, and the permeability of the bags.

The proposed models can be employed to assist in the design of the pulse-jet fabric filter, to understand the behavior of the system, and to predict the performance due to the change of an operating condition.

TABLE OF CONTENTS

CHAPTER		PAGE
I.	INTRODUCTION	1
	A. Statement of the Problem	1
	B. Overview of the Pulse-Jet Fabric Filter	3
II.	REVIEW OF THE LITERATURE	7
	A. Pulse-Jet Fabric Filter	7
	B. Flow Phenomena in the Pulse-Jet Fabric Filter	17
III.	EXPERIMENTAL FACILITY AND PROCEDURE	29
	A. Standard System	29
	B. Pilot System	31
IV.	A MODEL FOR THE PULSE PRESSURE IN A PULSE-JET FILTER	39
	A. Introduction	39
	B. Simplified Static Model	40
	C. Dynamic Model	70
V.	CONCLUSIONS	126
LIST OF REFERENCES		132
APPENDIXES		135
	A. Data Matrix of the Experiment and Example Photographs of Pulse-Pressure Wave	136
	B. Computer Program	146
VITA		153

LIST OF FIGURES

FIGURE		PAGE
1.1.	Schematic of a pulse-jet fabric filter (Strauss, 1966)	4
2.1.	The shock tube (Zckrow and Hoffman, 1977) . . .	24
3.1.	Schematic of the lateral pipe and bags	30
3.2.	Schematic diagram of the pulse-jet system . . .	33
3.3.	Schematic of the baghouse and the venturi . . .	35
3.4.	Schematic diagram of instrumentation	37
4.1.	Procedures for the development of a predictive model for the pulse pressure in a fabric filter	41
4.2.	The actual and the simplified system configuration	42
4.3.	Flow diagram of the calculation procedure for the simplified static model	54
4.4.	Reservoir and the lateral pipe pressure versus time	58
4.5.	Predicted and observed bag pressure versus time	59
4.6.	The pressure developed inside the bag with time for various reservoir volumes	62
4.7.	The pressure developed inside the bag with time for various lateral pipe volumes	64
4.8.	The pressure developed inside the bag with time for various bag volumes	65
4.9.	The pressure developed inside the bag with time for various orifice diameters	67
4.10.	The pressure developed inside the bag with time for various valve opening times	68

4.11. The electrical time setting versus actual valve opening times 69

4.12. Pulse pressures versus time for various reservoir pressures 71

4.13. The system of reservoir/lateral pipe 73

4.14. Procedure of the program development for the dynamic model 84

4.15. Flow diagram of the calculation procedure for the dynamic model 86

4.16. The pressure developed in the lateral pipe versus distance from the valve 98

4.17. Normalized pulse pressure versus the distance from the top of the bag 100

4.18. Calculated versus measured maximum pressure developed in the bag 102

4.19. Calculated versus measured maximum pressure corrected for the peak location 104

4.20. Photograph of pressure traces at the lateral pipe 105

4.21. The pressure developed in the lateral pipe versus reservoir pressure 107

4.22. A comparison of calculated versus measured lateral pipe pressure 111

4.23. A comparison of calculated versus measured pressure at the top of the bag 112

4.24. Pulse pressure developed in the bag versus the distance from the top of the bag (clean bag, without venturi, three bag locations) 116

4.25. Pulse pressure developed in the bag versus the distance from the top of the bag (clean bag, with venturi, three bag locations) 117

4.26. Pulse pressure developed in the bag versus the distance from the top of the bag (clean bag, with venturi, bag #2, 100 psi) 118

4.27. Pulse pressure developed in the bag versus the distance from the top of the bag (clean bag, with venturi, bag #2, 80 psi) 119

4.28. Pulse pressure developed in the bag versus the distance from top of the bag (clean bag, with venturi, bag #2, 60 psi) 120

4.29. Pulse pressure developed in the bag versus the distance from the top of the bag (dirty bag system, 100 psi) 121

4.30. Pulse pressure developed in the bag versus the distance from the top of the bag (Humphries and Madden,1981) 123

4.31. A comparison of calculated versus measured bag pressure 124

LIST OF TABLES

TABLE		PAGE
1.1.	The parameters that affect system performance .	6
2.1.	Notation used for discussion of the flow phenomena	19
2.2.	The governing equations for unsteady one dimensional flow	21
3.1.	Dimension of the standard configuration of the pulse-jet fabric filter	32
3.2.	Instrument specifications	38
4.1.	Notation for the simplified static model	44
4.2.	Summary of the equations for the simplified static model	52
4.3.	Example input to the simplified static model . .	57
4.4.	Summary of the equations for the dynamic model .	75
4.5.	Required input to the model	94
4.6.	Peak pressures observed in the lateral for reservoir pressures of 60,80 and 100 psig . . .	96
A.1.	Clean bag test (A)	138
A.2.	Lateral pipe test	139
A.3.	Clean bag test (B)	140
A.4.	Dirty bag test (c)	141

CHAPTER I

INTRODUCTION

A. Statement of the Problem

In recent years, because of increasing concern about visibility and acid rain, more stringent emission control standards (Clean Air Act and New Source Performance Standards, 1977) have been introduced. This regulation has led the utility industry to use high efficiency emission control devices. Currently, fabric filters and electrostatic precipitators (ESP) are the only control devices that are able to provide sufficient collection efficiency to meet the standard for particulate emissions. At present, fabric filters are the preferred choice over ESP by the utility industry because of (1) increasing use of low sulfur coals which generate high resistivity fly ashes (fabric filters are relatively insensitive to the characteristics of fly ash compared to ESP), (2) its ability to handle a wide range of particulate sizes, and (3) recent progress in design and operation.

Fabric filters are usually classified into three types (shaker, reverse-air and pulse-jet) depending on the dust dislodgement method employed. Among them, pulse-jet fabric filters have the potential of being one of the most promising technologies for collection of particulate matter

because they can be operated at a higher air-to-cloth ratio than more conventional fabric filters. This results in units which are smaller in size and more economical to build.

Although pulse-jet fabric filters have been widely used in various industries, little is known about the physical cleaning mechanism of pulse-jet fabric filters. The experience with pulse-jet fabric filters acquired in a small-scale industry cannot be applied directly to the pulse-jet fabric filters used for the public utility industry. For example, in the models for predicting the pressure drop in industrial-size pulse-jet fabric filters, it is usually assumed that the pressure wave travels rapidly and develops static pressure inside the bag instantaneously. Therefore, the force acting on the bag/dust is uniform throughout the bag. As a result, the dust is dislodged uniformly. This is not the case for utility-size pulse-jet fabric filters where the filter bags may be 9 to 15 feet in length. Preliminary laboratory investigations have shown that the maximum pressure at the bottom of the bag was typically only 20% of the value at the top, indicating that a significant part of the total energy of the pressure wave had been lost prior to reaching the bottom of the bag.

Given these circumstances, this research was carried out in order to identify and quantify the physical mechanisms associated with pulse-jet fabric filter cleaning

and to develop the basic steps for a predictive model which can be used for designing pulse-jet fabric filters.

B. Overview of the Pulse-Jet Fabric Filter

Pulse-jet cleaned fabric filters are being utilized to filter dust from particulate laden gas streams. A typical pulse-jet fabric filter is shown in Figure 1.1.

In this figure, dirty air is usually introduced from the bottom. Dust is collected on the exterior of the cylindrical bag, and clean air exits from the outlet at the top of the system. The dust deposited on the bag is periodically dislodged by utilizing a pulse jet. The compressed air stored in the tank (typically 100 psi) is released every several minutes through a solenoid valve. The duration of the pulse is typically 100 ms. This released air fills the lateral pipe, and high velocity air is ejected from a series of orifices (typically 3/8" in diameter) located at a certain distance (typically 4") from the top of the bag. The jet flow creates a low pressure zone and transfers momentum to the surrounding fluid, thereby inducing secondary flow (Bakke, 1974). The pressure of the air jet is recovered by a venturi placed at the top of the bag. Pressure waves created by the air mass travel down the bag at sonic velocities and transfer energy to the fabric/dust. The fabric/dust attains a certain outward velocity. However, the fabric must come back to its

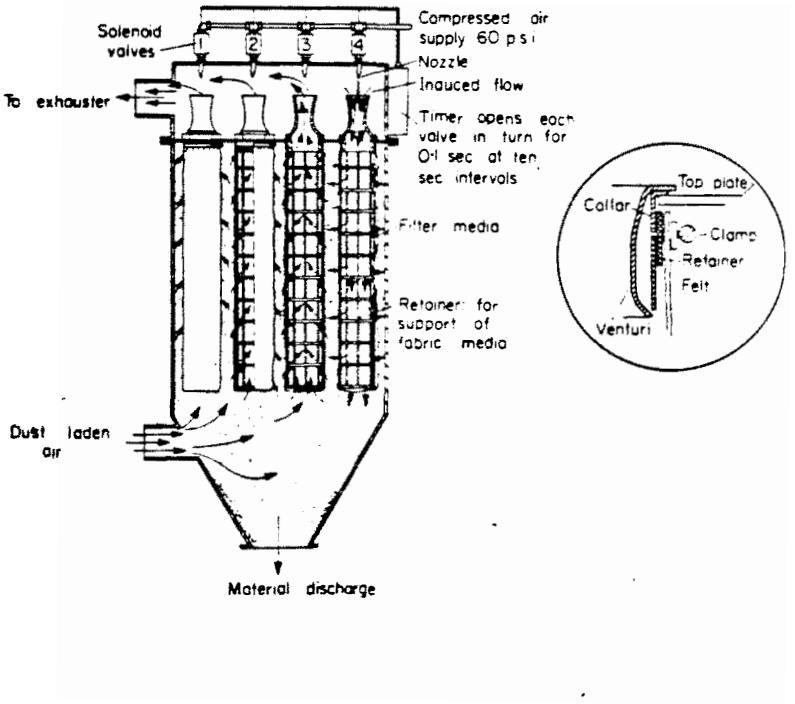

Figure 1.1. Schematics of a pulse-jet fabric filter. (Strauss, 1966)

original position so that dust is released from the bag. This is accomplished with the help of outward air flow.

The pulse jet fabric filter system involves two main processes. These processes are dust dislodgment and filtration. The effectiveness of these processes are considered in terms of the pressure drop across the bag and penetration of the dust, respectively. These processes are governed by operating conditions and characteristics of the system configuration including filtration velocity, pulse intensity, volume of baghouse, and the distance between the orifice and the venturi. A complete list of these parameters is given in Table 1.1. The objective of this study is to quantify the extent to which many of these parameters affect the operation of the pulse-jet fabric filter.

Table 1.1. Parameters that affect system performance.

A. Operating Conditions

a. Pulse characteristics
- compressed air pressure
- valve opening time
- volume of jet air flow
- pulse interval
- pulse duration
- pulse rise rate

b. Flow characteristics
- filtration velocity
- upward flow velocity
- gas temperature
- humidity
- corrosive components in gas

c. Dust Characteristics
- particle size distribution
- inlet concentration
- electrostatic charges
- agglomeration characteristics
- sticky, hydroscopic, corrosive

d. Others

B. System Configuration

- volume of reservoir tank
- valve diameter
- a lateral pipe diameter
- a lateral pipe length
- diameter of orifice
- distance between orifice and top of the bag
- alignment of orifice
- dimension of venturi
- diameter and length of a bag
- fabric type
- height of a baghouse
- volume of a baghouse
- inlet location (top or bottom)

CHAPTER II

REVIEW OF THE LITERATURE

A. Pulse-Jet Fabric Filter

There are two major areas of interest in determining the performance of pulse-jet fabric filters. One area is the efficiency of the system which focuses on the dust collection process. The other is the pressure drop of the system which is affected by the dust dislodgment process. The area of efficiency goes beyond the scope of this study. On the other hand, the subject of the pressure drop will be dealt with thoroughly in a later chapter. The following is a review of the literature related to the study of pressure drop.

The historical studies can be classified into two areas: macroscopic and microscopic. Early studies (Dennis and Silverman, 1962, Leith and First, 1977) are considered to be macroscopic. The method of study utilized was a "black box" type of approach. The relationship between the pressure drop and the parameters involved were determined empirically. The pressure drop in each system varied depending on a) the operating condition of the system, b) the configuration of the system, and c) the characteristics of the gas, dust and type of fabric. The combinations of

dependent parameters were numerous. Therefore, the empirical models developed were usually system-specific.

The microscopic studies have been conducted to clarify the physical processes which occur within the "black box" (i.e. investigation of the mechanism of the dust dislodgement process). The findings of these studies were incorporated into macroscopic models (Dennis and Wilder, 1975, Dennis and Klemn, 1980)

Also, theoretical studies based on the microscopic view have been conducted to eliminate the dependency of the model on empirical parameters (Dennis, Wilder and Harmon, 1981, and Leith and Ellenbecker, 1981). However, these models still rely on the experimental data to determine the factors derived from the theory.

There are several microscopic studies that are focused on the specific parameters such as pulse characteristics (Leith, First and Gibson, 1978), and the magnitude of the pulse pressure exerted along the bag (Humphries and Madden, 1981 and 1983).

The models mentioned above are summarized below in detail. Dennis and Silverman (1962) proposed the following empirical model.

$$\Delta P(\text{inch } H_2O) = 1.1 + (3.8\ C_i^{0.25})/(P_c^{2}\ f_c^{0.5}/100) \qquad (2\text{-}1)$$

where:

ΔP = pressure drop (inch H_2O)

C_i = dust loading (1-14 grains/ft^3 , fly ash)

P_c = compressed air (60-120 psig)

f_c = cleaning frequency (1-6 pulses/min/bag)

The equation applies to a nine-bag, single-compartment, sequentially pulsed system using wool felt bags at a filtration velocity of 8.0 ft/min. Although the relationship presented may be applicable to other systems, the model is still primitive.

Leith and First (1977) presented the following empirical model:

$$\Delta P = 2.72 \quad W^{0.45} P_p^{-1.38} V^{2.34} \qquad (2\text{-}2)$$

in which

ΔW = areal density of the dust deposited between pulses (i.e. $C_i V t$, mg/cm^2)

ΔP = pressure drop (cm of H_2O)

C_i = inlet dust concentration (mg/cm^3)

V = filtration velocity (cm/sec)

t = the time between pulses (sec)

P_p = pulse pressure (atmospheres)

The model was developed for fly ash collected on polyester bags.

An extensive study has been conducted by both groups (Dennis and Leith) in order to eliminate the weaknesses of

the models pressented. Both groups began by looking into the physical mechanism of dust dislodgment.

Dennis and Wilder (1975) and Dennis and Klemm (1980) considered that the bag acceleration created by the pulse played a major role in dust dislodgment, and the maximum acceleration of the bag in this model was approximated by

$$a_{max} = \frac{G}{\sqrt{\rho M_e}} \frac{dP_p}{dt} \qquad (2\text{-}3)$$

where:

a_{max} = maximum acceleration attained by bag (cm/sec^2)

G = flexibility of fabric ($cm/cm\ H_2O$)

M_e = elasticity of fabric ($cm/\ cm\ H_2O$)

ρ = mass per unit area for the dust laden bag (g/cm^2)

$\frac{dP_p}{dt}$ = pressure gradient ($cm\ H_2O/sec$)

The equation indicates that the pressure rise rate is directly related to acceleration, which is the main factor of dust dislodgment. They experimentally correlated the pressure rise rate and the effective pressure drop, and developed an empirical relationship.

$$\Delta P_e = A\ (dP_p/dt)^{-B} \qquad (2\text{-}4)$$

where:

ΔP_e = residual pressure drop (N/m^2)

$\frac{dP_p}{dt}$ = pressure rise rate (cm H_2O/sec)

A, B = correlation coefficients

Further, Dennis, Wilder and Harmon (1981) redefined the expression $d(P_p)/dt$, which is usually determined experimentally, in terms of readily determined design and operating parameters characterizing the filter system of interest. The rate of pressure increase $d(P_p)/dt$ was related to the solenoid opening time (t_s), jet volume (v_p), bag pressure before pulsing (P_b), entrained air (V_s) and bag volume (V_b).

$$\frac{dP_p}{dt} = \frac{V_p + V_s}{V_b} \quad \frac{P_b}{t_s} \qquad (2\text{-}5)$$

The primary jet volume was calculated on the basis of the jet flow from the orifice under critical flow conditions. It was assumed that the secondary air was proportional to the primary jet volume. In this case, the equation (2-5) is rewritten using readily available design and operating parameters.

$$\frac{dP_p}{dt} = (k \cdot P_{j,a} A_j / \sqrt{T_{j,a}})(P_b / V_b \rho_b) \qquad (2\text{-}6)$$

where:

k = constant

A_j = jet nozzle cross section (m^2)

$P_{j,a}$ = pulse jet reservoir pressure (kPa)

$T_{j,a}$ = absolute temperature of compressed air (^oK)

P_b = bag static pressure before pulsing (kPa)

V_b = bag volume (m^3)

ρ_b = ambient air density (kg/m^3)

For an instantaneous pressure drop model for a pulse jet fabric filter, Dennis and Klemm (1980) proposed the following model:

$$\Delta P = \Delta P_e + (k_2)_c V \; W_c + k_2 V \cdot W \qquad (2\text{-}7)$$

where:

ΔP = pressure drop (N/m^2)

ΔP_e = pressure drop effective (N/m^2)

$(k_2)_c$ = specific resistance coefficient for redeposited dust (N-min/g-m)

V = filtration velocity (m/min)

k_2 = specific resistance coefficient (N-min/g-m)

ΔW = dust deposited during filtration cycle (g/m^2)

ΔW_c = dust redeposited (g/m^2)

Although this model describes real physical situations, it is difficult to determine the second parameter involving redeposited dust. Therefore, the first two terms are replaced by equation (2-4) and the instantaneous pressure drop is given by the following expression:

$$\Delta P = \Delta P_e + k_2 \cdot V \cdot \Delta W \qquad (2\text{-}8)$$

Leith and Ellenbecker (1980) developed the pressure drop model which describes the physical dust dislodgment mechanism. First, they assumed that the fraction of the dust deposit removed from the fabric (E) is proportional to the force acting to separate the dust deposit from the fabric (F_s) such that

$$E = k(F_s/A) \qquad (2\text{-}9)$$

The force acting to separate the dust from the fabric was obtained from the impulse necessary to stop the outward momentum of the dust deposit and was given by the following equation:

$$F_s/A = \frac{(P_s - \Delta P)t_1}{t_2} - \frac{V^* W_b}{t_2} \qquad (2\text{-}10)$$

The first term on the left expresses the momentum applied by the pulse, and the second term expresses the momentum force required to stop the outward movement of fabric. In this equation,

F_s/A = area specific force acting to separate the dust deposit from its substrate (N/m^2)

P_s = maximum static pressure developed inside the bag as the result of the cleaning pulse (N/m^2)

ΔP = pressure drop across the bag anddust deposit (N/m^2)

t_1 = time during which Ps acts (sec)

t_2 = time during which Fs acts (sec)

V^* = maximum velocity achieved by fabric and dust cleaning (m/sec)

W_b = areal density of fabric (kg/m^2)

Combining equation (2-9) and (2-10),

$$E = \frac{(P_s - \Delta P)t_1 k}{t_2} - \frac{V^* W_b k}{t_2}$$

$$= k_3(P_s - \Delta P) - k_4 \qquad (2\text{-}11)$$

Here, k_3 and k_4 are determined experimentally for the system of interest due to the difficulty of estimating t_1 and t_2.

The mass balance equation for the dust mass per unit area on a bag was written for one filtration cycle, dN, which includes by definition exactly one cleaning pulse as follows:

Additional areal density due to dust added to the bag per cycle	Decrease in areal density due to dust removed from the bag per cycle	Accumlation of areal density on the bag per cycle

$$W_o - W \cdot E = \frac{dW}{dN} \qquad (2\text{-}12)$$

While models for the pressure drop across a fabric are generally written as follows:

$$\Delta P = k_1 V + k_2 \cdot V \cdot W \qquad (2\text{-}13)$$

where:

ΔP = pressure drop (N/m^2)

k_1 = fabric resistance constant (N/m^3 sec)

k_2 = specific resistance of dust deposit (1/sec)

V = filtration velocity (m/sec)

W = areal density of dust deposit (kg/m^2)

Equations (2-11) and (2-13) are inserted into (2-12) and solved for an equilibrium condition. The pressure drop equation was given as:

$$\Delta P = \frac{P_s - k_4/k_3 + k_1 V}{2} - \frac{(P_s - k_4/k_3 - k_1 V)^2 - 4W_o V k_2/k_3}{2} \qquad (2\text{-}14)$$

The equation presented describes the system behavior fairly well. It allows prediction of operating conditions under which filter operation will become unstable and causes pressure drop to increase without limit.

In addition, Ellenbecker and Leith (1981) conducted an experiment to determine the fraction of dust removed by the pulse. They found that the fraction of dust deposit removed

from the bag correlated most closely with the dust deposit kinetic energy acquired.

$$E = 0.22\ E_k \qquad (2\text{-}15)$$

where:

$$E_k = \frac{1}{2} V_c^2 \cdot W$$

V_c = maximum velocity during cleaning (m/sec)

W = dust deposit areal density (kg/m^2)

Kingel and Loffer (1983) directly utilized the Darcy equation for the pressure drop through the dust cake instead of relying on the experimental data. The pressure drop equation can be written as:

$$\Delta P = \mu \frac{L}{Bo} V + \mu \frac{1}{(1 - E)} c V^2 t \phi \qquad (2\text{-}16)$$

where:

ΔP = pressure drop (N/m^2)

μ = dynamic gas viscosity ($N\ sec/m^2$)

L = thickness of the filter layer (m)

E = porosity of the dust cake

c = dust concentration (g/m^3)

ϕ = collection efficiency

Bo = permeability of the filter (m^2)

V = filtration velocity (m/h)

ρ_s = solid density (g/m^3)

t = time (h)

It is assumed that the flow is classified in the low Reynolds regions (Re < 1) and the filter cake is incompressible. The thickness of dust cake which is required by the model was directly measured by a device based on the absorption of x-rays. In this model, although the number of empirical parameters have been reduced, some parameters still have to be determined experimentally.

Leith, First and Gibson (1978) investigated the effect of pulse pattern and concluded that dust seepage through a fabric and excessive fabric wear can be minimized by gradually reducing air pressure at the end of the cleaning pulse instead of using the square wave pattern.

Humphries and Madden (1981) have measured the pulse pressure along the bag. They found that the peak pressure was highest at the top portion of the bag where negative pressures were recorded during the pulse. They claimed that the bag is sucked on to its support cage due to this negative pressure and causes mechanical wear of the fabric. They recommended use of support cages with much smaller mesh size than conventional cages.

B. Flow Phenomena in the Pulse-Jet Fabric Filter

In the pulse-jet fabric filter, the dust deposited on the bag is dislodged by the force of the pulse-jet. When a

valve of a pressurized tank is opened, the pressurized air flows into the lateral pipe and the air jet is injected into the bag from the hole on the lateral pipe. The high pressure gas released from the tank expands to the atmospheric pressure almost instantaneously through the course of the dust dislodgment process. The pressure of the flowing gas changes rapidly with time. Also, the air is considered to be an ideal and perfect gas. In addition, the pulse-jet fabric filter consists of a series of ducts whose cross sectional area are constant and the flow properties are the same within the cross section. Hence, the type of flow that must be dealt with is an unsteady one-dimensional flow of a perfect gas. Much useful literature is available such as Shapiro (1953), Liepman and Loshko (1960), Owczarek (1964), and Zckrow and Hoffman (1977). Fundamentals of Gas Dynamics (1964) by Owczarek and Gas Dynamics (1977) by Zucrow and Hoffman were referenced extensively in the development of the governing equation for unsteady one dimensional flow. Table 2.1 is a list of notations used for discussion of the flow phenomena in a pulse-jet fabric filter. The governing equations for unsteady one dimensional flow are discussed in Gas Dynamics (1977) and are summarized in Table 2.2.

These equations shown in Table 2.2 are said to be a system of three quasi-linear partial differential equations. The equation can be classified into three types: hyperbolic,

Table 2.1. Notation used for discussion of the flow phenomena.

Symbol	Meaning
A	flow cross-sectional area
C	the unsteady flow Mach lines
f	Fanning friction coefficient
δF_f	friction force
h	static specific enthalpy
H	stagnation specific enthalpy
$\dot{m}_i$	mass addition
δQ	heat transfer
$\dot{m}$	mass flow rate
γ	specific heat ratio
t	time
T	absolute static temperature
u	velocity of the gas
U	velocity of a shock wave relative to the gas
M	Mach number
p	pressure of the gas
ρ	density of the gas
a	speed of sound
x	spatial coordinate in flow direction
β	combined friction and mass addition term in the momentum equation
E	mass addition term in the continuity equation

Table 2.1. (Continued)

Symbol	Meaning
$\lambda_{\pm}$	= 1/(u $\pm$ a) slope of the Mach lines
ψ	combined friction, heat transfer, and mass addition term in the energy equation
1,2, etc	subscript of numbers indicate flow regions associated with the flow properties

Table 2.2. The governing equations for unsteady one dimensional flow.

Continuity Equation:

$$\rho_t + u\rho_x + \rho u_x = E \qquad (2\text{-}17)$$

Momentum Equation:

$$\rho u_t + \rho u u_x + P_x = \beta \qquad (2\text{-}18)$$

Energy Equation:

$$P_t + uP_x - a^2(\rho_t + u\rho_x) = \psi \qquad (2\text{-}19)$$

where:

$$E = \frac{1}{A}\frac{d\dot{m}_i}{dx}$$

$$\beta = -\left[\frac{\rho u^2}{2}\frac{4f}{D} + \rho u^2 (1-y)\frac{d\dot{m}_i}{\dot{m}dx}\right]$$

$$\psi = (r-1)(\rho u \delta Q_x - dH_i - u\beta)$$

parabolic and elliptic types. The governing equation for unsteady one-dimensional flow belongs to the hyperbolic type. The method of characteristics is usually employed to solve the equations.

The factors involved in the equations have been evaluated for the flow condition at the bag and the lateral pipe. Then, the equations are simplified under several assumptions. For the bag, the equations have been simplified by assuming that a lump of high pressure air mass is traveling along the bag at a constant velocity while it is losing its mass through the permeable bag. For the lateral, the entropy is assumed to be constant. Also, loss of mass and friction are considered to be insignificant. Consequently, the equations have been reduced to a system of quasi-linear homogeneous partial differential equations of the hyperbolic type.

It was considered that the flow phenomena of the reservoir/lateral-pipe system is similar to that of a shock tube. Hence, the theory developed for a shock tube is applicable to the system of the reservoir/lateral-pipe.

Theoretical and experimental studies on a simple shock tube have been conducted extensively and the theory for a simple shock tube are well established. Discussions of a simple shock tube can be found in the literature mentioned previously. The development of equations to predict the pressure in the shock tube was conducted in the following

section. Fundamental discussions on unsteady one dimensional homentropic flow including characteristic and compatibility equations for the type of waves generated in the lateral such as a simple wave, a centered expansion wave, a moving shock wave, and a reflected shock wave from a stationary wall can be also found in the literature mentioned previously.

A Simple Shock Tube

A shock tube is a device in which high-speed transient flows are generated by the rupture of a diaphragm separating a gas at high pressure from a gas at low pressure. The rupture of the diaphragm separating gases at different pressures results in the formation of wave a pattern as illustrated in Figure 2.1. The wave pattern consists of a shock wave moving into the low pressure gas, a contact surface, and a centered expansion wave moving into high pressure gas.

Owczarek (1964) derived the set of equations that determines the property of regions 2, 3, and 5 based on the intial condition of region 1 and 4. The Mach number in region 3 (M_3) is expressed in terms of the initial pressure ratio(P_4/P_1) , speed of sound ratios (a_4/a_1), and the ratio of specific heats of the gas (r_1/r_4). The pressure ratio across the expansion wave (P_3/P_4) and the pressure ratio across the shock wave (P_2/P_1) are expressed in terms of M_3.

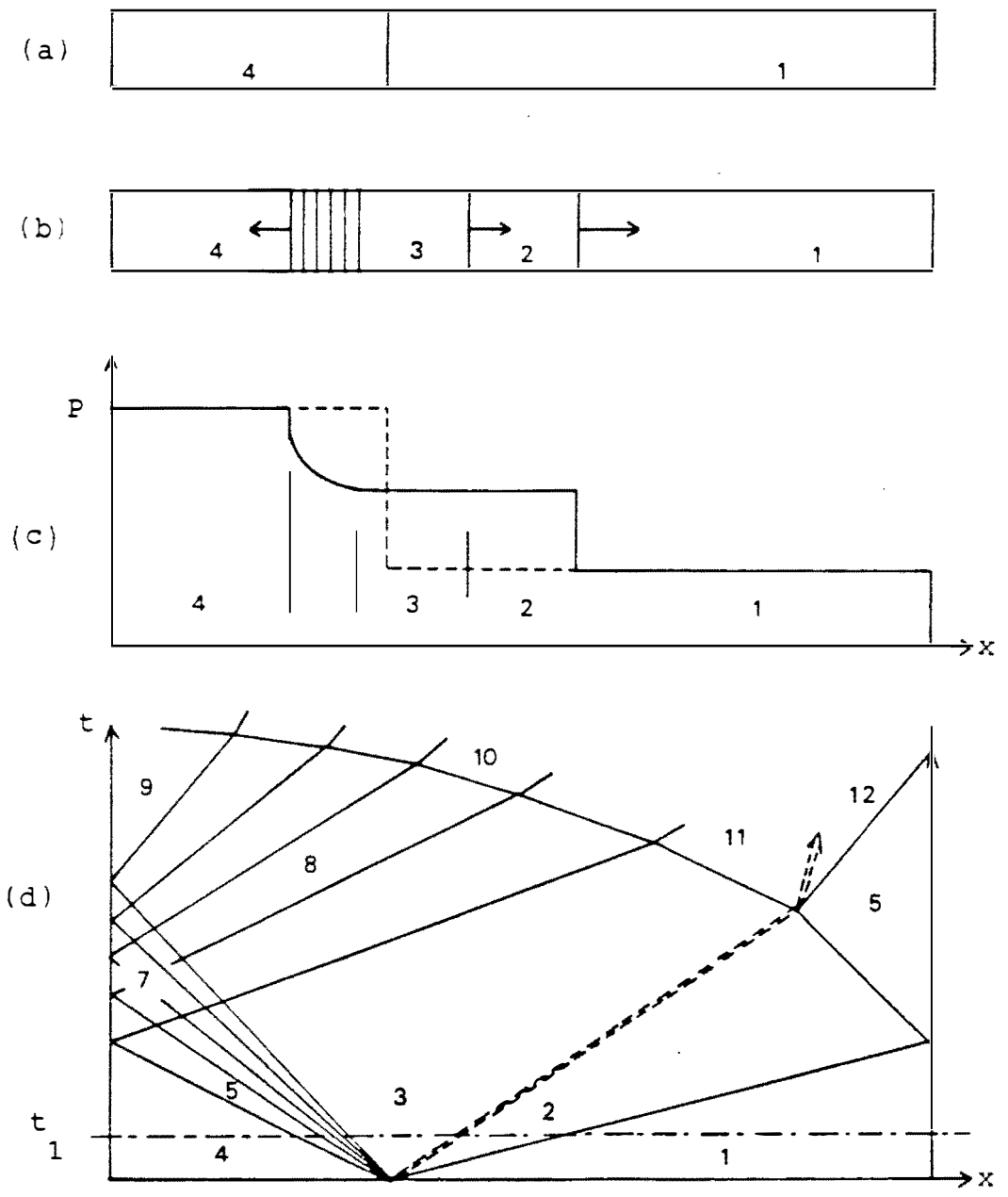

Figure 2.1. The shock tube (Zckrow and Hoffman,1977)
(a) Flow field before the rupture of the diaphragm
(b) Flow field at time t_1 after rupture of the diaphragm
(c) Pressure distribution at time t_1
(d) Wave pattern in the physical plane

The equations which relate the states of gas ahead of and behind a moving shock wave are obtained as follows:

$$\frac{u_2 - u_1}{a_1} = \frac{2}{\gamma + 1}\left(\frac{U}{a_1} - \frac{a_1}{U}\right) \qquad (2\text{-}20)$$

This equation expresses the dimensionless change in the speed of the gas across a moving shock wave with the function of dimensionless speed of propagation of the shock wave relative to the gas ahead of it.

The pressure ratio across a moving shock wave is also obtained as:

$$\frac{P_2}{P_1} = 1 + \frac{2\gamma}{\gamma + 1}\left[\left(\frac{U}{a_1}\right)^2 - 1\right] \qquad (2\text{-}21)$$

Eliminating the shock wave Mach number $M_s=U/a_1$ from these two equations and substituting $u_1=0$ yields:

$$\frac{u_2}{a_3} = \frac{\frac{P_2}{P_1} - 1}{r_1\sqrt{1 + \frac{\gamma + 1}{2\gamma}\left(\frac{P_2}{P_1} - 1\right)}} \qquad (2\text{-}22)$$

The pressure ratio across the centered expansion wave and the dimensionless change in the gas velocity are related by:

$$\frac{u_3}{a_4} = \frac{2}{\gamma_4 - 1}\left[1 - \left(\frac{P_3}{P_4}\right)^{\gamma_4 - 1/2\gamma_4}\right] \qquad (2\text{-}23)$$

Since $u_2=u_3$ and $p_2=p_3$, equations (2-22) and (2-23) can be combined to yield:

$$\frac{\frac{a_1}{a_4}\left(\frac{P_2}{P_1}-1\right)}{\gamma_1\sqrt{1+\frac{\gamma_1-1}{2\gamma_1}\left(\frac{P_2}{P_1}-1\right)}} = \frac{2}{\gamma_4-1}\left[1-\left(\frac{P_2}{P_4}\right)^{\gamma_4-1/2\gamma_4}\right] \qquad (2\text{-}24)$$

The pressure ratio across the wave p_3/p_4 can be expressed as a function of the Mach number behind an expansion wave propagating in a gas at rest.

$$\frac{P_3}{P_4}=\frac{P_2}{P_4}=\left(1+\frac{\gamma_4-1}{2}M_3\right)^{-2\gamma_4/\gamma_4-1} \qquad (2\text{-}25)$$

Further, equation (2-25) is rearranged as follows.

$$\frac{2}{\gamma_4-1}\left[1-\left(\frac{P_2}{P_4}\right)^{\gamma_4-1/2\gamma_4}\right]=\frac{M_3}{1+\frac{\gamma_4-1}{2}M_3} \qquad (2\text{-}26)$$

Substitution of the equation (2-26) into equation (2-24) and solving for the pressure ratio p_2/p_1 gives

$$\frac{P_2}{P_1} = 1 + \frac{1}{2}\left(\frac{a_4}{a_1}\right)^2\left(\frac{\gamma_1 M_3}{1 + \frac{\gamma_4 - 1}{2} M_3}\right)^2 \left[\frac{\gamma_1 + 1}{2\gamma_1}\right.$$

$$\left. + \left(\frac{\gamma_1 + 1}{2\gamma_1}\right)^2 + \frac{4}{\left(\frac{a_4}{a_1}\right)^2 \left(\frac{\gamma_1 M_3}{1 + \frac{\gamma_4 - 1}{2} M_3}\right)^2}\right] \quad (2\text{-}27)$$

In view of equation (2-25)

$$\frac{P_4}{P_1} = \frac{P_4}{P_2}\frac{P_2}{P_1} = \frac{P_2}{P_1}\left(1 + \frac{\gamma_4 - 1}{2} M_3\right)^{2\gamma_4/\gamma_4 - 1} \quad (2\text{-}28)$$

Combining the last two equations gives the relationship

$$\frac{P_4}{P_1} = 1 + \frac{1}{2}\left(\frac{a_4}{a_1}\right)^2\left(\frac{\gamma_1 M_3}{1 + \frac{\gamma_4 - 1}{2} M_3}\right)^2 \left[\frac{\gamma_1 + 1}{2\gamma_1}\right.$$

$$\left. + \left(\frac{\gamma_1 + 1}{2\gamma_1}\right)^2 + \frac{4}{\left(\frac{a_4}{a_1}\right)^2 \left(\frac{\gamma_1 M_3}{1 + \frac{\gamma_4 - 1}{2} M_3}\right)^2}\right]$$

$$x \left(1 + \frac{\gamma_4 - 1}{2} M_3\right)^{2\gamma_4/\gamma_4 - 1} \quad (2\text{-}29)$$

The ratio of the speed of sound a_4/a_1 can be expressed as

$$\frac{a_4}{a_1} = \sqrt{\frac{\gamma_4 m_1 T_4}{\gamma_1 m_4 T_1}} \qquad (2\text{-}30)$$

where m_1 and m_4 are the molecular weights of the gases.

The equation relating the Mach number behind the shock wave, moving into a gas at rest, with the pressure ratio across it is:

$$M_2^2 = \frac{2}{\gamma_1(\gamma_1 - 1)} \frac{\frac{P_2}{P_1} + \frac{P_1}{P_2} - 2}{\frac{\gamma_1 + 1}{\gamma_1 - 1} + \frac{P_2}{P_1}} \qquad (2\text{-}31)$$

Further the pressure behind the reflected shock wave can be determined by:

$$\frac{P5 - P1}{P2 - P1} = 1 + \frac{\frac{2\gamma}{\gamma - 1}}{\frac{\gamma + 1}{\gamma - 1}\frac{P1}{P2} + 1} \qquad (2\text{-}32)$$

The above equations are utilized in Chapter IV for the prediction of the pressures in the lateral pipe.

CHAPTER III

EXPERIMENTAL FACILITY AND PROCEDURE

Two different experimental facilities were used to study the pulse-jet fabric filter. The standard system (clean system) was designed to analyze the pulse pressure exerted on the bag for various system configurations and operating conditions for the utility-size pulse-jet fabric filter. The system was such that modification of the system configuration and the operating conditions could be made easily. For example, a lateral pipe, a bag, and a tank can be replaced within a short period of time. Also, the pressure ports can be accessed easily.

The pilot plant system (dirty system) was designed to analyze the pulse pressure exerted on the bag under normal operating conditions and to find the relationship between the pulse pressure exerted on the bag, pressure drop across the system, and the filtration efficiency.

A. Standard System

A complete profile pulse system including a compressed air tank, solenoid valve, standard lateral pipe, bags, venturies, and the spacing between the components was constructed. The configuration of the system is shown in Figure 3.1. The lateral and the bags were placed horizontally at two feet above the floor. The bags were

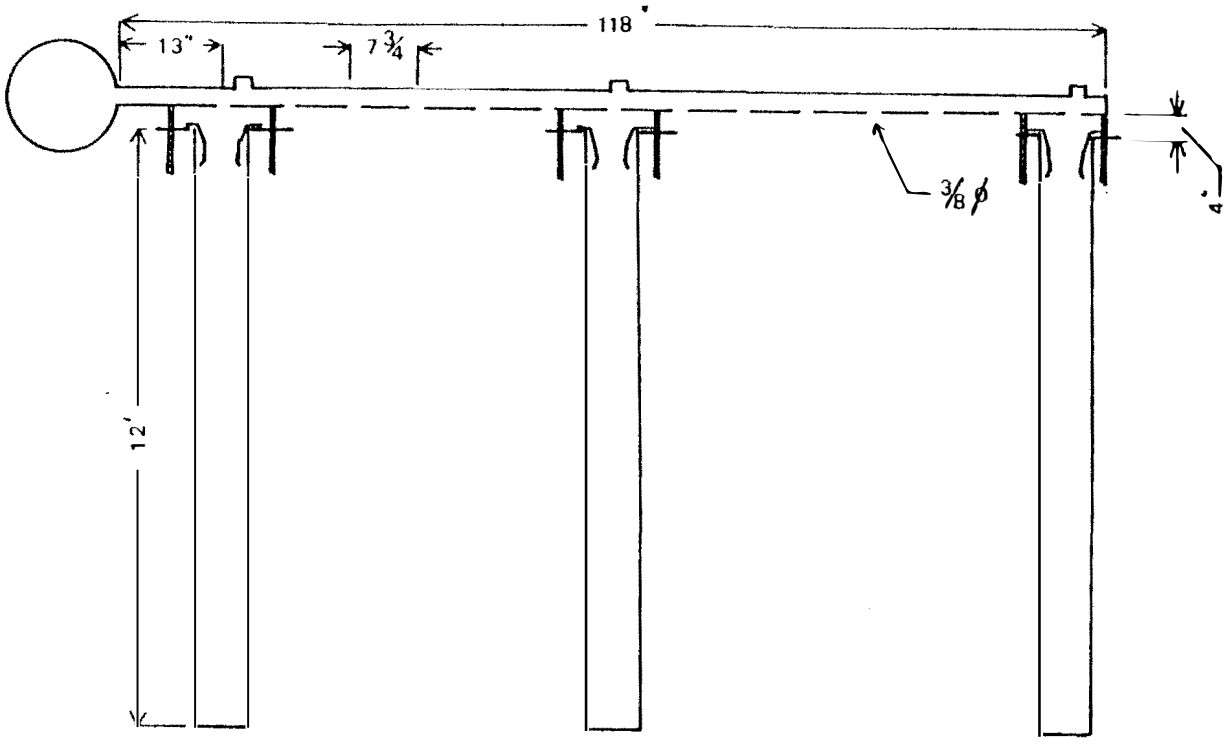

Figure 3.1. Schematic of the lateral pipe and bags.

located on the lateral hole 1 (nearest the valve), hole 7 (middle of the lateral pipe), and hole 14 (last bag on the lateral). The lateral to bag spacing was adjustable from a spacing of 2" to 20". Pressure taps were installed at 1.5 ft intervals on each bag and 17, 64 and 110 inches from the tank on the lateral pipe. The static pressure developed inside of the bag during the pulse was measured by a high sensitivity pressure transducer and a storage oscilloscope. The pressure was recorded for one pressure port at a time. The dimensions of the system are shown in Table 3.1.

B. Pilot System

An existing pulse-jet system was modified to serve the objectives of the tests conducted in this study. Figure 3.2 shows the system schematic. The test compartment was placed in a closed loop with an environmental control room which was utilized to maintain system temperature and humidity. Compartment flow was regulated by a damper which was controlled by a Dwyer Photohelic on/off controller. The controller was activated by the pressure differential across an orifice plate located in the ductwork on the down stream side of the compartment.

Flyash test dust was injected from a Vibrascrew dust feeder (located in the environmental control room) into the duct leading to the filter compartment. The flyash utilized was obtained from the hoppers of an electrostatic

Table 3.1. Dimension of the standard configuration of the pulse-jet fabric filter.

Lateral	1 1/2 in. diameter, sch. 40 pipe
Bag dimension	12 ft in length
	6 in. in diameter, felted
Bag spacing	7 3/4 in. center to center
Number of bags per lateral	14 bags
Lateral hole diameter	3/8 in.
lateral to bag space	4 in.
Volume of tank	0.92 ft
Valve	ASCO 1 1/2 in. diameter
Tank pressure	100 psi
Pulse duration	50 ms

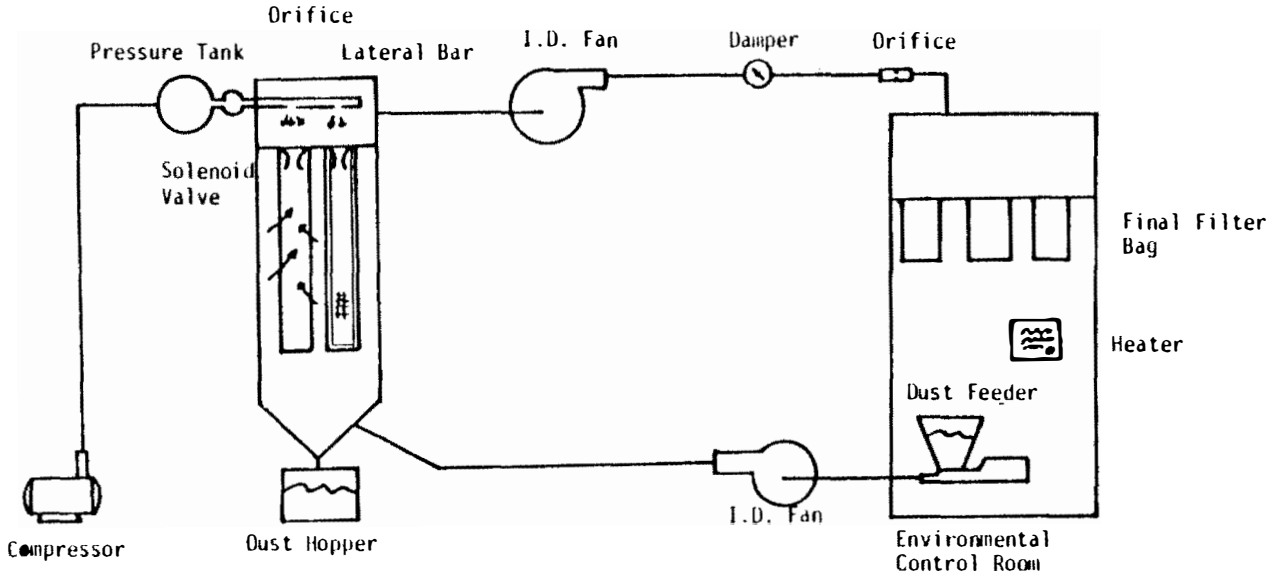

Figure 3.2. Schematic diagram of the pulse-jet system.

precipitator installed at a nearby pulverized coal fired boiler (Kingston Steam Plant, Tennessee Valley Authority).

Figure 3.3 is a detailed description of the pulse jet fabric filter collecter. The cleaning mechanism consisted of a rapid pulse of high pressure air which was transfered from a pressurized tank through a lateral pipe into the top of each filter bag. The tank pressure was variable from 0-100 pounds per square inch (psig). Two identical laterals transfered the compressed air from the tank to the bags. Each lateral pulsed two filter bags. During the filtration cycle, a row of bags (2 bags in each row) was pulsed by activating a solenoid valve located between the tank and the lateral. At a pre-determined interval (2-5 minutes) the bags were cleaned by alternating between laterals 1 and 2.

Each1 - 1/4 " diameter lateral had a 3/8" diameter hole located above each bag at the center of the hole at the top of the bag. The laterals were adjustable from a spacing of 4" to 20"(centerline of the pipe to the top edge of the filter bag) in increments of 4".

The filter system housed 4 filter bags (6" diameter by 12' long). Pressure taps were installed at one foot intervals on one of the bags to allow pressure waves to be measured along the length of the bag. Access doors (10" diameter) were also installed on one side of the housing wall to allow both visual inspection and access to the

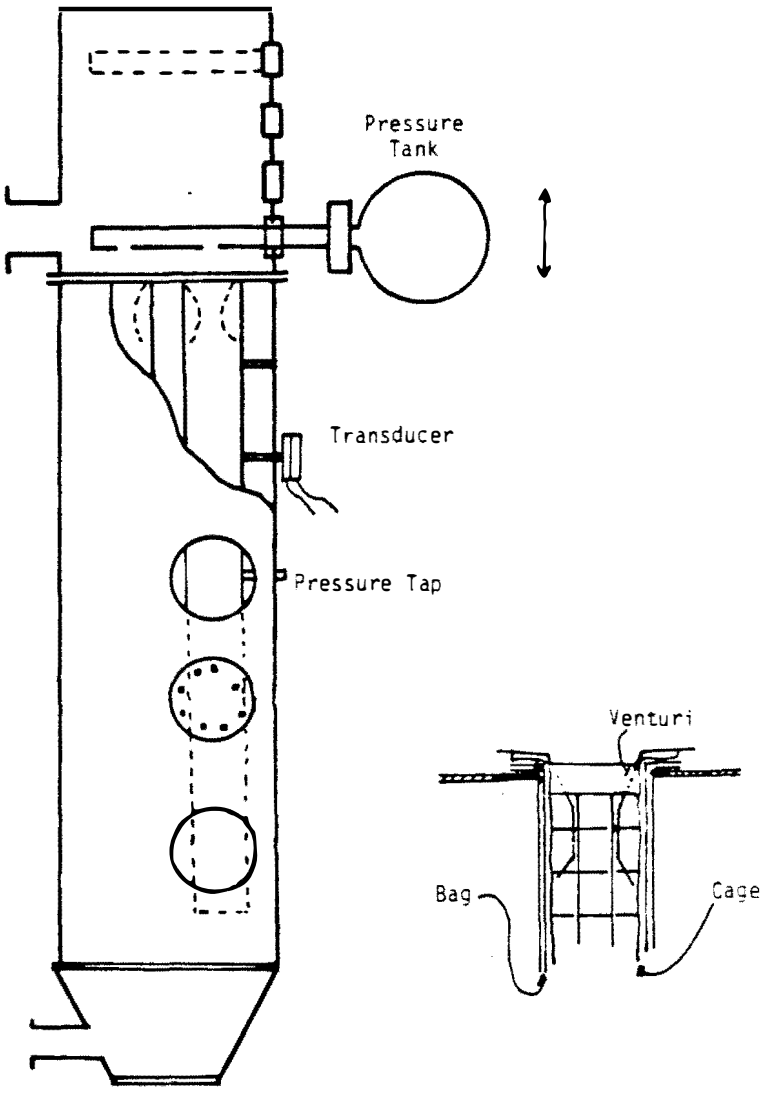

Figure 3.3. Schematic of the baghouse and venturi.

filter bag which was used to measure the pressure wave. A venturi was mounted in the top of each filter bag.

A schematic diagram of instrumentation is shown in Figure 3.4 . Also the specifications of the instruments are listed on Table 3.2. The pressure drop across the bag was continuously monitored by a low range, low sensitivity pressure transducer and a x-y recorder. The static pressure developed inside of the bag during the pulse was measured by a high-sensitivity pressure transducer and a storage oscilloscope. The particle removal efficiency was measured by sampling upstream of the collector with an optical particle counter (Climet 208 and Climet 210).

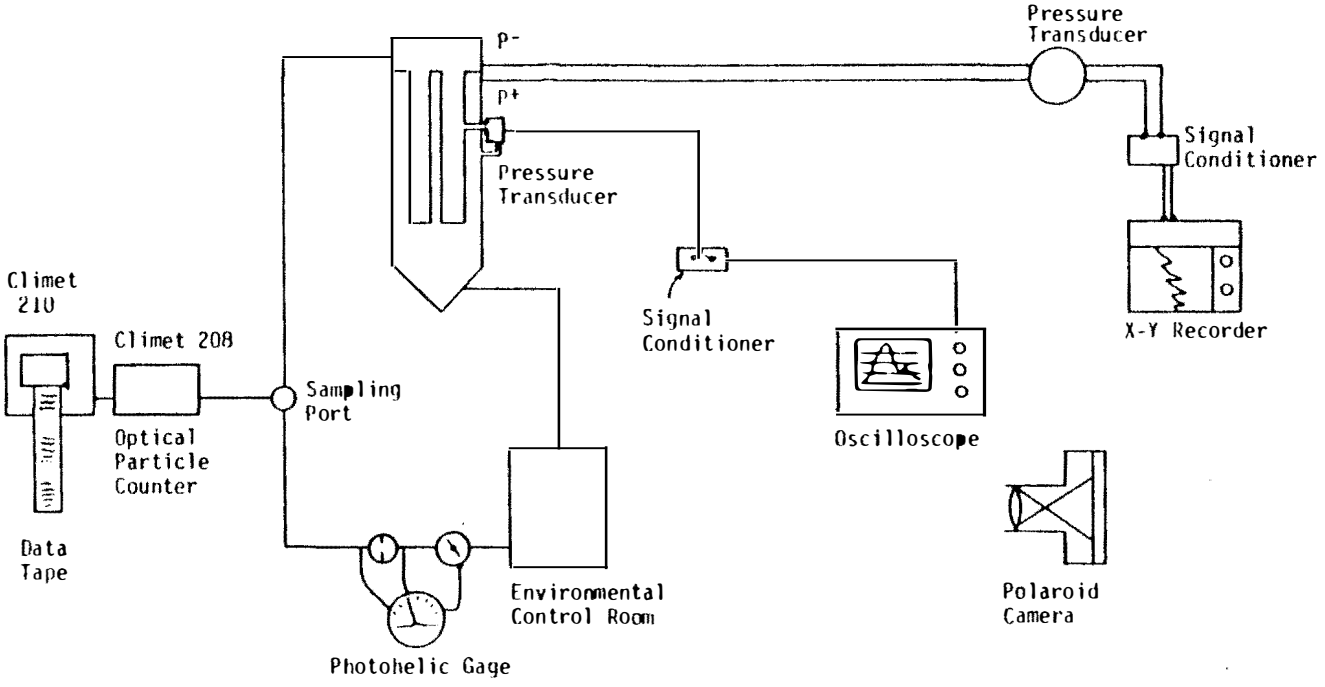

Figure 3.4. Schematic diagram of instrumentation.

Table 3.2. Instrument specifications.

Differential Pressure Transducer	Validyne Model DP15-50 S/N 49392 Range: 0-125 psi Output: 35 mv/v at 3000 Hz Celesco Model P7D +.1 PSID Range: +.1 to +500, differential Output: 25 mv/v min FS @ 3000Hz Robert Shaw Model No. 117-A1-A Range: 0-10/50" W.G., SP:2000psi Input:12/80 VDC Output:4-20 MADC
Oscilloscope	Tektronix 434 Storage Oscilloscope
Camera	Tektronix Type C30AP
Film	Kodak Polaroid Film Type 667
Solenoid Valves	ASCO Valves 2-way diaphragm type Quick opening 1 1/2 N.P.T Normally closed operation
X-Y Recorder	Cole-Parmer Instrument Company
Optical Particle Counter	Climet 208 Climet 210 Multi Channel Monitor Range: 0.3 μ - 10 μ
Pressure Gauge	Magnehelic Range : 0 - 5" W.G. 1 - 2" W.G. Photohelic Range: 0 - 1.0 " W.G

CHAPTER IV

A MODEL FOR THE PULSE PRESSURE IN A PULSE-JET FABRIC FILTER

A. Introduction

The amount of the dust dislodged from a fabric filter is a function of pulse pressure developed inside of the bag. Thus, an understanding of the pressure developed in the lateral pipe and bag is very important for the design of a pulse-jet type of fabric filter. This task becomes more complex if the shape of the lateral pipe and the bag is taken into account since the pressure does not develop uniformly throughout the system due to its long-tube shape. Furthermore, due to the permeability of the bag, the pulse pressure developed inside the bag dissipates toward the bottom of the bag.

The analysis of the pressure exerted in the system is approached in two steps. The first step is to develop a predictive model without consideration of the system configuration. This model is referred to herein as the simplified static model. The model developed under the simplified configuration is capable of estimating the general pressure wave pattern and the representative magnitude of the pressure developed in the lateral pipe and the bag. In this model, the predicted pressure can be

considered to be somewhere between the lower and upper value in terms of the pressure developed although the model is not able to predict the pressure at specific locations and/or times. Nonetheless, the simplified static model is a very effective tool in understanding the behavior of the pulse-jet fabric filter. For example, the effect of varying the design parameters on the pulse pressure can be examined with the model. Such analyses have been conducted and are included in a later section.

The second step is to consider the dynamic aspects of the system. The configuration and the permeability of the bag are taken into account in the dynamic model. This section provides the information needed to understand the behavior of the dynamic aspects of the pulse-jet fabric filter and to solve the problems associated with designing the pulse-jet fabric filter.

Figure 4.1 illustrates the procedure used in the analysis of the pulse pressure in the pulse-jet fabric filter.

B. Simplified Static Model

Development of the Model

The system can be viewed as an energy distribution system consisting of the compressed air tank, the solenoid valve, the lateral pipe, the venturi, and the bag as illustrated in Figure 4.2. When the valve is opened, the

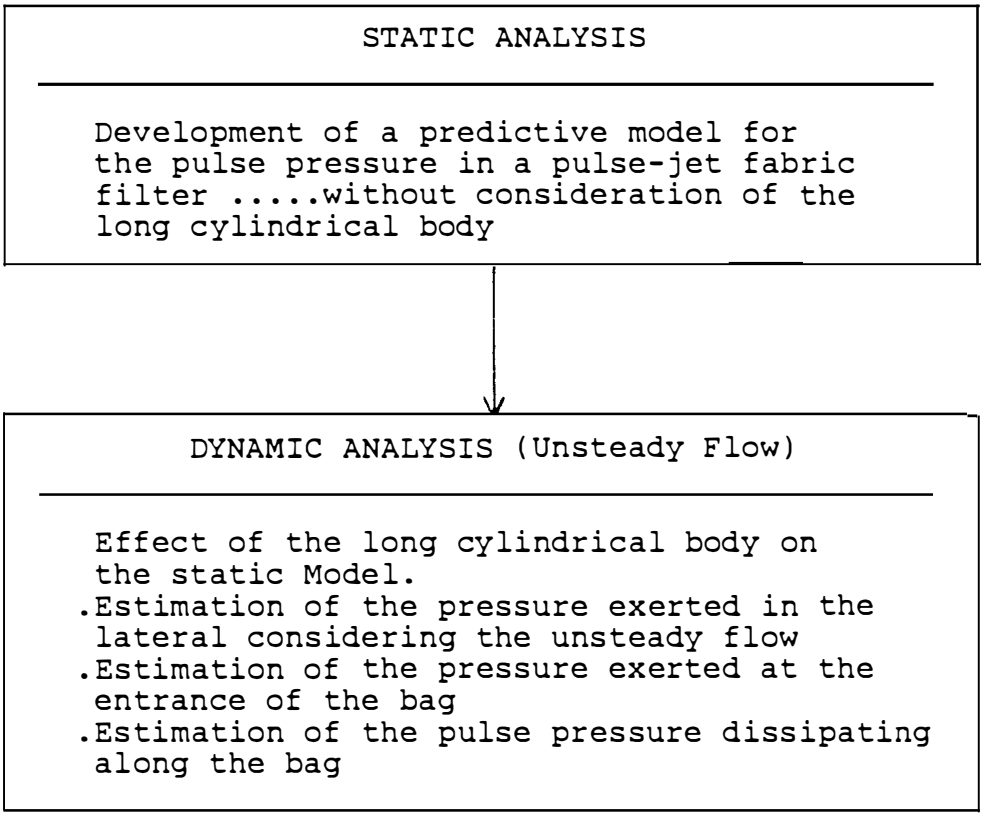

Figure 4.1. Procedures for the development of a predictive model for the pulse pressure in a fabric filter.

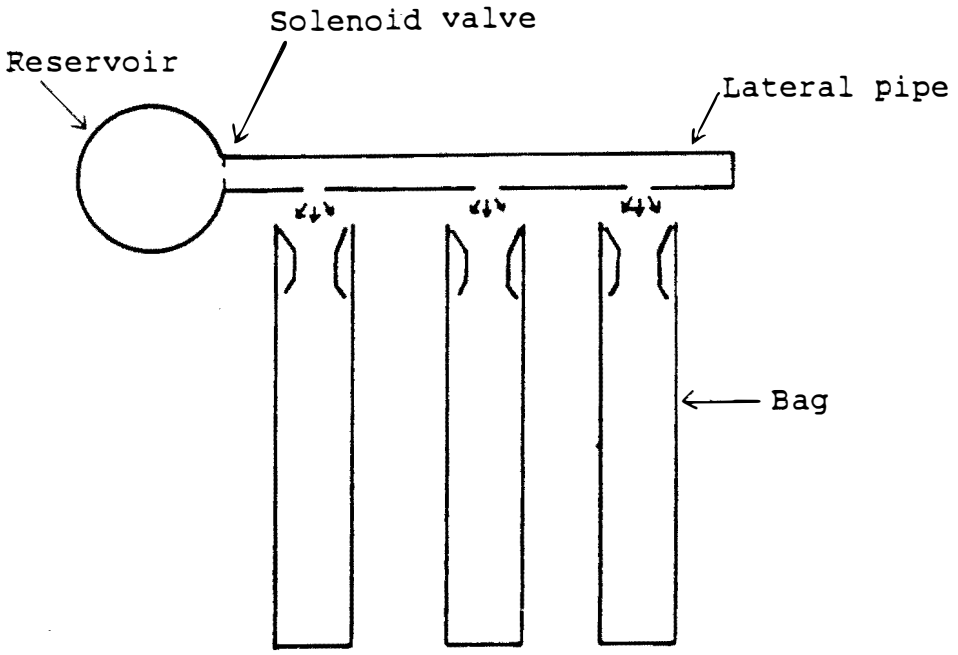

(a)

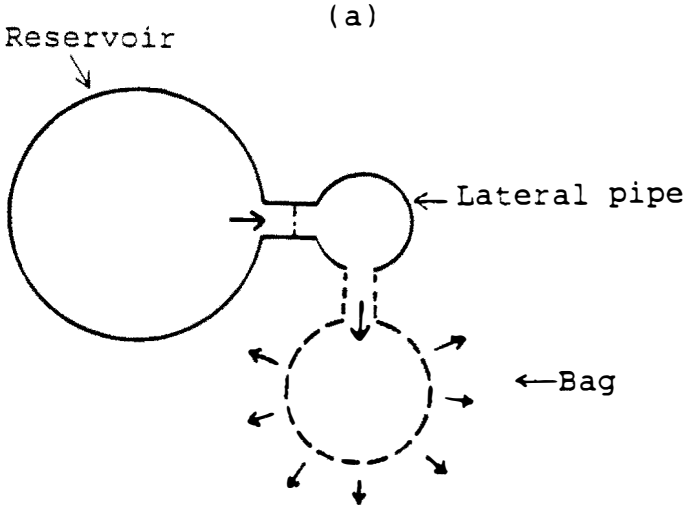

(b)

Figure 4.2. The actual and the simplified system configuration.
(a) Actual system.
(b) Simplified system.

compressed air flows into the lateral pipe and the lateral pipe is pressurized. While the pressure of the lateral pipe is being developed, some air begins to be discharged into the bag located below each orifice in the pipe. Then the bag is pressurized while some air permeates through the bag surface. The amount of air mass flowing into the lateral and the amount of air mass discharged from the lateral are regulated by the pressure conditions at the valve and the orifice. The amount of air flowing into the bag is regulated by the pressure condition at the bag entrance. The amount of the air permeating through the bag surface is controlled by the material/construction of the bag and dust loading conditions.

In the simplified static model, in order to eliminate the problem of configuration, an ideal configuration is considered. The lateral pipe and the bag are treated as spherical containers in which the pressure develops uniformly throughout the container.

Figure 4.2(a) and (b) illustrate the actual system and the idealized system configurations used for model development respectively. Table 4.1 is a list of notation used in the course of the model development.

When the valve of the reservoir opens, the high pressure air expands into the lateral pipe. The mass of air which has flowed into the lateral in a specific time increment is equivalent to the amount of the air which was

Table 4.1. Notation for the simplified static model.

Symbol	Meaning
v_r	Reservoir Volume (ft^3)
v_l	Lateral Volume (ft^3)
ρ_r	Density of air in the reservoir (lbm/ft^3)
ρ_l	Density of air in the lateral (lbm/ft^3)
ρ_v	Density of air at the valve (lbm/ft^3)
T_r	Temperature of air in the reservoir ($^\circ R$)
T_l	Temperature of air in the lateral ($^\circ R$)
T_a	Temperature of air in the atmosphere ($^\circ R$)
T_v	Temperature of air at the valve ($^\circ R$)
T_o	Temperature of air at the orifice ($^\circ R$)
P_r	Pressure of the reservoir (psi)
P_l	Pressure of the lateral (psi)
P_a	Pressure of the atmosphere (psi)
P_v	Pressure at the valve (psi)
P_o	Pressure at the orifice (psi)
P_b	Pressure in the bag (psi)
P_e	Pressure exerted by a jet at a bag entrance (psi)
M_r	Mass flow rate from the reservoir (lbm/sec)
M_o	Mass flow rate from the lateral (lbm/sec)
M_b	Mass flow rate from the bag (lbm/sec)
V_v	Velocity of air at the valve (ft/sec)
V_o	Velocity of air at the orifice (ft/sec)

Table 4.1. (continued)

Symbol	Meaning
V_b	Velocity of air permeating the bag (ft/sec)
A_v	Area of the valve (ft^2)
A_o	Area of the orifice (ft^2)
A_s	Surface area of the bag (ft^2)
A_c	Area of the bag cross section (ft^2)
K_p	Permeability coefficient (ft/sec/in. w.g.)
M	Mach number V/a , a=sound of speed
M_v	Mach number at the valve
M_o	Mach number at the orifice
g_c	Numerical value of the standard acceleration due to gravity (ft/sec^2)
R	Gas constant (ft.lbf/lbm°R)
ɤ	Specific heat ratio
Subscripts	
r	Reservoir
l	Lateral pipe
b	Bag
v	Valve
o	Orifice
a	Atmosphere

lost from the reservoir in that same time increment. Therefore, the mass balance equation can be established such that (John, 1969):

$$\frac{\partial}{\partial t}\iiint \rho_r \, dv + \iint_s \rho_r \vec{V}_v \, d\vec{A}_v = 0 \qquad (4\text{-}1)$$

where:

ρ_r = the density of air in the reservoir

$\vec{V}_v$ = the velocity of the air escaping through the valve

$d\vec{A}_v$ = the unit area of the valve

dv = the unit volume of the reservoir

Since the volume of the reservoir and the area of the valve are constant, equation (4-1) can be rewritten as

$$\frac{\partial \rho_r}{\partial t} v_r + \rho_v V_v A_v = 0 \qquad (4\text{-}2)$$

change of mass in the reservoir | mass flow from the valve

where:

A_v = the area of the valve

v_r = the total volume of the reservoir

For the ideal gas,

$$P = \rho RT \qquad (4\text{-}3)$$

Substitution of equation (4-3) into equation (4-2) results in the following expressions:

$$\frac{v_r}{R\,T_r}\,\frac{\partial P_r}{\partial t} + \frac{P_v}{R\,T_v}\,V_v\,A_v = 0 \qquad (4\text{-}4)$$

where it is considered that the temperature is constant during the discharge of air.

In the same manner as above, a mass balance equation can be set up between the reservoir, the lateral pipe, and the atmosphere:

$$\underset{\substack{\text{accumulation of}\\ \text{mass in the}\\ \text{lateral pipe}}}{\frac{v_l}{R\,T_l}\,\frac{dP_l}{dt}} - \underset{\substack{\text{mass flow-in}\\ \text{from valve}}}{\frac{P_v}{R\,T_v}\,A_v\,V_v} + \underset{\substack{\text{mass flow-out}\\ \text{from orifice}}}{\frac{P_o}{R\,T_o}\,A_o\,V_o} = 0 \qquad (4\text{-}5)$$

Also, a mass balance can be set up between the lateral, the bag and the atmosphere as follows:

$$\underset{\substack{\text{accumulation of}\\ \text{mass in the bag}}}{\frac{v_b}{R\,T_o}\,\frac{dP_b}{dt}} - \underset{\substack{\text{mass flow-in}\\ \text{from orifice}}}{\frac{P_o}{R\,T_o}\,A_o\,V_o} + \underset{\substack{\text{mass flow-out}\\ \text{from bag surface}}}{\frac{P_b}{R\,T_b}\,A_s\,V_b} = 0 \qquad (4\text{-}6)$$

where:

V_b = the permeation velocity

The entrainment of the air at the entry of bag was considered to be negligible in this development.

The velocity of the air discharged through the valve (V_v) and the orifice (V_o) is calculated in one of two ways depending on the pressure condition at the valve and orifice. The following equations (John, 1979) are used for each condition:

$$V_v = M_v \sqrt{r\ g_c\ R\ T_v} \qquad (4\text{-}7)$$

where:

$$T_v = T_r \ / \ (\ 1 + \frac{r - 1}{2} M_v^2)$$

When critical pressure conditions exist at the valve (i.e. $P_l/P_r < 0.528$):

$$P_v = 0.528\ P_r$$

$$M_v = 1$$

When non-critical pressure conditions exist at the valve (i.e. $P_l/P_r > 0.528$):

$$P_v = P_l$$

$$M_v = \left[\frac{2}{r - 1} \left\{ \left(\frac{P_l}{P_r} \right)^{-(r-1)/r} - 1 \right\} \right]^{1/2}$$

The value of the pressure ratio, 0.528, is the critical pressure ratio for the air ($r = 1.4$), below which the nozzle is choked. M_v is the Mach Number at the valve.

In the same manner as above, the velocity at the orifice is determined as follows.

$$V_o = M_o \sqrt{r\, g_c\, R\, T_o} \qquad (4\text{-}8)$$

where:

$$T_o = T_1 \,/\, \left(1 + \frac{r - 1}{2} M_o^2 \right)$$

For critical pressure condition at the orifice (i.e. $P_a/P_1 < 0.528$):

$$P_o = 0.528\, P_1$$

$$M_o = 1$$

For non-critical pressure condition (i.e. $P_a/P_1 > 0.528$):

$$P_o = P_a$$

$$M_o = \left[\frac{2}{r - 1} \left\{ \left(\frac{P_a}{P_1} \right)^{-(r-1)/r} - 1 \right\} \right]^{1/2}$$

According to Darcy's Law (Berrer, 1941), it is considered that the velocity of the air permeating the bag is proportional to the pressure difference between the pressure developed in the bag and the pressure surrounding the bag:

$$V_b = K_p \left(P_b - P_a \right) \qquad (4\text{-}9)$$

where K_p is the permeation constant.

Substituting equation (4-9) into equation (4-6), gives the expression:

$$\frac{V_b}{R\,T_b}\,\frac{dP_b}{dt} - \frac{P_o}{R\,T_o}\,A_o\,V_o + \frac{P_b}{R\,T_b}\,K_p\,A_b\,(P_b - P_a) = 0 \qquad (4\text{-}10)$$

Further, it is assumed that the momentum possessed by the air jet is conserved until the air jet reaches the entry point of the bag (see Figure below).

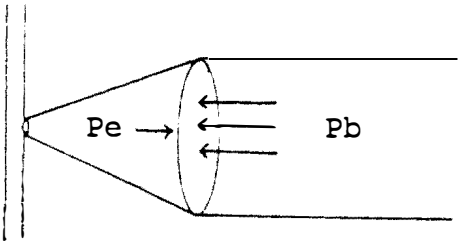

Then the pressure force acting on the bag entrance plane developed by the air jet is calculated by

$$P_e = m_o\,V_o\,/\,A_c \qquad (4\text{-}11)$$

As long as the pressure force developed by the air jet at the entrance of the bag is larger than the pressure in the bag, the air jet flows into the bag. However, once the pressure force developed by the air jet at the entrance of the bag reaches the pressure inside of the bag, the bag

pressure is controlled by the pressure force possessed by the air jet. Therefore, when the pressure of air jet (P_e) is less than the pressure in the bag (P_b), mass flow into the bag (the second term of the equation 4-10) becomes zero and the pressure of the bag (P_b) becomes equal to the pressure of the air jet (P_e).

Table 4.2 is a summary of equations for the simplified static model.

Development of the Computer Program

The set of mass balance equations shown in Table 4.2 has been solved by using a step by step solution method. Figure 4.3 shows a flow diagram of the calculation procedure. The calculation procedure is explained in seven steps as follows. In step 1, input data required for the model is prepared. They include physical parameters, conversion factors, design and operating parameters, and program parameters. In step 2, current time and time increment are set and the loop for time is initiated. In step 3, a set of velocity equations is selected for the air flow from the reservoir depending on the pressure condition at the valve. Then, the amount of air released from the reservoir for the time period t and the reservoir pressure at time T are calculated. In step 4, the velocity of air flow from the orifice is determined in the same manner as the velocity of air flow at the valve. The set of velocity

Table 4.2. Summary of the equations for the simplified static model

---

$$\frac{V_r}{R\,T_r}\frac{dP_r}{dt} + \frac{P_v}{R\,T_v} V_v\,A_v = 0 \qquad (4\text{-}4)$$

$$\frac{V_l}{R\,T_l}\frac{dP_l}{dt} - \frac{P_v}{R\,T_v} A_v\,V_v + \frac{P_o}{R\,T_o} A_o\,V_o = 0 \qquad (4\text{-}5)$$

$$\frac{V_b}{R\,T_o}\frac{dP_b}{dt} - \frac{P_b}{R\,T_o} A_o\,V_o + \frac{P_b}{R\,T_b} A_s\,V_b = 0 \qquad (4\text{-}6)$$

where:

$$V_b = K_p\,(P_b - P_a)$$

$$V_r = M_v\sqrt{\varkappa\,g_c\,R\,T_v} \qquad (4\text{-}7)$$

$$T_v = T_r / \left(1 + \frac{\varkappa - 1}{2} M_v^2\right)$$

If $P_l/P_r < 0.528$ then

$$P_v = 0.528\,P_r$$

$$M_v = 1$$

If $P_l/P_r > 0.528$ then

$$P_v = P_l$$

$$M_v = \left[\frac{2}{\varkappa - 1}\left\{\left(\frac{P_l}{P_r}\right)^{-(\varkappa-1)/\varkappa} - 1\right\}\right]^{1/2}$$

Table 4.2 (continued)

$$V_o = M_o \sqrt{\kappa\, g_c\, R\, T_o} \qquad (4\text{-}8)$$

$$T_o = T_1 \,/\, \left(1 + \frac{\kappa - 1}{2} M_o^2 \right)$$

If $P_a/P_1 < 0.528$ then

$$P_o = 0.528\, P_1$$

$$M_o = 1$$

If $P_a/P_1 > 0.528$ then

$$P_o = P_a$$

$$M_o = \left[\frac{2}{\kappa - 1} \left\{ \left(\frac{P_a}{P_1} \right)^{-(\kappa-1)/\kappa} - 1 \right\} \right]^{1/2}$$

$$P_e = \frac{P_o}{R\, T_o} A_o\, V_o^2 \,/\, A_c$$

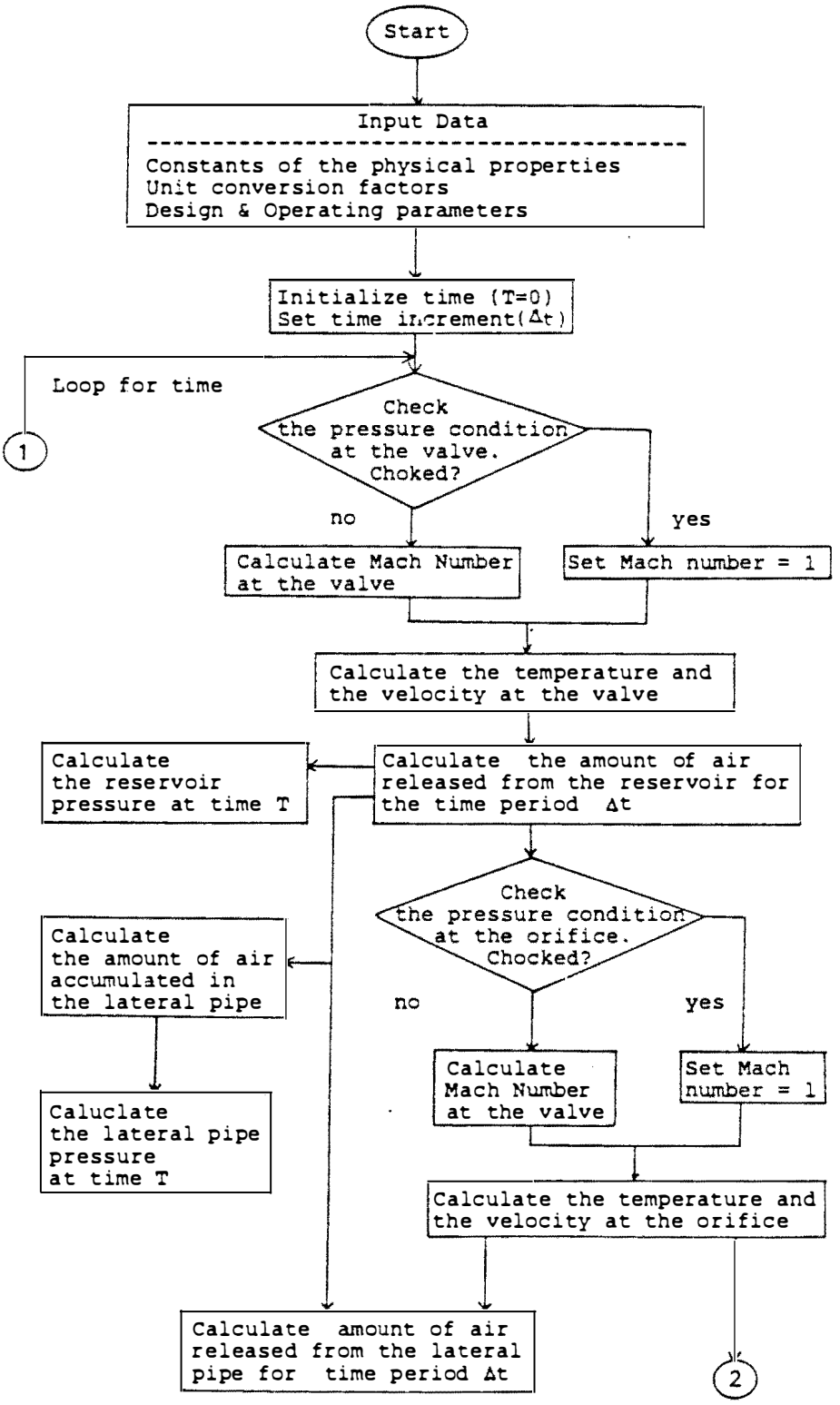

Figure 4.3. Flow diagram of the calculation procedure for the simplified static model.

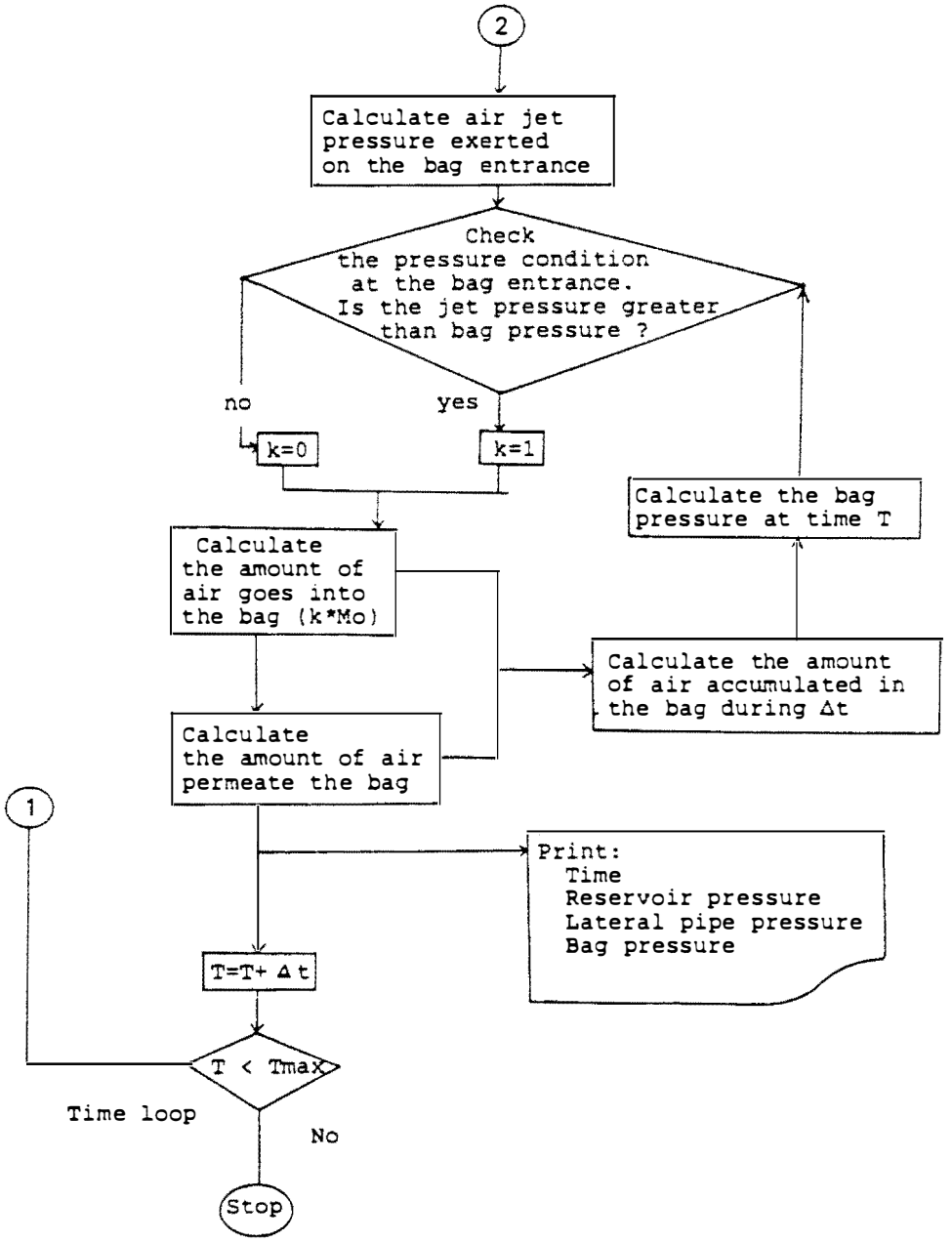

Figure 4.3. (Continued)

equations is chosen depending on the pressure condition at the orifice. The amount of air released from the lateral, the amount of air accumulated in the lateral during time period Δt, and the pressure developed at time T are then calculated. In step 5, the air jet pressure exerted on the bag entry plane is calculated and compared with the bag pressure. If the jet pressure is less than the bag pressure, no air mass flow is allowed into the bag (i.e. K equals to zero). The amount of air injected into the bag during time period Δt, the amount of air permeating the bag during time period Δt, and the bag pressure developed at time T are then obtained. In step 6, desired values such as the reservoir pressure,the lateral pipe pressure, and the bag pressure are printed for the time T. In step 7, the time increment is added to current time and returns to the beginning of the loop for time. If the current time is greater than the pre-set time, the loop is terminated.

Application of the Model and Comparison with the Experimental Results

Table 4.3 is an example input to the model. The results are exhibited on Figure 4.4 and 4.5 with the observed pressure curve.

Figure 4.4 is a graph of predicted pressure versus time for the reservoir and the lateral. The observed pressure in the lateral is also shown for the conditions illustrated in

Table 4.3. Example input to the simplified static model.

Design parameters:	
Reservoir volume, v_r	0.92 ft^3
Lateral pipe volume, v_l	0.12 ft^3
Bag volume, v_b	2.35 ft^3
Valve area, A_v	1.767 $inch^2$
Orifice area, A_o	1.546 $inch^2$ (14 holes)
Area of bag inlet, A_c	28.274 $inch^2$
Area of bag surface, A_s	2714 $inch^2$
Operating parameters:	
Reservoir Pressure, P_r	100 psig
Temperature, T	530 °R
Valve opening time, t_s	100 ms
Calculation parameters:	
Time increment, Δt	0.5 ms

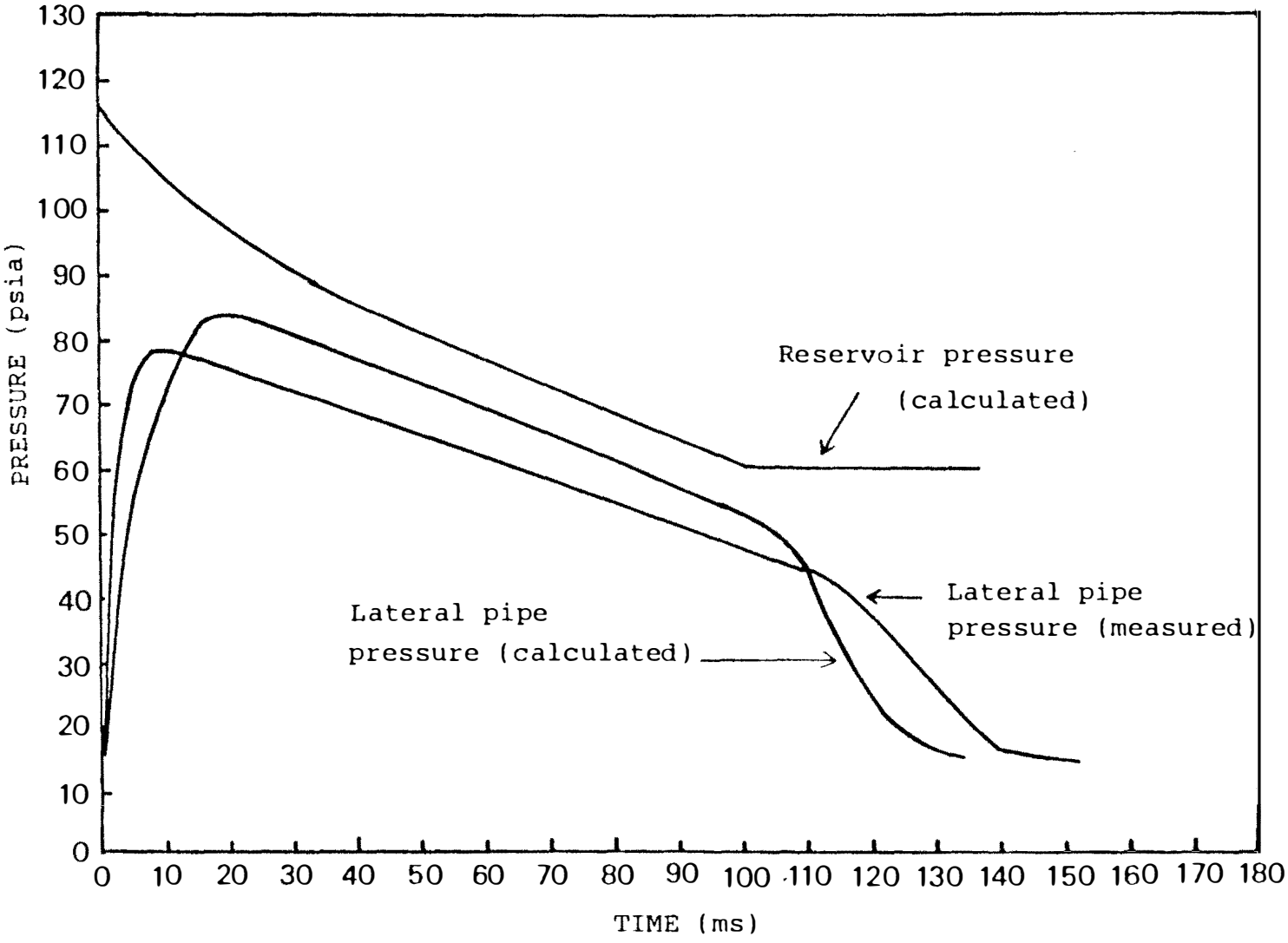

Figure 4.4. Reservoir and lateral pipe pressure versus time.

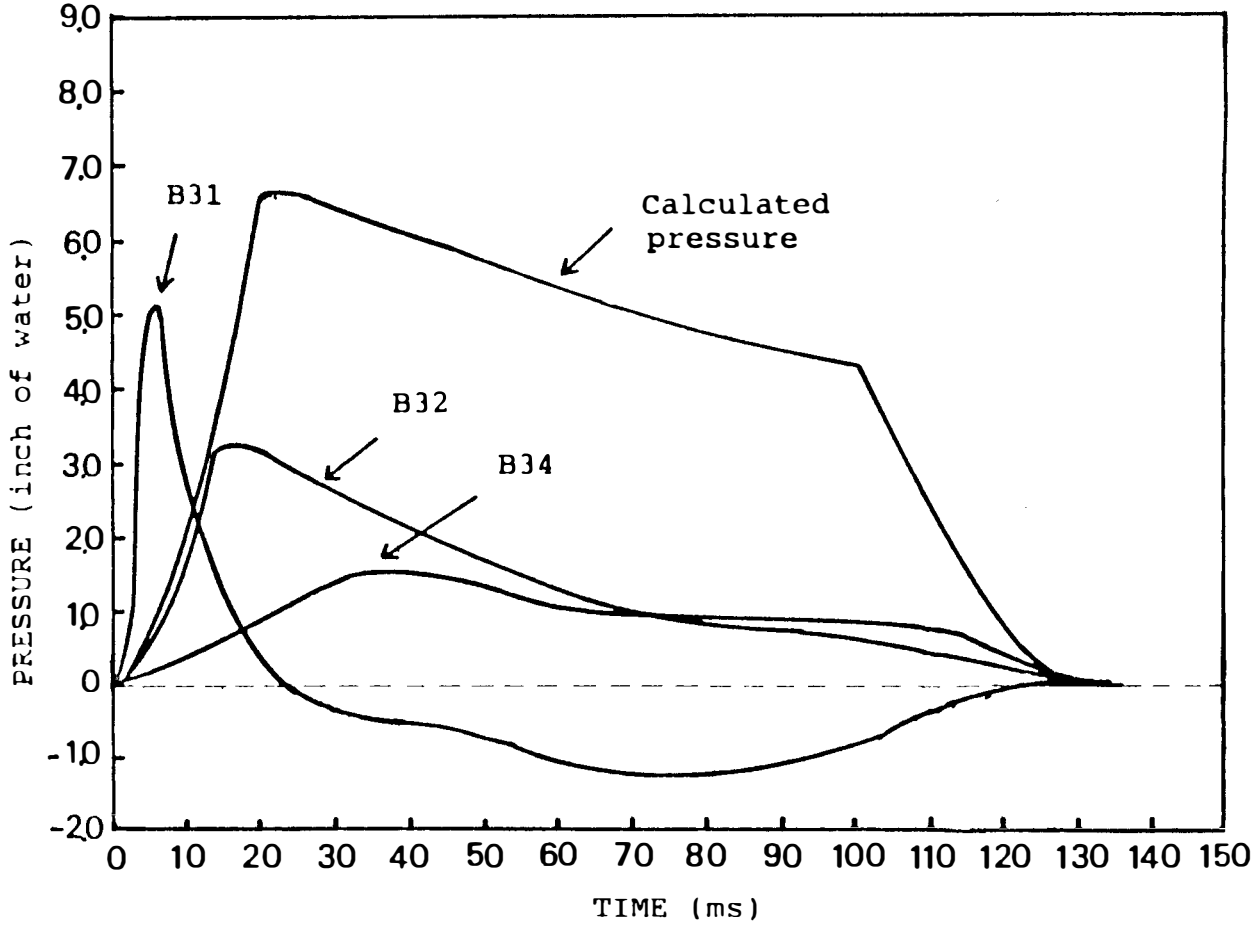

Figure 4.5. Predicted and observed bag pressure versus time.

Table 4.3. The magnitude of the observed pressure is approximately 10% smaller than the predicted value. However, the pattern of the predicted pressure curve is very similar to that of the observed pressure curve.

Figure 4.5 shows the predicted and observed bag pressure for three different locations along the bag. Bag #3 is located at the closed-end of the lateral. B31, B32, B34 are located at 1.5, 3, and 6 ft from the top of the bag, respectively. Bag #3 is chosen for illustration because the characteristics of dissipating pulse are manifested most clearly on this bag. The characteristics of the pulse pressure exerted on the other bags are similar to the charcteristics of the pulse pressure for bag #3. The bag nearest the closed-end or far end of the lateral consistently had a higher pressure than the other bags.

The pulse pressure at B31 is a sharp pulse(impulse-like) accompanied by an observed negative pressure after the initial short-lived pulse. The shape of pressure curve at B32 is similar to that of the lateral pressure curve. As the pulse travels down the bag, the shape of the pressure curve is rapidly deforming as shown in the pulse pressure curve for B34.

Theoretically, the observed pulse pressure of the bag at the far end of the lateral is expected to be higher than the predicted pulse pressure because the dynamic nature of the system has not been taken into account by the model.

Likewise, the observed pressure at the bottom of bag #1 should be lower than the predicted pulse pressure using the model. The observed pressure curve of bag #3 was consistently lower than the predicted one. It was hypothesized that the energy losses (i.e. entry loss, friction loss, momentum loss, and loss due to air entrainment) in the system which were not considered might have been considerably large. The energy losses incurred between the orifice on the lateral and the entry of the bag required further investigation and will be discussed in more detail in a later section.

Sensitivity Analysis

To better understand the behavior of the pulse-jet system, sensitivity analyses have been conducted by utilizing the model developed. These analyses examined the effect of varying the design parameters on the pulse pressure wave. The analyses conducted were, (1) effect of reservoir, lateral, and bag volume, (2) effect of reservoir pressure, (3) effect of orifice diameter, (4) effect of valve opening time.

Effect of reservoir volume. Figure 4.6 shows the change in the pressure wave for the various reservoir volumes. The reservoir volume affects the rate of decrease in pressure after the peak pressure is developed. As the reservoir volume becomes smaller, the pressure pattern

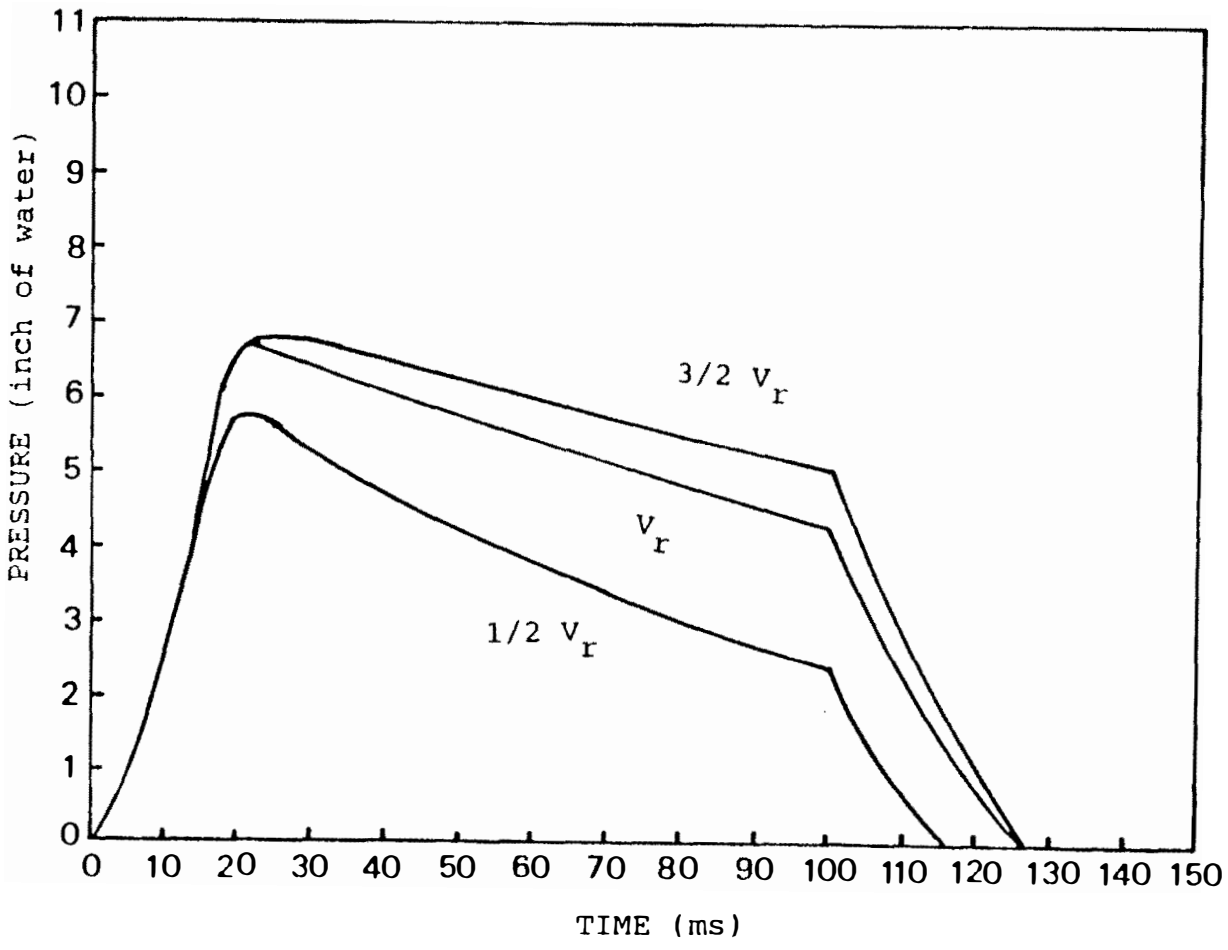

Figure 4.6. The pressure developed inside the bag with time for various reservoir volumes.

approaches a triangular shape since the reservoir cannot maintain the pressure. As the reservoir volume becomes larger, the pressure wave pattern approaches a rectangular shape. The magnitude of the predicted peak pressure developed in the standard reservoir volume and the reservoir volume which was 50 % larger than the standard reservoir volume are almost the same. On the other hand, when the reservoir volume becomes one half of the standard reservoir volume, the exerted peak pressure decreases significantly. This low peak pressure may not provide enough force to dislodge the dust from the bag. Therefore, it is recommended that the use of an excessively small reservoir be avoided.

Effect of a lateral pipe volume. Figure 4.7 shows the change in the pressure wave for the various lateral volumes. The lateral volume affects the peak pressure and pressure rise rate only slightly. It should be noted that the dynamic nature of the flow has been excluded from the simplified static model.

Effect of a bag volume. Figure 4.8 shows the change in pressure wave for various bag volumes. The bag volume will affect the pressure rise rate. Theoretically, the pulse pressure rise rate increases proportionally as the bag volume decreases.

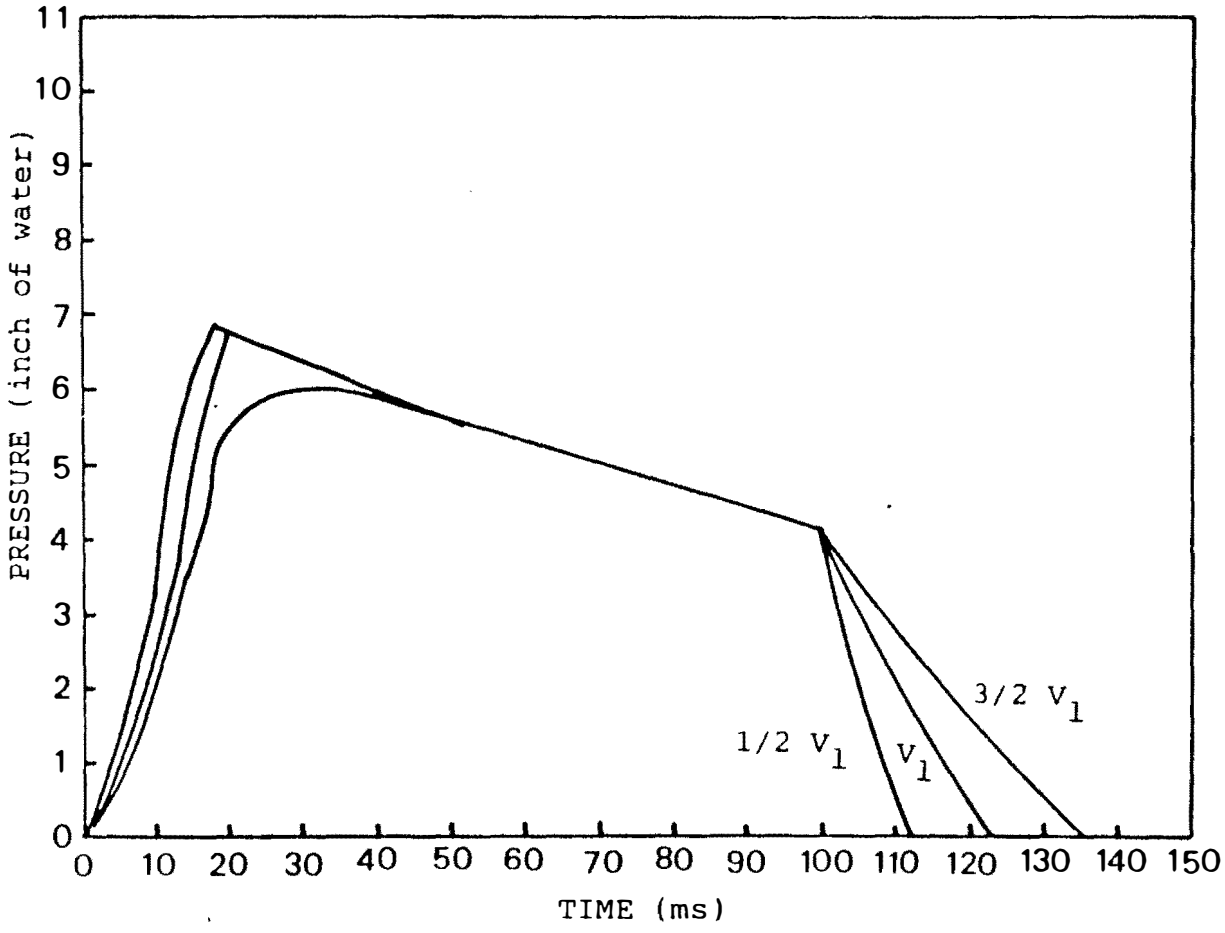

Figure 4.7. The pressure developed inside the bag with time for various lateral pipe volumes.

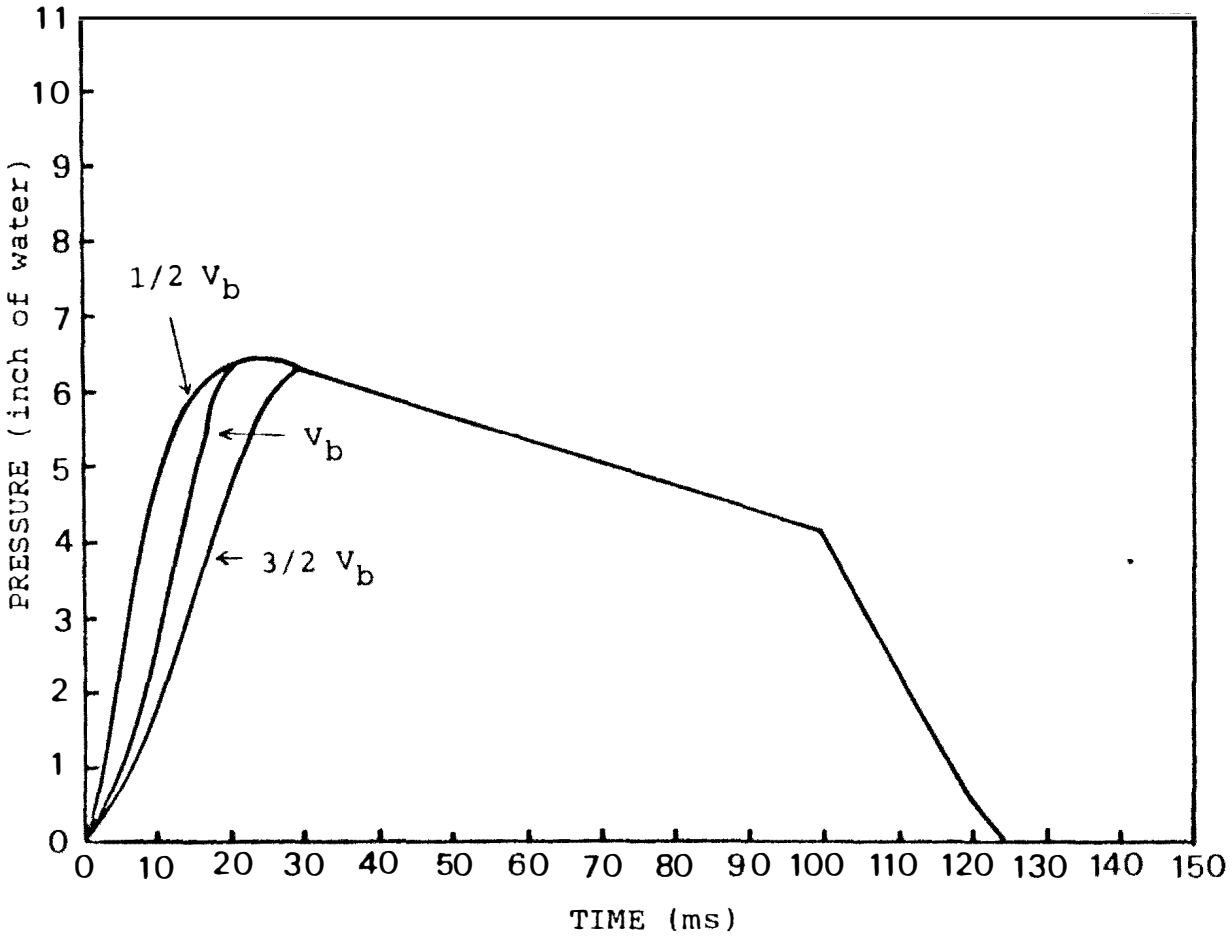

Figure 4.8. The pressure developed inside the bag with time for various bag volumes.

Effect of an orifice diameter. Figure 4.9 shows the change in pressure wave for the various orifice diameter. The orifice diameter affects the maximum pressure and pressure rise rate. Theoretically, if the orifice diameter becomes larger, the momentum of the air jet and the mass of air injected will increase. Consequently, the peak pressure and the pressure rise rate will increase.

Effect of a valve opening time. Figure 4.10 shows The change in the pressure wave for the various valve opening times. The pressure waves are essentially the same except for duration. The pulse duration should be long enough to avoid significant dust redeposition since the area under the pressure curve is related to the volume of reverse air flow through the bag.

Also, the relationship between actual valve opening time and electrical time setting was investigated. Figure 4.11 shows the actual valve opening time versus the electrical valve opening time setting. The mechanical response time appears to be 40ms. The actual duration of valve opening time is about 80ms longer than the electrical time setting in the range tested. Therefore, it should be noted that the proportion of electrical time differs from actual proportion of valve opening time. For example, when the electrical time setting is increased two times (50ms to

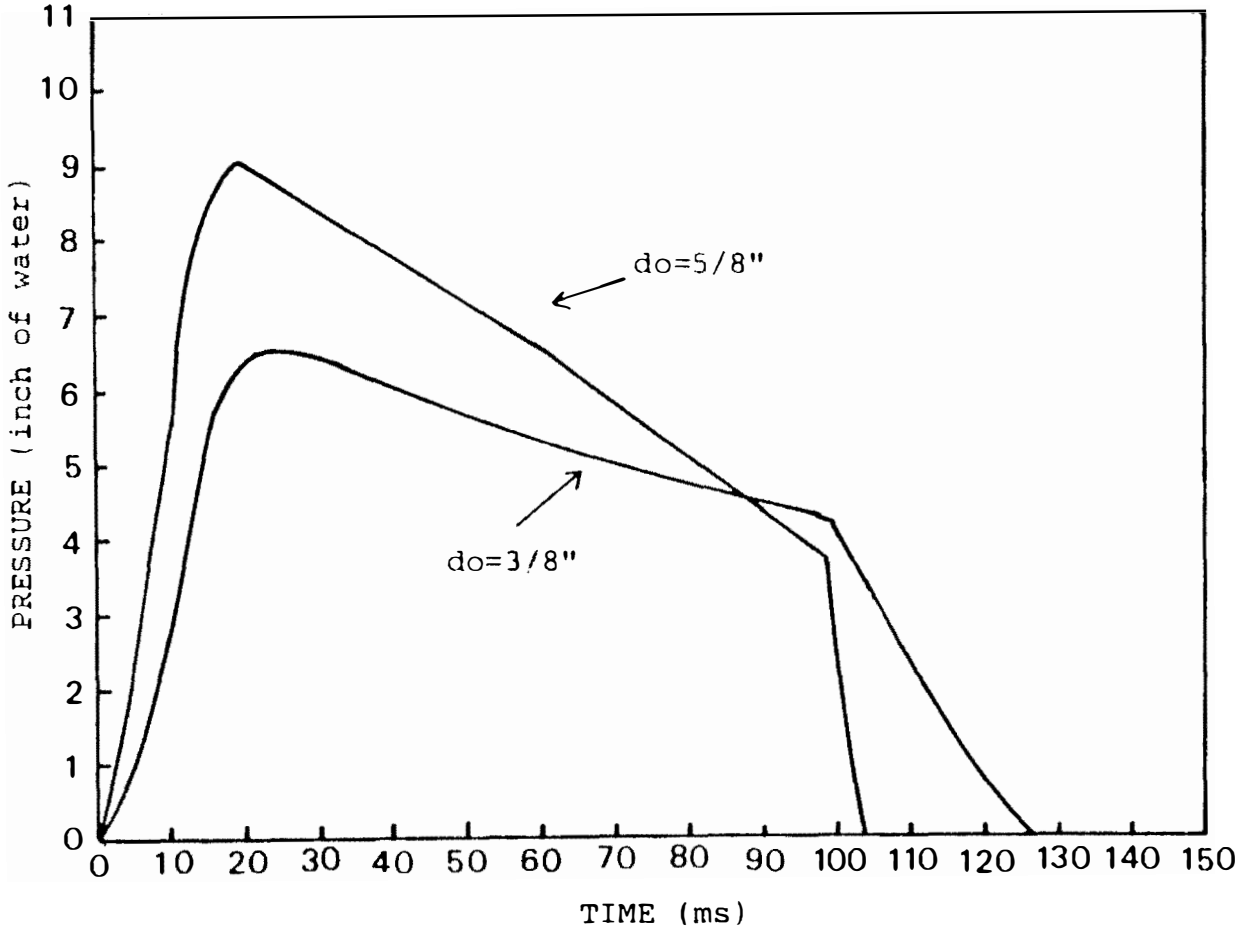

Figure 4.9. The pressure developed inside the bag with time for various orifice diameters.

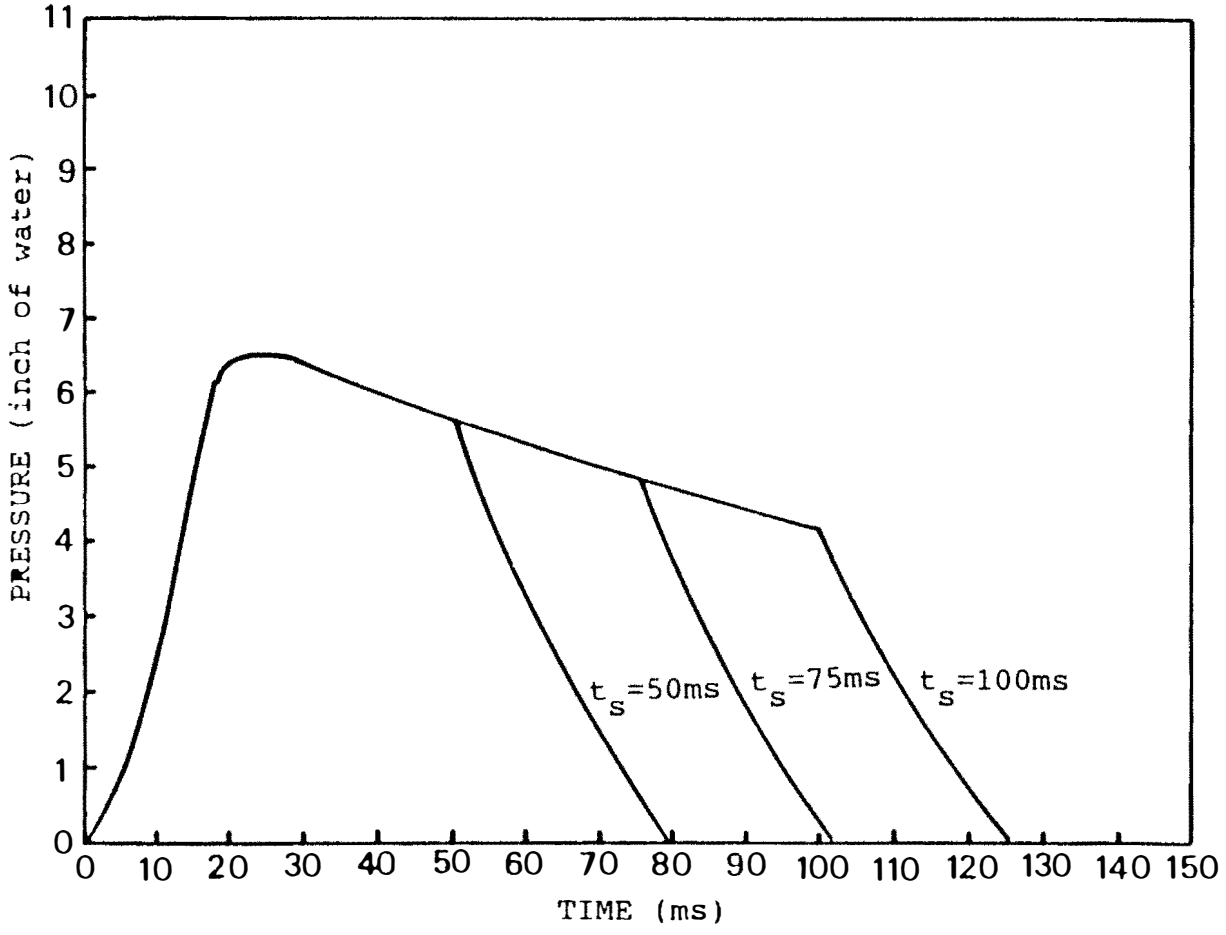

Figure 4.10. The pressure developed inside the bag with time for various valve opening times.

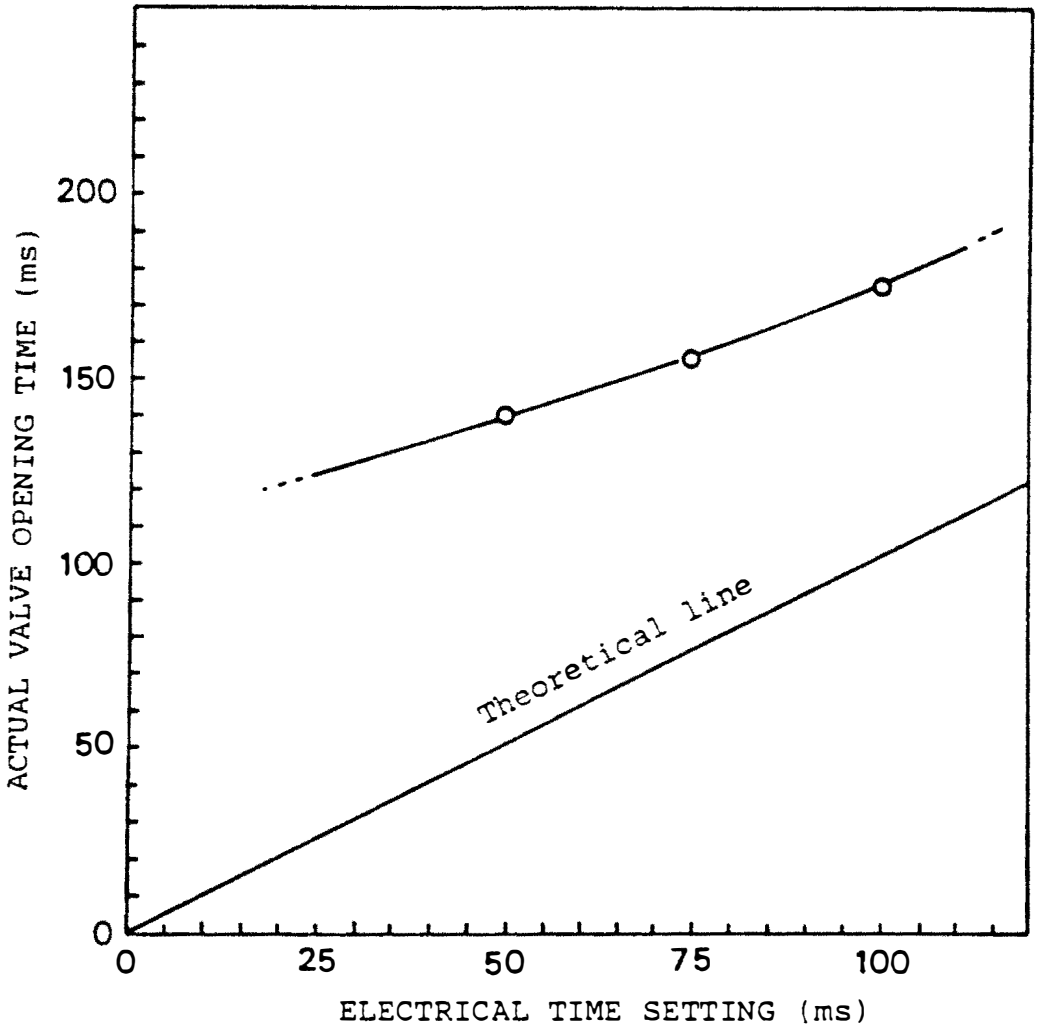

Figure 4.11. The electrical time setting versus actual valve opening time.

100ms), the actual opening time increases only 25% (140ms to 175 ms)

Effect of reservoir pressure. Reservoir pressure is a point of major interest from the view of the energy consumption of the system. Figure 4.12 shows the change in pressure for reservoir pressure. The magnitude of the pressure wave and the initial pressure rise rate become proportionally smaller as the reservoir pressure decreases.

C. Dynamic Model

Development of the Dynamic Model

The development of the Dynamic Model can be divided into five sections:

(a) Determination of the pulse pressure in the lateral
(b) Determination of the velocity of the air jet
(c) Determination of the pulse pressure generated by the injected air
(d) Determination of the pulse pressure dissipating along the bag
(e) Determinationof the pulse pressure reflected at the bottom of the bag

Determination of the pulse pressure in the lateral. Determination of the pulse pressure in the lateral was accomplished by introducing a set of analytical equations

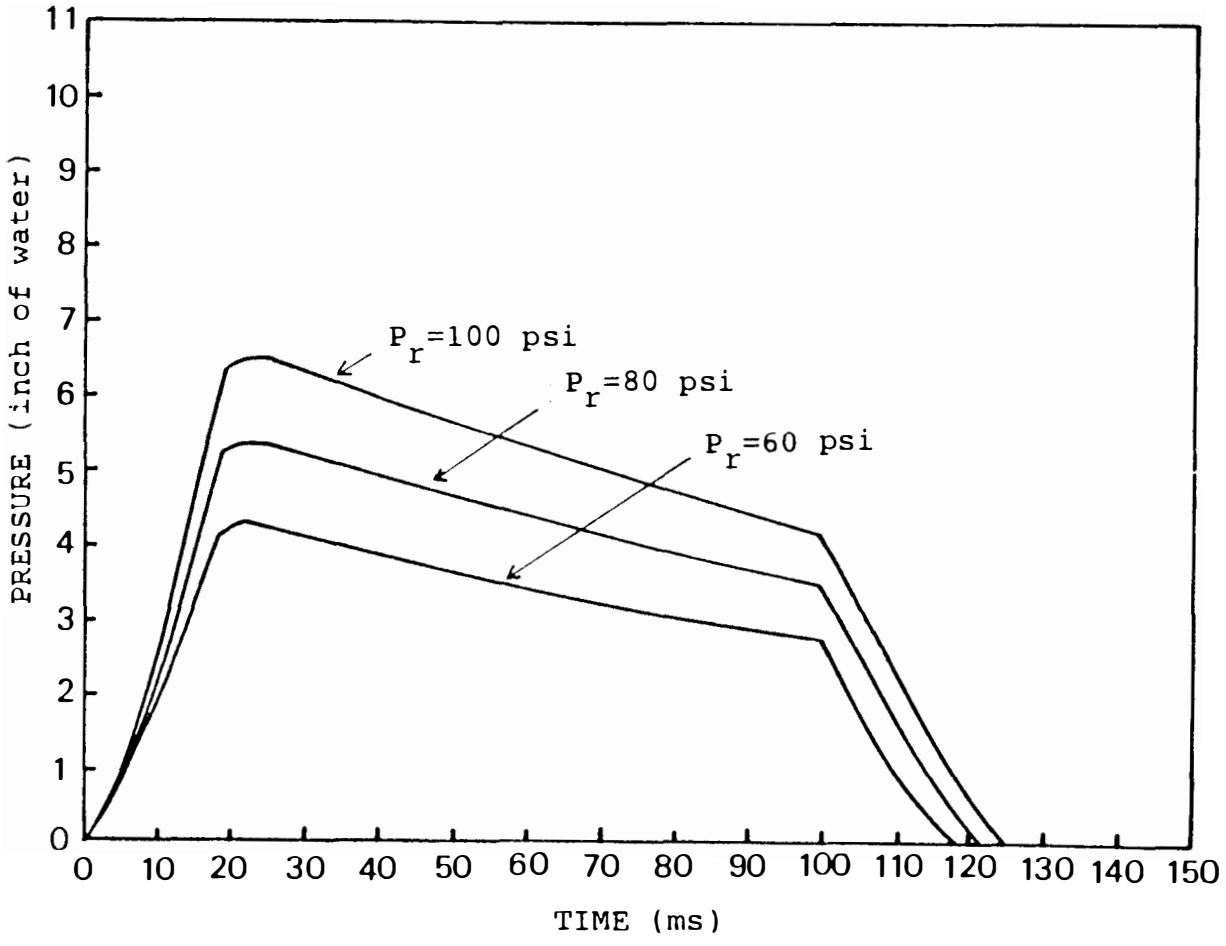

Figure 4.12. Pulse pressure versus time for various reservoir pressures.

derived for a shock tube. It was considered that the reservoir/lateral can be treated as a shock tube in which high-speed transient flows are generated by the rupture or rapid opening of the diaphram separating a gas at high pressure from a gas at low pressure.

Figures 4.13 (a), (b), (c), and (d) show the system of reservoir/lateral, the flow field at time t_1 after opening of the valve, pressure distribution at time t_1, and the wave pattern in a physical plane(xt plane), respectively.

The reservoir is filled with a high pressure gas and the lateral pipe is filled with low pressure gas. When the valve is opened, a right-facing shock wave travels into the low pressure gas and a left-facing expansion wave propagates into the high pressure gas. The wave pattern consists of a shock wave moving into the low pressure gas, a contact surface, and a centered expansion wave moving into the high pressure gas.

As shown in the physical plane (Figure 4.13 (d)), it is a very complicated task to predict the pressure in the lateral with time because the pressure wave pattern becomes complex after the pressure wave is reflected at the closed-end of the lateral creating non-simple flow regions. Here, the pressure of interest is the peak pressure developed in the lateral since this peak pressure creates the maximum pressure in the bag which is one of the major factors associated with dust dislodgement. In the lateral, the

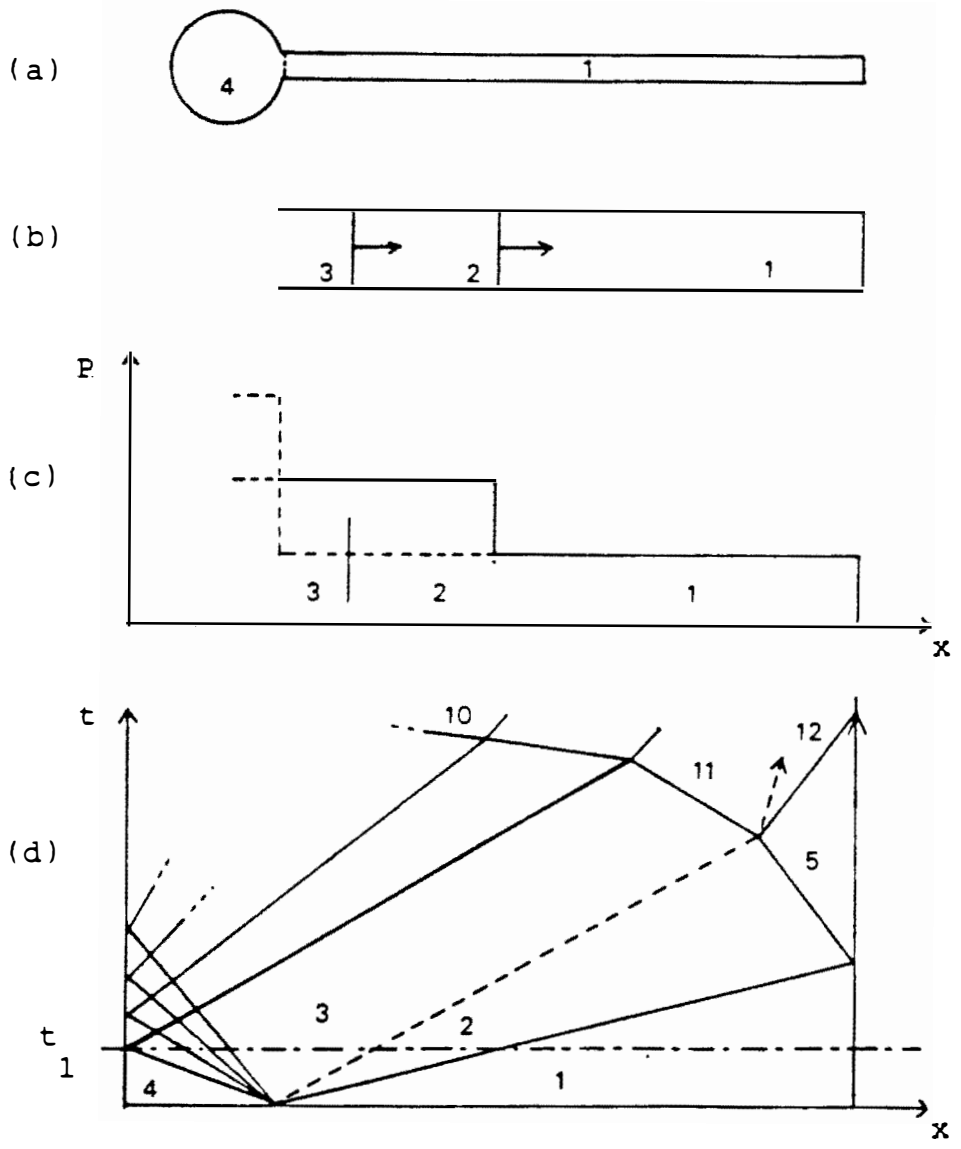

Figure 4.13. The system of reservoir/lateral pipe
(a) System of reservoir/lateral-pipe
(b) Flow field at time t after opening of the valve
(c) Pressure distribution at time t
(d) Wave pattern in the physical plane

first peak pressure is observed when the incident pressure (regions 2 and 3) traveling toward the closed-end arrives at the point of observation and the second peak pressure is observed when the reflected pressure traveling toward the reservoir arrives at the point of observation. It is assumed that the reflected expansion wave is very weak and flow properties of the flow regions 10, 11, and 12 can be approximated by the flow properties of region 5. Hence, the flow properties that must be required to predict the pressure in the lateral are the flow properties of the flow regions 2, 3, and 5.

Owczarek(1964) derived the set of equations that determine the property of region 2, 3, and 5 based on the initial condition of regions 1 and 4. The derivation of the equations is conducted in Fundamentals of Gas Dynamics (1964). Table 4.4 is a summary of the equations for prediction of the peak pressure in the lateral pipe. It was assumed that the friction of the wall in the lateral and the loss of mass through the holes in the lateral are neglegible. Effects of these assumptions on the prediction have been evaluated in a later section.

Determination of the velocity of the air jet. The principle of conservation of mass is applied between the orifice and the entry of the bag (see Figure below).

Table 4.4. Summary of the equations for the dynamic model.

$$\frac{P_2}{P_1} = 1 + \frac{1}{2}\left(\frac{a_4}{a_1}\right)^2\left(\frac{\kappa_1 M_3}{\psi}\right)^2 \times \left\{\left(\frac{\kappa_1 + 1}{2\kappa_1}\right) + \left[\left(\frac{\kappa_1 + 1}{2\kappa_1}\right)^2 + 4\left(\frac{a_1}{a_4}\right)^2\left(\frac{\psi}{\kappa_1 M_3}\right)^2\right]^{1/2}\right\} \qquad (2\text{-}27)$$

$$\frac{P_4}{P_1} = \left(\frac{P_2}{P_1}\right)\psi^{2\kappa_4/(\kappa_4-1)} \qquad (2\text{-}29)$$

$$M_2^2 = \frac{2}{\kappa_1(\kappa_1 - 1)}\left[\frac{\frac{P_2}{P_1} + \frac{P_1}{P_2} - 2}{\frac{\kappa_1 + 1}{\kappa_1 - 1} + \frac{P_2}{P_1}}\right] \qquad (2\text{-}31)$$

$$\frac{P_5}{P_2} = \frac{\left(\frac{3\kappa - 1}{\kappa + 1}\right)\frac{P_2}{P_1} - \frac{\kappa - 1}{\kappa + 1}}{\left(\frac{\kappa - 1}{\kappa + 1}\right)\frac{P_2}{P_1} + 1} \qquad (A\text{-}82)$$

where:

$$\psi = 1 + (\kappa_4 - 1)M_3/2$$

$$\left(\frac{a_4}{a_1}\right)^2 = \left(\frac{\kappa_4 R_4 T_4}{\kappa_1 R_1 T_1}\right)$$

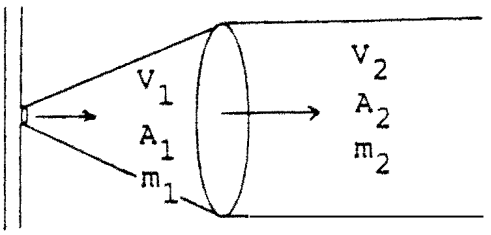

It is assumed that the jet flow is fully developed and that the cross sectional area of the jet coincides with that of the bag. The velocity of the air at the entry of the bag can be calculated as follows:

Mass balance equation is written as

$$m_1 = m_2 \qquad (4\text{-}12)$$

where:

$$m = \rho \frac{\pi D^2}{4} V \qquad (4\text{-}13)$$

$$P = \rho R T \qquad (4\text{-}14)$$

Substituting (4-13) and (4-14) into (4-12) and simplifying

$$V_2 = \frac{P_1}{P_2} \frac{T_2}{T_1} \left(\frac{D_1}{D_2} \right)^2 V_1 \qquad (4\text{-}15)$$

where the velocity of the air jet from the orifice is calculated by the following equation discussed in a previous section:

$$V_1 = M_o \sqrt{\kappa g_c R T_o}$$

where:

$$T_o = T_1/\left(1 + \frac{\gamma-1}{2} M_o^2 \right)$$

if $P_a/P_1 < 0.528$ then

$$P_o = 0.528\ P_1$$

$$M_o = 1$$

if $P_a/P_1 > 0.528$ then

$$P_o = P_1$$

$$M_o = \left[\frac{2}{\gamma - 1} \left\{ \left(\frac{P_a}{P_1} \right)^{-(\gamma-1)/\gamma} - 1 \right\} \right]^{1/2}$$

Determination of the pulse pressure generated by the injected air. Because air mass is forced into the bag, the air at rest in the top of the bag must accelerate to the velocity of the air jet. Consequently, the shock wave travels ahead of the air jet and pulse pressure is developed behind the shock wave. The pressure developed by the injected air can be obtained by applying the principle of a mass balance across the shock wave as discussed in Chapter II.

The velocity difference across a moving shock wave in terms of the speed of propagation of the wave can be obtained as follows (see Chapter II):

$$\frac{u_2 - u_1}{a_1} = \frac{2}{\gamma+1} \left(\frac{U}{a_1} - \frac{a_1}{U} \right) \qquad (2\text{-}20)$$

Since the velocity, u_1, of the air mass in front of the shock wave is zero, then:

$$\frac{u_2}{a_1} = \frac{2}{\kappa + 1}\left(\frac{U}{a_1} - \frac{a_1}{U}\right) \qquad (4\text{-}16)$$

Also, the pressure ratio across a moving wave can be written as follows.

$$\frac{P_2}{P_1} = 1 + \frac{2\kappa}{\kappa + 1}\left[\left(\frac{U}{a_1}\right)^2 - 1\right] \qquad (2\text{-}21)$$

Since u_2 can be obtained empirically or theoretically, the incident pressure developed at the top of the bag can be obtained from equation (4-16) and (2-21).

Determination of the pulse pressure dissipating along the bag. The type of flow phenomena created by the air jet can be considered unsteady one dimensional flow. The governing equations are developed in Gas Dynamics (1977) and are summarized here:

Continuity equation:

$$\rho_t + u\rho_t + \rho u_x = E \qquad (2\text{-}17)$$

Momentum equation:

$$\rho u_t + \rho u u_x + P_x = \beta \qquad (2\text{-}18)$$

Energy equation:

$$P_t + uP_x - a^2(\rho_t + u\rho_x) = \psi \qquad (2\text{-}19)$$

where:

$$E = \frac{1}{A}\frac{d\dot{m}}{dx}$$

$$\beta = -\left[\frac{\rho u^2}{2}\frac{4f}{D} + \rho u^2(1-y)\frac{d\dot{m}}{dx\,\dot{m}}\right]$$

$$\psi = (1-r)(dH_i + u\beta)$$

According to the experimental results to be discussed later, the loss of mass as the flow permeates through the bag plays the major role, while pressure loss due to friction along the bag contributes little to the pulse dissipation. Also, it can be assumed that the pulse is traveling at a constant velocity in the bag. Further it is assumed that the entropy of the flow element is constant. In light of the above statement, the equation has been examined. Since the velocity of the flow is constant, the equations become linear equations and the solution of the equations are additive. Therefore, those factors involved in the equations are evaluated individually and summed up later. Assumptions introduced in the course of the model development have been evaluated in a later section. The following is a discussion of the dominant factors in the equations.

(a) Loss of mass due to diffusion

The term of loss of mass in the equation is written as follows:

$$E = \frac{\dot{dm}}{A\ dx} \qquad (4\text{-}17)$$

where:

A = area of cross section

dx = unit length in flow direction

$\dot{dm}$ = mass flow rate

The flow through a porous medium obeys the Hagen-Poiseuille Law (Barrer, 1941) since the pore diameter is very small(pore size of 50-100 um) and the Reynold's number is less than 10 (Handbook of fabric filter technology, volume I, 1970). Therefore, the equation of flow for a compressible gas in a porous system (Barrer, 1941) can be written as:

$$\frac{VP}{t} = A_p\ P_g\ \frac{P_1 + P_2}{2}\ (P_1 - P_2) \qquad (4\text{-}18)$$

where:

A_p = the cross-sectional area of a pore

V = the volume measured at a pressure p

P_1, P_2 = the pressure of high and low pressure gases, respectively

t = the duration of measurement

P_g = the permeability of medium

This equation is known as Darcy's Law.

Since P_1 is the bag pressure (P_b), P_2 is atmospheric pressure, and the area is the bag surface area ($ds=\pi Ddx$), the equation can be rewritten as follows:

$$\frac{V}{t} = ds \cdot P_g \cdot \frac{P_b + P_a}{2P_a} (P_b - P_a) \qquad (4\text{-}19)$$

In terms of mass flow, the equation is written as:

$$dm = \frac{V}{t} \rho_a = ds\ P_g \frac{P_b + P_a}{2Pa} \rho_a (P_b - P_a) \qquad (4\text{-}20)$$

Substituting equation (4-20) to (4-17) and simplified to:

$$E = \frac{4}{D} P_g \frac{P_b + P_a}{2P_a} \rho_a (P_b - P_a) \qquad (4\text{-}21)$$

(b) Friction loss and momentum loss

The term of friction loss and momentum loss due to loss of mass in the equation is rewritten as follows:

$$\beta = - \left[\frac{\rho u^2}{2} \frac{4f}{D} dx + \rho u^2 (1-y) \frac{d\dot{m}}{dx\ \dot{m}} \right] \qquad (4\text{-}22)$$

The first term is a friction loss:

$$\beta_1 = - \frac{\rho u^2}{2} \frac{4f}{D} \qquad (4\text{-}23)$$

The second term is a loss of momentum caused by the loss of mass:

$$B_2 = -\rho u^2 (1-y) \frac{d\dot{m}}{dx\ \dot{m}} \quad] \tag{4-24}$$

Since $y=0$, $\dot{m}=puA$, B_2 can be rewritten as:

$$B_2 = \rho\ u^2 \frac{dm}{dx\ \rho uA} = u \frac{dm}{dx\ A} = u\ E \tag{4-25}$$

The above discussion can be summarized as follows:

1) the pressure drop due to loss of mass:

$$E = \frac{4}{D} P_g \frac{P_b + P_a}{2P_a} \rho_a (P_b - P_a) \tag{4-26}$$

2) the pressure drop due to momentum loss which is caused by the loss of mass:

$$B_2 = uE \tag{4-27}$$

3) the pressure loss due to friction of the bag wall is

$$B_1 = \frac{\rho u^2}{2} \frac{4f}{D} dx \tag{4-28}$$

4) the total pressure loss in unit length (dx) and unit time (dt)

$$dp = [\ E\ dt\ R\ T\ ] + [\frac{\rho u^2}{2} \frac{4f}{D} dx] + [u\ E\ dt] \tag{4-29}$$

Determination of the pulse pressure reflected at the bottom of the bag. The pulse of incident pressure travels along the bag while the pulse is losing its mass through the

bag surface. At the bottom of the bag, the incident pressure is reflected and travels back toward the entrance of the bag. The magnitude of the reflected pressure is calculated by Equation (2-20). The equation is written as follows:

$$\frac{P_5 - P_1}{P_2 - P_1} = 1 + \frac{\frac{2\kappa}{\kappa - 1}}{\frac{\kappa + 1}{\kappa - 1}\frac{P_1}{P_2} + 1} \qquad (2\text{-}20)$$

Development of a Computer Program

The equations developed in each section were integrated into a systematic modeling program for the prediction of the pulse pressure in the pulse jet fabric filter. Figure 4.14 illustrates the general procedure of the program development.

The first step of the program is the input data preparation. In this step the input values required by the program are established. The input parameters include configuration and operating parameters. The configuration parameters consist of the diameter of the orifice, the lateral/bag spacing, the diameter of the bag, the friction coeffiient of the bag and the permeability of the bag. The operating parameters are the reservoir and lateral

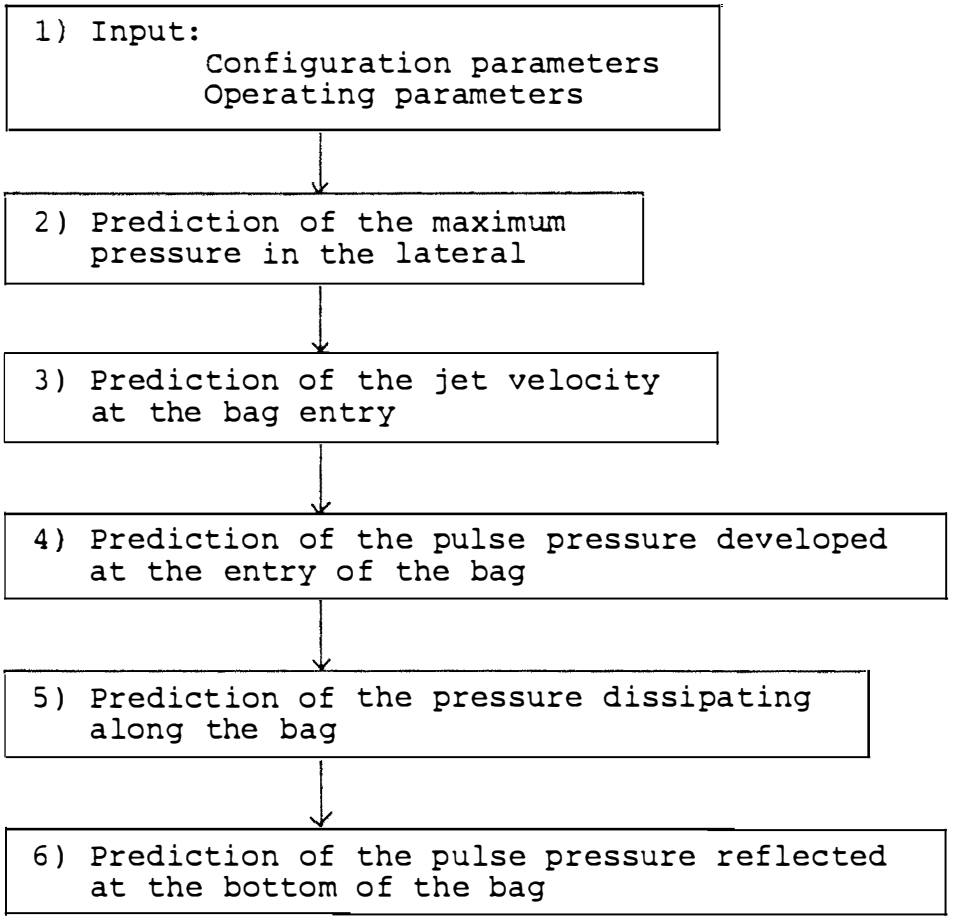

Figure 4.14. Procedure of the program development for the dynamic model.

pressures and temperatures. Input parameters are summarized in Figure 4.15(a).

The second step of the program predicts the maximum pressure in the lateral. The maximum pressure developed in the lateral can be obtained by the simultaneous solution of Equations (2-27) and (2-29). Due to the nonlinear nature of these equations, the solution must be accomplished by an iterative procedure where an initial value for M3 is assumed. The terms P_2/P_1 and P_4/P_1 are determined from equations (2-27) and (2-29), respectively. The procedure is repeated until the specified value of P_4/P_1 is obtained. Figure 4.15(b) shows a detailed flow diagram of the program step. Input parameters required for this step are the initial reservoir and lateral pressures. Output parameters for this step are the initial incident and the reflected pressure. The reflected pressure is the maximum pressure developed in the lateral.

The third step is the prediction of the jet velocity at the entry of the bag. Inputs to the model are the lateral pressure, and the orifice and the bag diameters. The output parameter is the jet velocity at the entry of the bag. The detailed flow diagram is shown in Figure 4.15(c).

The fourth step is the prediction of the pulse pressure developed at the entry of the bag. The input to the module is the air jet velocity and the output from the module is

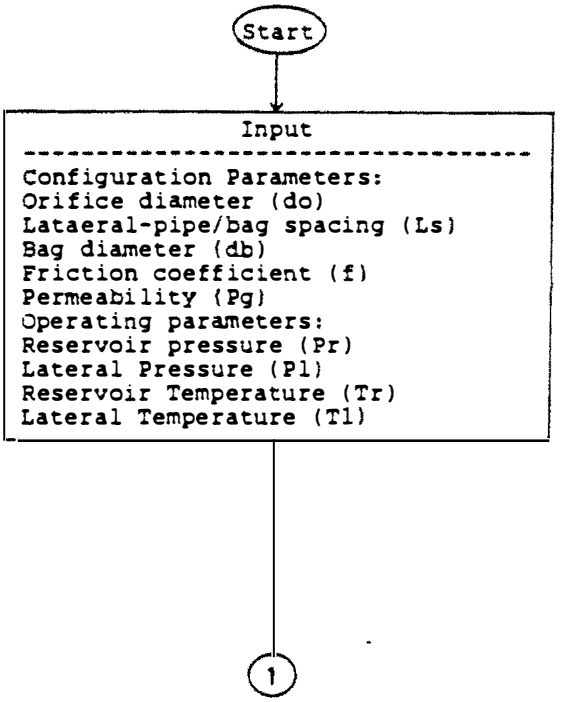

(a)

Figure 4.15. Flow diagram of the calculation procedure for the dynamic model.

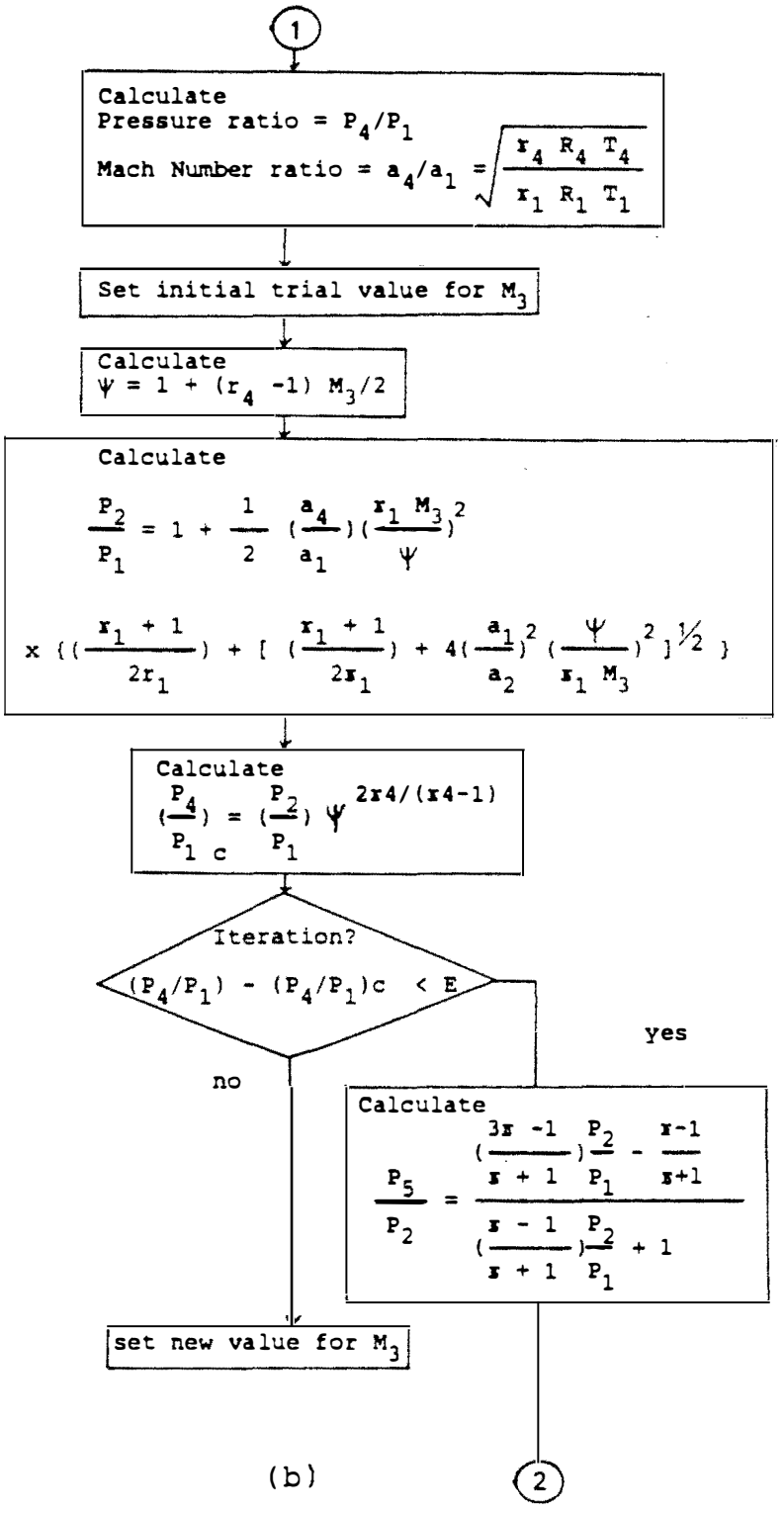

Figure 4.15. (Continued)

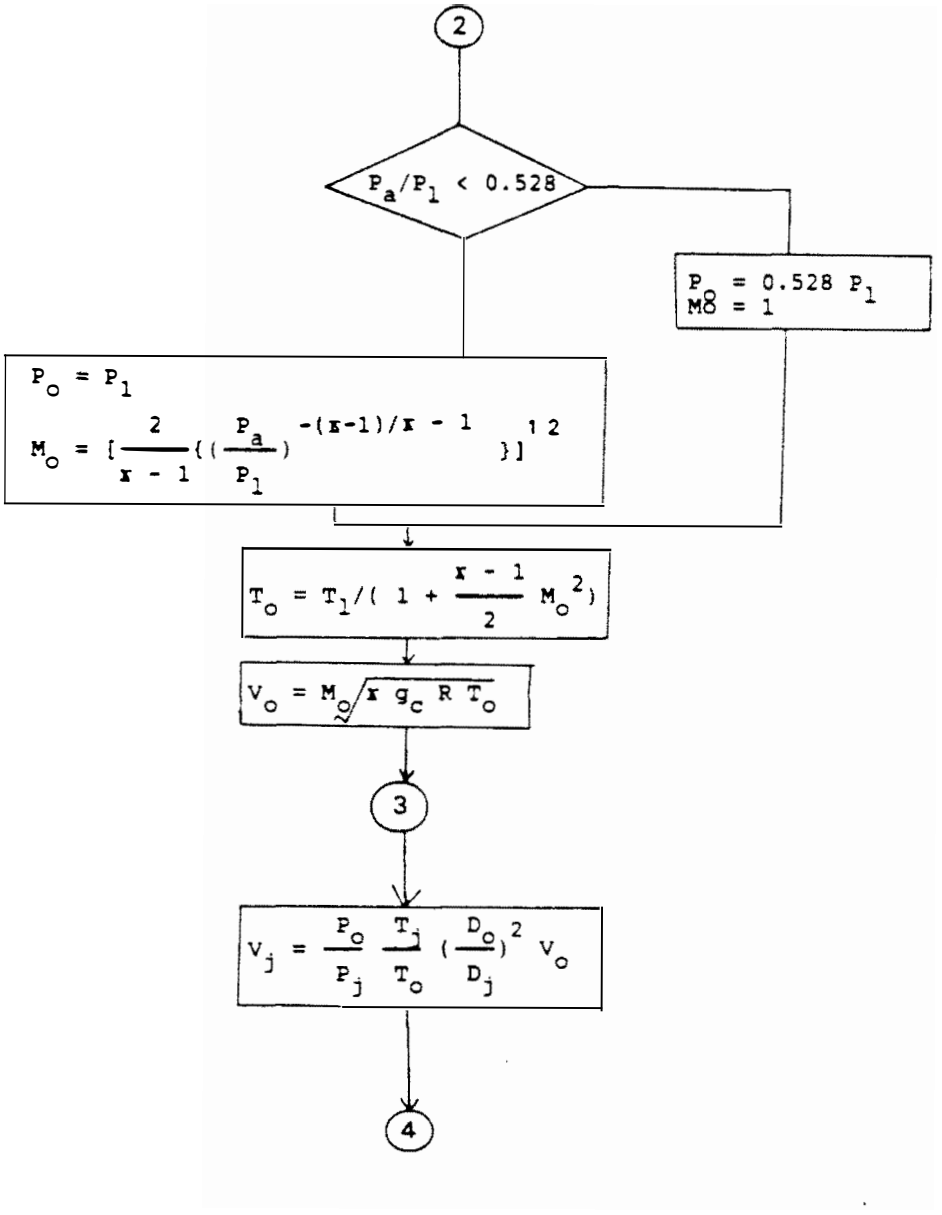

(c)

Figure 4.15. (Continued)

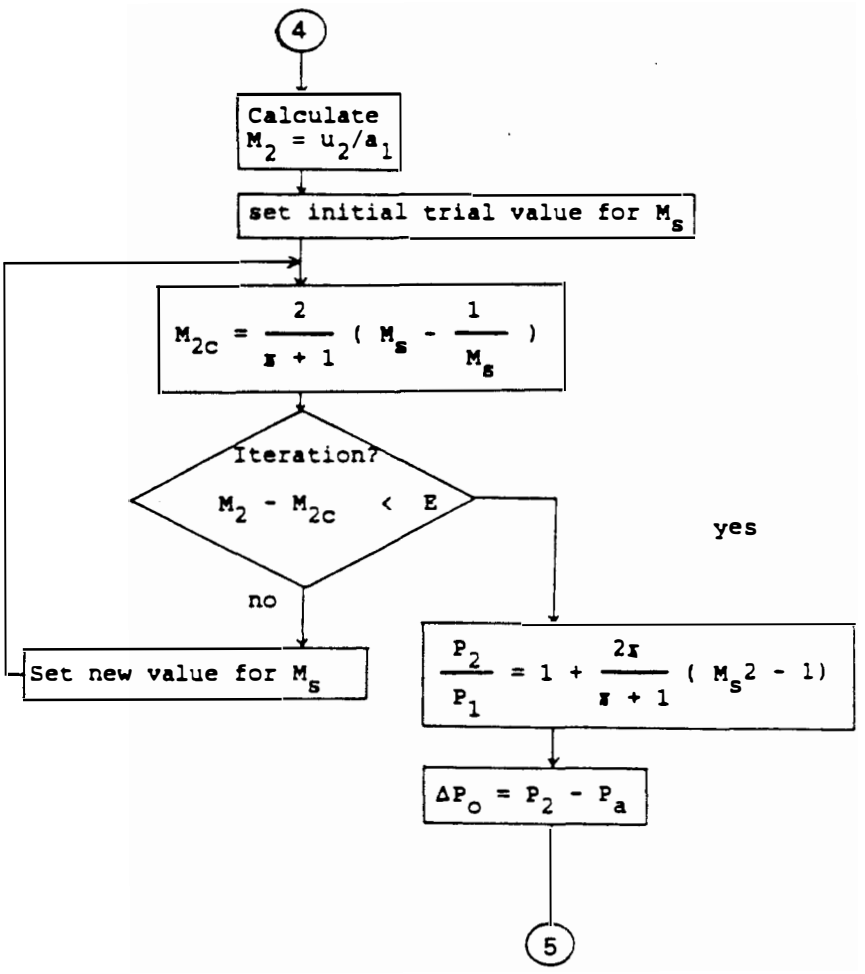

(d)

Figure 4.15. (Continued)

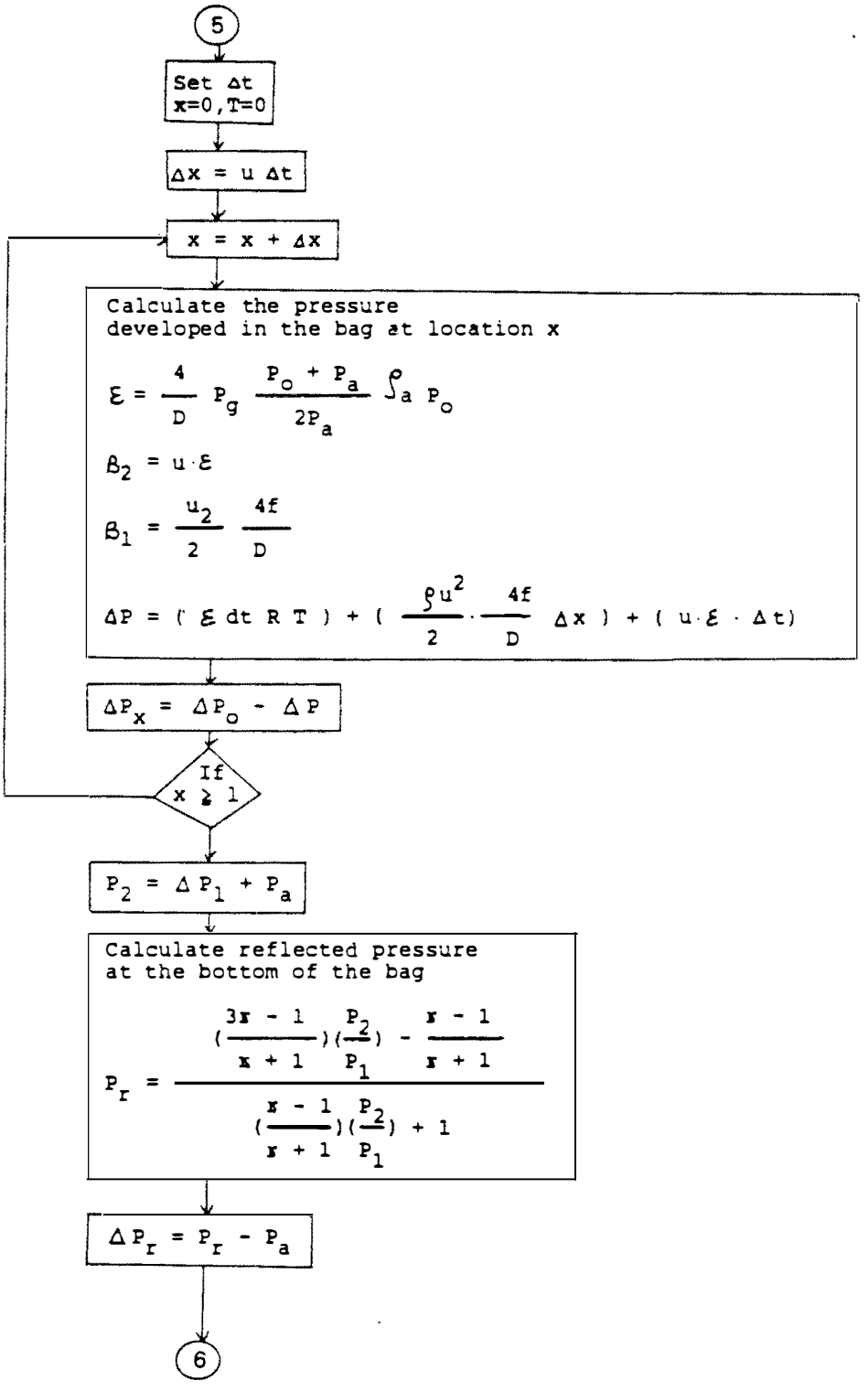

(e)

Figure 4.15. (Continued)

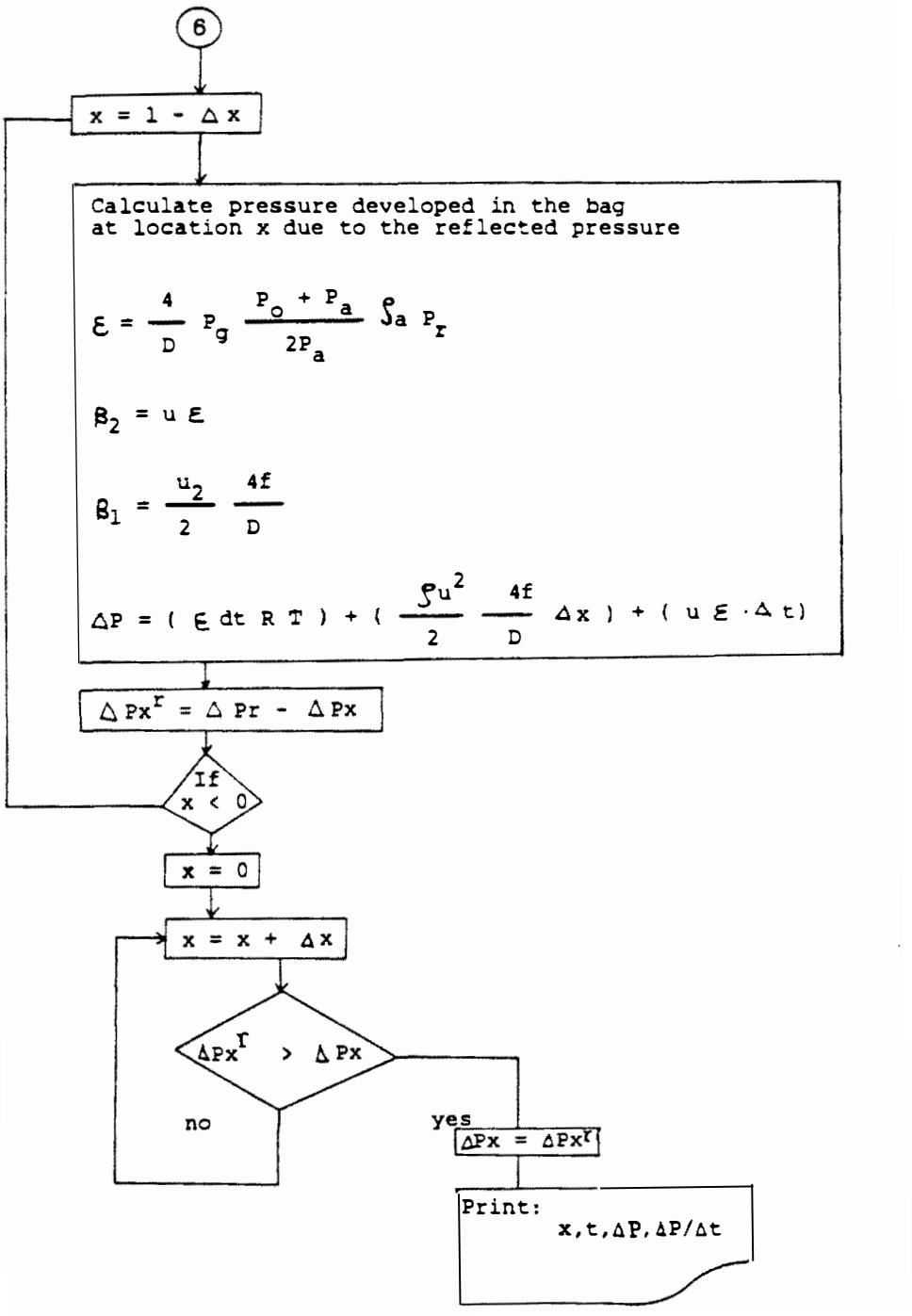

(f)

Figure 5.15. (Continued)

the pressure developed by the injected air jet. The detailed flow diagram is shown in Figure 4.15(d).

The fifth step of the program is the prediction of the pulse pressure dissipating along the bag. A stepwise solution method was applied to the equations. Inputs to the module are the maximum pressure developed at the entry of the bag, the friction coefficient, and the permeability of the bag. Output from the module is the pulse pressure exerted at location x along the bag. The detailed flow diagram is shown in Figure 4.15(e).

The last step of the program is the prediction of the pulse pressure reflected at the bottom of the bag. Input to the module is the pulse pressure at the bottom of the bag. The magnitude of the reflected pressure at location x is compared with the magnitude of the incident pressure at location x and the larger value is registered as the maximum pressure exerted at that location. The detailed flow diagram is shown in Figure 4.15(f).

Application of the Model and Comparison with the Experimental Results

Model Inputs. The model is applied to a pulse-jet fabric filter configuration commonly used in utility industries. The configuration and dimensions of the system are shown in Chapter III.

Three values of reservoir pressures (100, 80 and 60 psig), three locations of the bag (bag #1, #2 and #3 are located 17, 64 and 110 inches from the reservoir respectively) and two types of bag-entry configurations (type 1: without venturi, type 2: with venturi) are considered, with comparisons to experimental results. In this example, the prediction of the reflected pressure at the end of the bag was not conducted.

Table 4.5 shows the required input to the model. The temperature and the pressure are considered to be constant throughout the pulsing process and are assumed to be 70 F and 14.7 psi respectively.

Empirical Correction Factors Applied to the Dynamic Model

Empirical correction factors. The theoretical dynamic model developed in the previous section does not consider the energy losses inherent in this type of system. Development of a theoretical approach to estimate the energy losses is very complex. Therefore, empirical correction factors are introduced into the model. The model with empirical correction factors is refered to herein as the Adjusted Dynamic Model (ADM). The empirical correction factors incorporated in the dynamic model are: 1) the friction coefficient in the lateral, 2) the pressure loss factor at the entrance of the bag, and 3) the permeability of the bag. The data have been collected to determine these

Table 4.5. Required input to the model.

Design Parameters:
Orifice diameter, d_o (inches)
Lateral/Bag spacing, l (inches)
Diameter of the bag, d_b (inches)
Friction coefficient, f
Permeability of the bag, P_g (ft/sec/in w.g)
Operating Parameters:
Reservoir pressure, P_r (psi)
Lateral prssure, P_l (psi)
Reservoir Temperature, T_r ($^\circ$R)
Lateral Temperature, T_l ($^\circ$R)

factors. The discussion of the empirical correction factors is conducted below.

Friction coefficient of the lateral. The friction coefficients were estimated by (1) the von Karman-Nikurade formula and (2) by experiment. The velocity and the density of air in the lateral which are required to determine the Reynolds number and the pressure drop along the lateral are estimated according to Equations (2-27) and (2-31) developed for a shock tube.

(1) The von Karman-Nikurade formula (Owczarek, 1964) is written as:

$$\frac{1}{4f} = -0.8 + 2 \log_{10}(R_{eD}\sqrt{4f}) \qquad (4\text{-}30)$$

where:

$$R_{eD} = \frac{\rho V D}{\mu}$$

For the range of the reservoir pressures from 60 to 100 psi, the Reynold's number is calculated to be from 9.7×10^5 (u=584 ft/sec, ρ=0.143 lbm/ft) to 1.42×10^6 (u=714 ft/sec, ρ=0.36lbm/ft) and the friction coefficient was determined to be from f=0.0027 to 0.0029.

Table 4.6 shows the peak pressure observed in the lateral for the reservoir pressure of 60, 80 and 100psig. At 60 psig of reservoir pressure, an open-ended lateral pipe is used to observe the pressure at the end of the lateral

Table 4.6. Peak pressures observed in the lateral for reservoir pressures of 60, 80, and 100 psig.

tank pressure	P1 (17") peak 1st	P1 (17") peak 2nd	P2 (64") peak 1st	P2 (64") peak 2nd	P3 (110") single peak
a)100	22.4 (1.3)	45.44 (1.9)	-	-	56.0 (1.6)
b)100	22.7	49.3	13.3	45.3	53.3
a) 80	-	-	-	-	41.2 (1.6)
a) 60	-	-	-	-	30.7 (2.1)
b) 60	13.3	26.7	10.7	29.9	32.0
b)*60	13.1		10.7		12.8,6.7 double peak

Note: a) Data set A: multiple measurement (units: psig)
b) Data set B: single measurement
* open-end lateral
( ) standard deviation

pipe so that it was not affected by the closed end. Figure 4.16 is the graphical presentation of the table 4.6.

Based on the equation($\Delta P = (1/2)\, \rho \cdot u^2\, (4f/D) \cdot \Delta x$), the friction coefficients are calculated to be 0.0021 (100 psi for reflected pressure), 0.0024(60 psi for the refrected pressure), 0.00395 (60 psi for incident pressure), 0.00495 (60 psi for the incident pressure, open-ended lateral).

In the determination of the friction coefficients, the predicted velocity obtained from Equation (2-31) is used as mentioned previously. However, the average velocity of the air mass in the lateral pipe can also be determined by measuring the time lag between the first peak and the second peak of the pressure wave and the distance between the pressure port and the closed-end of the lateral. According to this method, the velocity of the air mass in the lateral pipe is calculated to be 804 ft/sec(measurement error = 10%) for both reservoir pressures (60 and 100psi). The velocity difference between the reservoir pressure of 60 and 100 psi was not recognized because of the limitation of accuracy in measurement technique. If this velocity (804 ft/sec) is used for determination of the friction coefficients, the friction coefficients are recalculated as follows ; 0.0016 (100 psi for the reflected pressure), 0.0013 (60 psi for the reflected pressure), 0.0021 (60 psi for incident pressure), and 0.0026 (60 psi for the incident pressure, the open-ended lateral pipe).

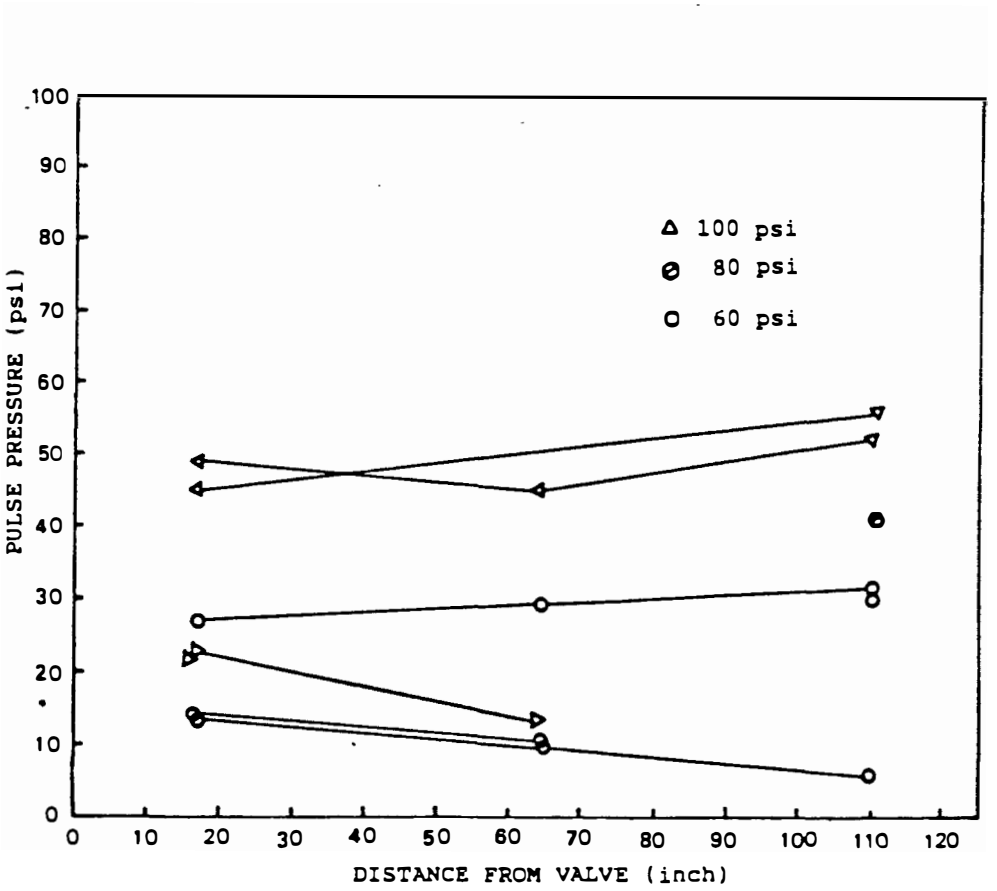

Figure 4.16. The pressure developed in the lateral pipe versus distance from the valve.

In summary, the friction coefficient ranges from 0.0013 to 0.005. The friction coefficient should be chosen depending on the property of the flow. Theoretically, the friction coefficient decreases as the velocity and the density of the air increase since the friction coefficient is a function of Reynold's number.

Permeability of the bag. The permeability of the fabrics is usually provided by the fabric manufacturers in terms of volume flow rate (CFM) at 0.5 inches of water pressure drop. The permeability of the typical fabric ranges between 15 cfm and 40 cfm (C.E. Billings et al., 1970). However, these values do not reflect the nature of unsteady flow, which is the case in this discussion. Therefore, the permeability was determined experimentally. The permeability for steady flow may be used by applying the correction factor for unsteady flow.

Figure 4.17 shows the normalized pulse pressure versus the location from the top of the bag for a clean bag. The pressures measured at various location along the bag are normalized by the pressure at port 1 (1.5 ft from the top of the bag). The equation for the pressure dissipating along the bag is written as:

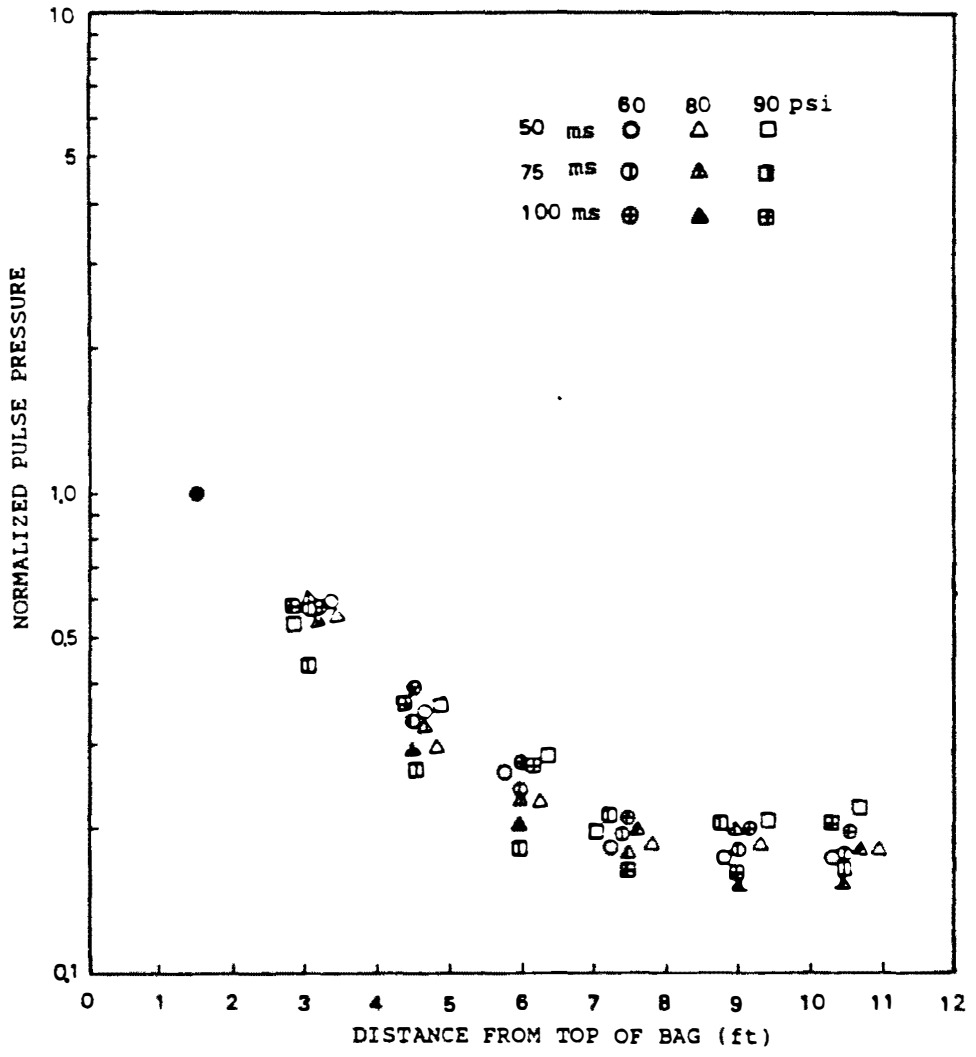

Figure 4.17. Normalized pulse pressure versus the distance from the top of the bag.

$$d(\Delta P) = \frac{4}{D} P_g \frac{P_b + P_a}{2P_a} \rho_a (P_b - P_a) R T \frac{dx}{u} + \frac{1}{2} \rho u^2 \frac{4f}{D} dx \quad (4\text{-}29)$$

The slope of the curve is a function of the friction of the bag surface(f), the velocity of the air mass(u), diameter of the bag (D), and the permeability of the bag(Pg). The pressure dissipation due to friction (2nd term of equation (4-29)) is considered to be very small compared to the pressure dissipation due to the permeation. Therefore the friction term was ignored. The average velocity for the 60, 80 and 100 psi is used for determination of permeability (P_g). It was assumed that the solenoid valve opening time and reservoir pressure did not affect the permeability of the bag. Since the pressure at the bottom of the bag is altered (increased) by the reflection at the bottom, the pressures observed at the bottom half of the bag were omitted from the analysis. Linear regression analysis was applied to the data and the permeability of the clean bag was determined to be Pg=0.0067 ft/sec/in w.g (slope=-0.26 1/ft, R=0.85 ,N=36).

The pressure loss factor at the entry of the bag. Two types of bag entrance configurations are considered: type 1: without venturi and type 2: with venturi. Figure 4.18 shows calculated versus measured maximum pressure developed in the bag. The measured value is substantially lower than

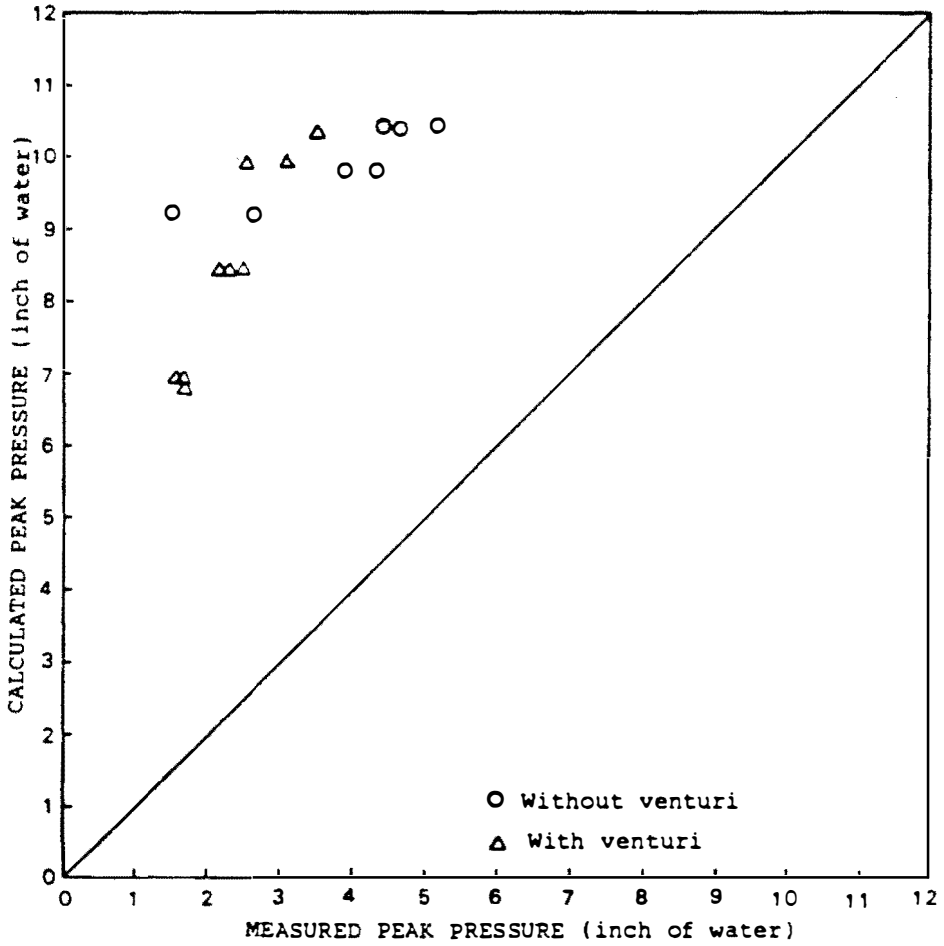

Figure 4.18. Calculated versus measured maximum pressure developed in the bag.

calculated value. There are two sources of error:(1) the measured pressure is not the maximum pressure developed in the bag. The measured location is at 1.5 ft from the top of the bag where the pressure has already begun to dissipate. On the other hand, the location of the calculated maximum pressure is 10" from the top of the bag. It should be noted that the spacing of orifice to top of the bag is fixed based on the jet diameter. (2) the pressure loss at the entry of the bag. The relationship between calculated and measured can be expressed as:

$$Pc=E1(Pm + E2) \qquad (4\text{-}31)$$

where:

E1= pressure loss coefficient at the entry of the bag

E2= pressure difference between the actual peak pressure and measured pressure

In order to eliminate the error term E2, The pressure at the calculated location is obtained by extrapolation of the experimental data. Figure 4.19 shows a corrected measured pressure versus calculated maximum pressure. Least Square Analysis is applied and loss factor E1 is determined to be 1.74 and 2.80 for the entry configuration type 1 and type 2 respectively. This indicates that there are 43 % and 64 % losses respectively for type 1 and 2.

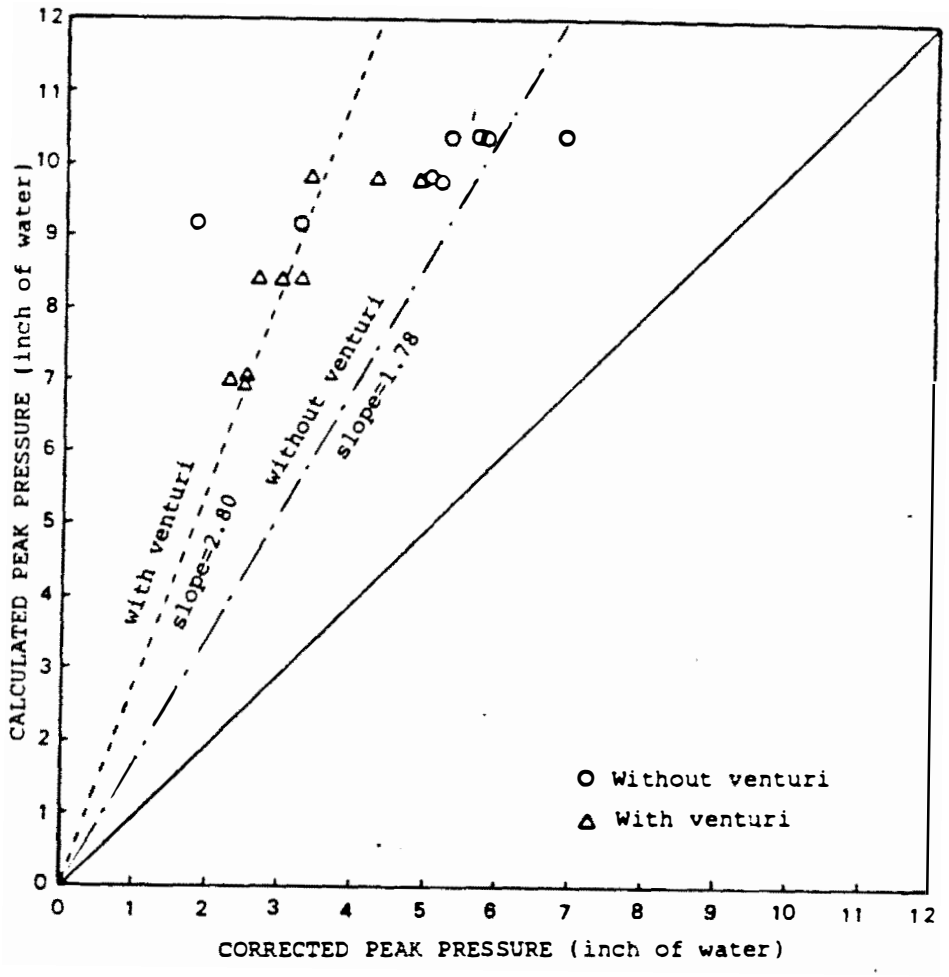

Figure 4.19. Calculated versus measured maximum pressure corrected for the peak location.

Discussions of the Results

Pressure developed in the lateral. The odel was applied for the three values of the reservoir ressure 100, 80, and 60 psig. The low pressure gas in the lateral is at atmospheric pressure.

Figure 4.20 (a) and (b) are typical pre sure traces observed near the inlet of the lateral pipe(.e. port #1) and the closed end of the lateral pipe(i.e. port #3).The location of the ports are shown in Figure 2. . As shown in Figure 4.20 (a), the pressure trace observed near the inlet of the lateral pipe peaks out in two steps. he first peak is incident pressure and the second peak is due to the reflected shock wave. In this pressure trac shown in Figure 4.20(a), the incident pressure was me sured to be 24 psig and the pressure behind the reflected s ock wave was measured to be 56 psig.

Figure 4.21 shows the observed inciden pressure (measured at port #1) and reflected pressur (measured at port #3) for three values of reservoir pres res (100, 80, and 60 psi). Theoretical curves for the inc ent pressure (the lowest curve among five curves) and re ected pressure without friction loss (the top curve) are a o shown in the figure.

The incident pressure (measured at por #1) agrees well with the theoretical curve since the measur location is

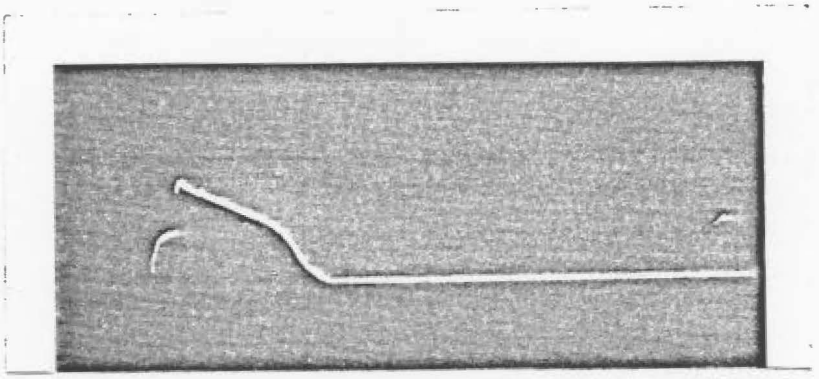

(a) Port #1

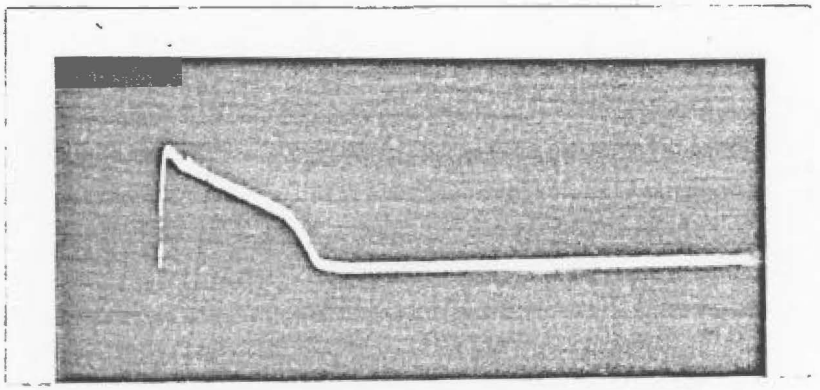

(b) port #3

Figure 4.20. Photograph of pressure traces at the lateral pipe.
(a) measured near the tank (i.e. port # 1)
(b) measured near the closed-end of the lateral pipe (P_r = 100 psi, t_s = 50 ms)

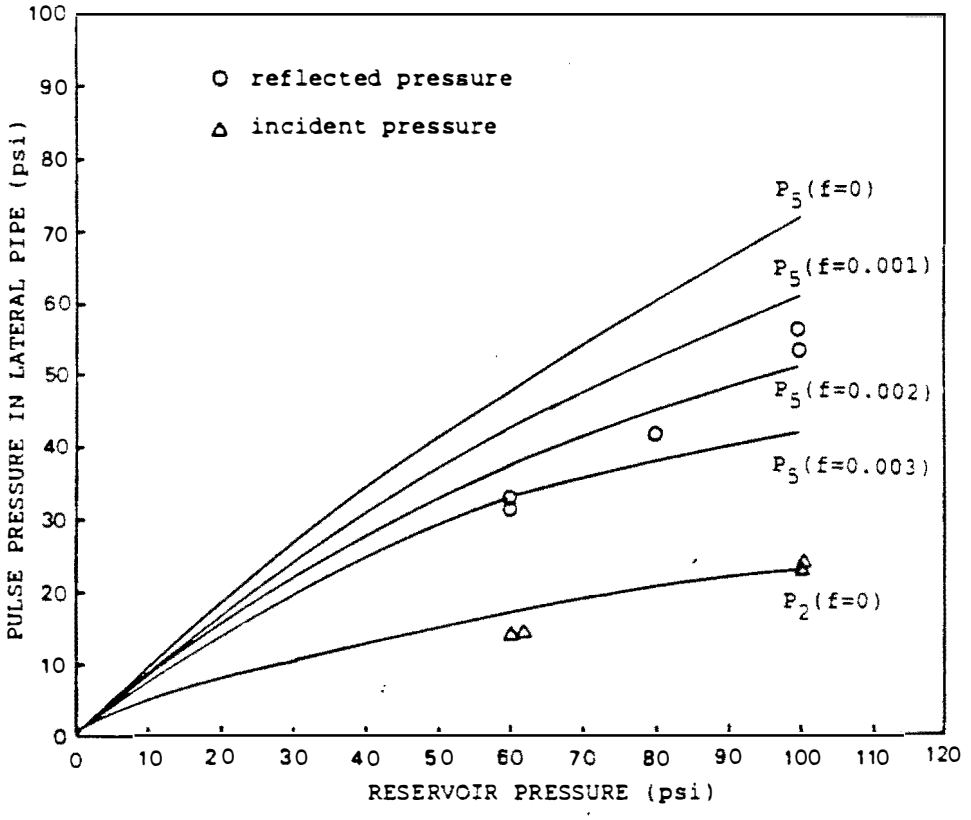

Figure 4.21. The pressure developed in the lateral pipe versus reservoir pressure.

close to the valve. Consequently, there is no effect of friction or loss of mass. However, the reflected pressure measured at the end of the lateral is much lower than the predicted value because the incident pressure decreases due to friction as it travels toward the end of the lateral. Although the friction factor was originally ignored from the equations, the effect of friction is reconsidered by introducing the friction parameter after the incident pressure is determined by Equation (2-27) It is assumed that the velocity and density of air mass are constant in the incident wave. The incident pressure at the end of the lateral is corrected by subtracting the pressure drop due to friction and the equation is written as:

$$P_2^c = P_2 - \frac{1}{2} \rho V^2 \frac{4f}{D} l \qquad (4\text{-}32)$$

where:

P_2^c = predicted incident pressure corrected for friction

P_2 = predicted incident pressure by Equation 2-27.

V = predicted velocity

ρ = predicted density

f = friction coefficient

D = diameter of the lateral

l = length of the lateral

This corrected incident pressure is used for prediction of the reflected pressure. Predicted reflected pressure for three values of friction coefficient (f=0.001, 0.002 and 0.003) against reservoir pressures are shown in the Figure 4.21. As the reservoir pressure increases, the curve gradually bends over because as the reservoir pressure increases, the density of air and the velocity of air mass increases. Consequently, the magnitude of pressure drop due to friction becomes larger when a constant friction coefficient is used. The friction coefficient is a function of the Reynold`s number so that the friction coefficient must be varied depending on the reservoir pressure.

Friction coefficients acquired by the Karman-Nikradse formula and the experimental data ranged between 0.0013 and 0.005. Since these values also involve errors (prediction of velocity, density and measurement of pressure (12 %)), empirical results of the friction coefficients were employed for the purpose of illustration of the model. These values were obtained such that they provided an accurate prediction of the reflected wave. The friction coefficients for 100, 80, and 60 psi were determined to be 0.0015, 0.0025, and 0.003 respectively. More research is needed here to accurately predict the friction coefficient in the lateral.

It is assumed that the reflected pressure travels back to the reservoir with the same velocity as the incident

pressure. The maximum pressure at location x in the lateral is calculated by following equation:

$$P_5(x) = P_5 - \frac{1}{2} \rho V^2 \frac{4f}{D}(l-x) \qquad (4\text{-}33)$$

where:

P_5 = reflected pressure

ρ = density of air

V = velocity of air particle traveling toward the reservoir

f = friction coefficient

l = length of the lateral

x = distance from the end of the lateral

Figure 4.22 shows the calculated versus measured lateral pressure. It can be concluded that the calculated pressure agrees well with the measured pressure (R^2=0.85, N=15)..

Jet velocity and pulse pressure exerted at the entry of the bag. According to the theoretical Equation (4-15), the velocity of the air jet at the bag entry can be calculated for the reservoir pressure of 100 , 80, and 60 psig . The pressure developed by the air jet is calculated based on Equations (2-20) and (2-21) and is compared with measured values in the Figure 4.23. The pressure loss factors (type1: 43% loss, type2: 64% loss) are applied for the

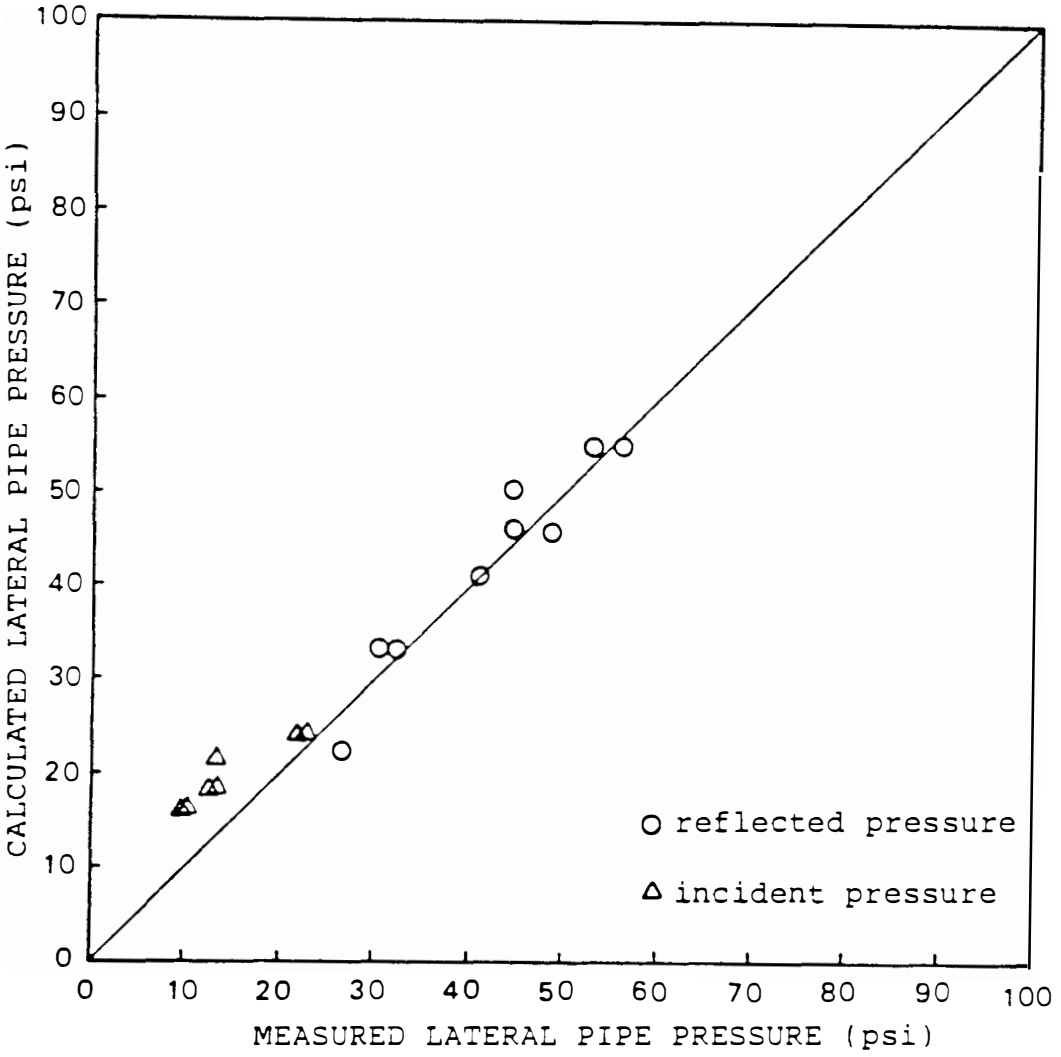

Figure 4.22. A comparison of calculated versus measured lateral pipe pressure.

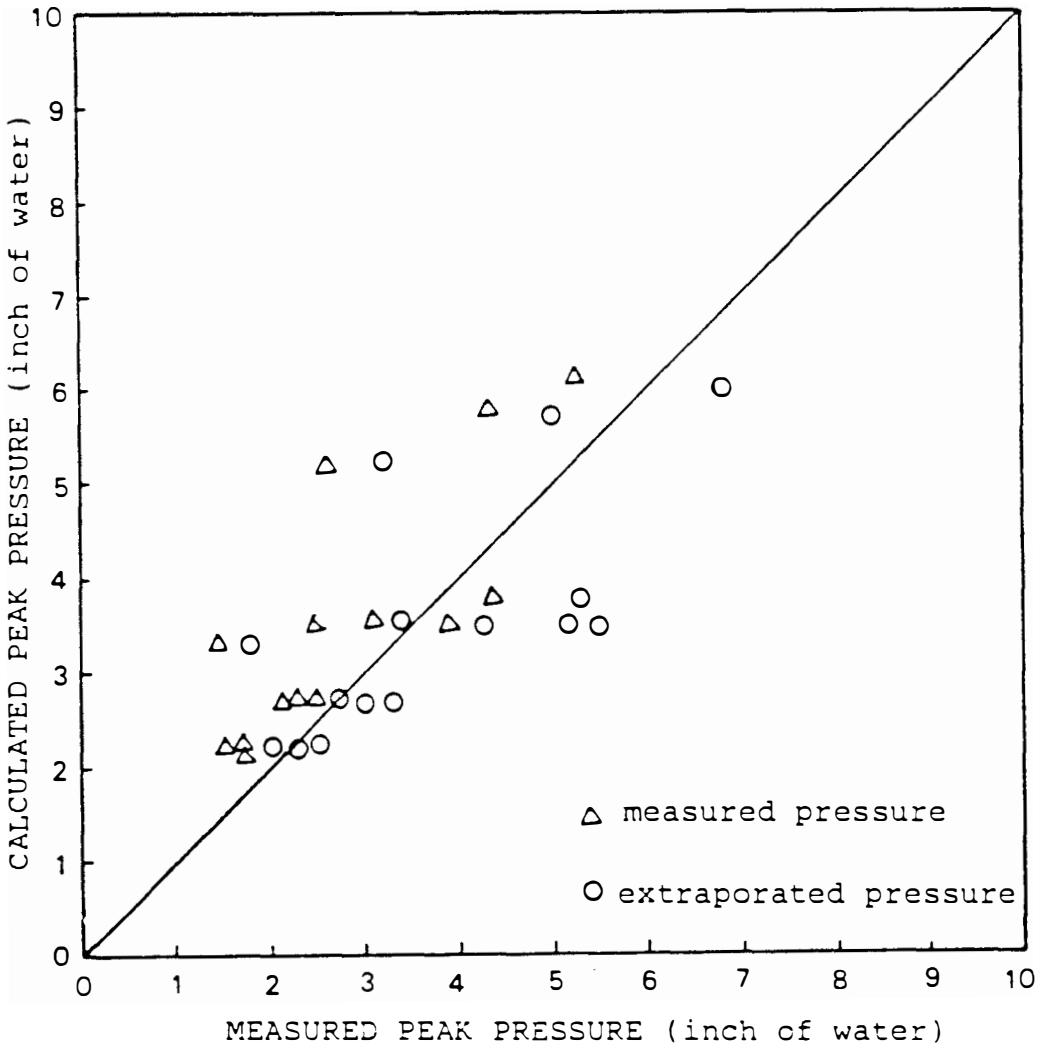

Figure 4.23. A comparison of calculated versus measured pressure at the top of the bag.

predicted pressure depending on the bag entry configuration. Predicted pressure versus the measured maximum pressure extraporated for the calculated point are also plotted on the figure (symbol=○). The calculated value agrees reasonably well with the measured value.

Pulse pressure dissipating along the bag. The pulse pressure dissipating along the bag can be described by Equation (4-29) and written as:

$$d(\Delta P) = \frac{4}{D} P_g \frac{P_b + P_a}{2P_a} \rho_a (P_b - P_a) R T \frac{dx}{u} + \frac{1}{2} \rho u^2 \frac{4f}{D} dx \qquad (4\text{-}29)$$

Since ρa, R,T are constant, and P_b is nearly equal to p_a, the equation can be rewritten as:

$$d(P) = \frac{4}{D} P_g K \frac{dx}{u} + \frac{1}{2} \rho u^2 \frac{4f}{D} dx \qquad (4\text{-}34)$$

where:

$$K = 4 \frac{P_b - P_a}{2P_a} R T$$

By examining parameters in the equation, the following observation can be made.

(1) As the velocity of the flow decreases, the dissipation rate in the first term increases. This indicates that more air is allowed to permeate until the air mass reaches the

bottom of the bag. On the other hand, the second term of the equation due to friction decreases. Therefore, the velocity affects the pressure dissipation in opposite directions for the first and second terms. Therefore the first and second terms seem to be compensating each other in the range of velocity considered.

(2) When the bag diameter increases, the first and the second term in the equation decrease. Consequently, the rate of pressure dissipation decreases.

(3) Permeation coefficient directly controls the rate of pulse pressure dissipation. When the permeation coefficient increases, the rate of pressure dissipation increases.

Based on the above observations, it is concluded that the friction term contributes very little to the pulse dissipation. Since the friction term was excluded from the equation, the velocity in the first term is considered to be constant. Then the equation can be simplified to

$$d(\Delta P) = - \frac{K}{D} P_g (\Delta P) \, dx \qquad (4\text{-}35)$$

Integating the equation

$$P(x) = P_i \exp\left(- \frac{K}{D} P_g x \right) \qquad (4\text{-}36)$$

This form of the equation is applied for the experimental data.

Figure 4.24 shows the pressure exerted along the bag for bags #1, #2, and #3. The data is acquired from standard system configuration without venturi at 100 psig reservoir pressure. The solid lines show the ADM (Equation 4-36) predicted pressure (Pg = 0.0067 ft/sec/inch w.g., d = 0.5 ft, entry loss = 43%).

Figure 4.25 shows the pressure exerted along the bag for bags #1, #2, and #3. The data is acquired from standard system configuration with venturi at 100 psig reservoir pressure. The solid lines show the ADM (Equation 4-36) predicted pressure (Pg = 0.0067 ft/sec/ inch w.g, d = 0.5 ft, entry loss = 64%).

Figure 4.26 shows the pressure exerted along bag #2 for three values of valve opening time(50, 75, and 100 ms) The data is acquired from standard system configuration with venturi at 100 psig reservoir pressure. The solid lines show the ADM (Equation 4-36) predicted pressure (Pg = 0.0067 ft/sec/inch w.g., d = 0.5 ft, entry loss = 64%).

Figure 4.27 shows the pressure exerted along bag #2 for three values of valve opening time(50, 75, and 100 ms) The data is acquired from standard system configuration with venturi at 80 psig reservoir pressure. The solid lines show the ADM (equation 4-36) predicted pressure (Pg=0.0067 ft/sec/inch w.g., d=0.5 ft, entry loss = 64%).

Figure 4.28 shows the pressure exerted along bag #2 for three values of valve opening time(50, 75, and 100 ms) The

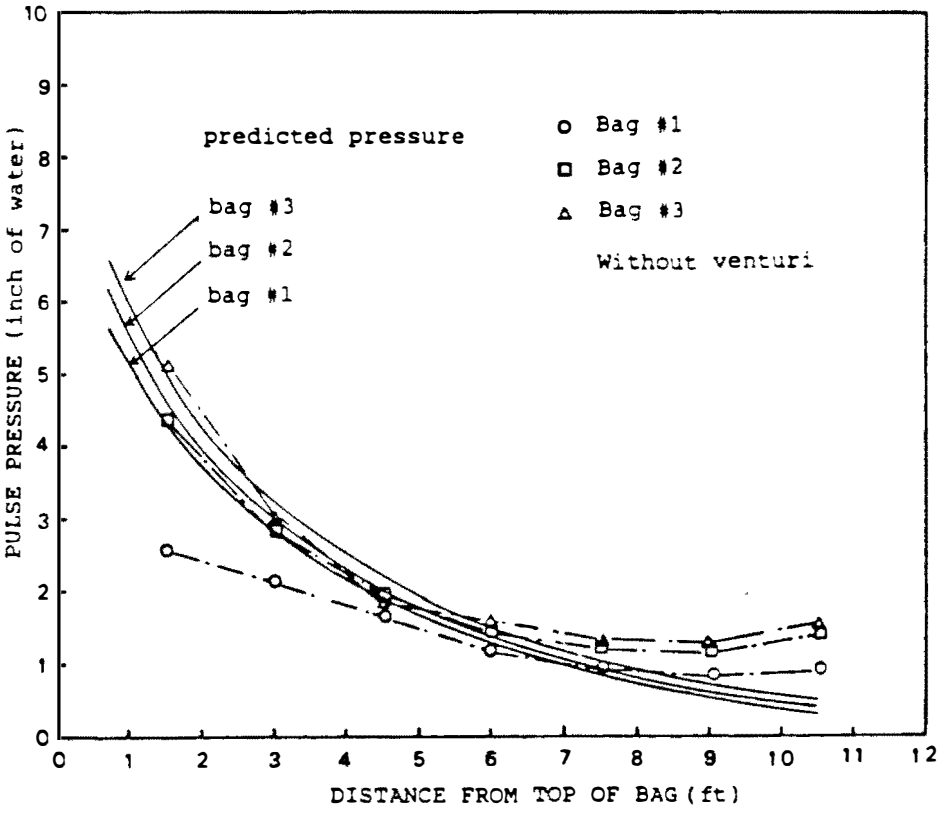

Figure 4.24. Pulse pressure developed in the bag versus the distance from the top of the bag (clean bag, without venturi, three bag locations).

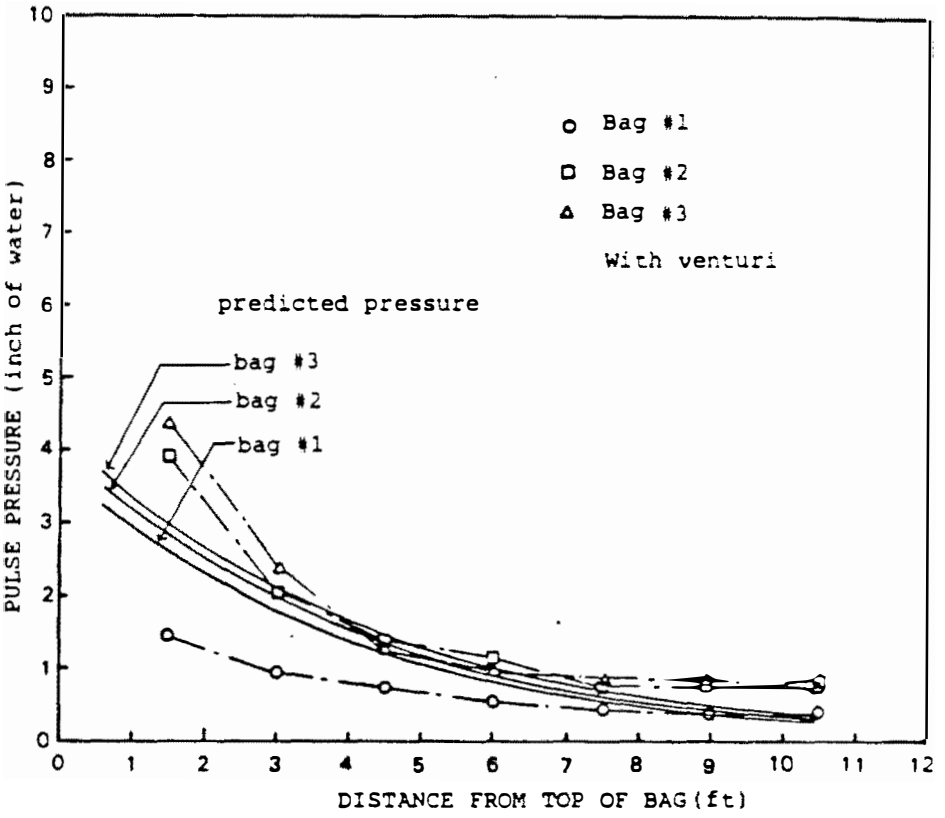

Figure 4.25. Pulse pressure developed in the bag versus the distance from the top of the bag (clean bag, with venturi, three bag locations).

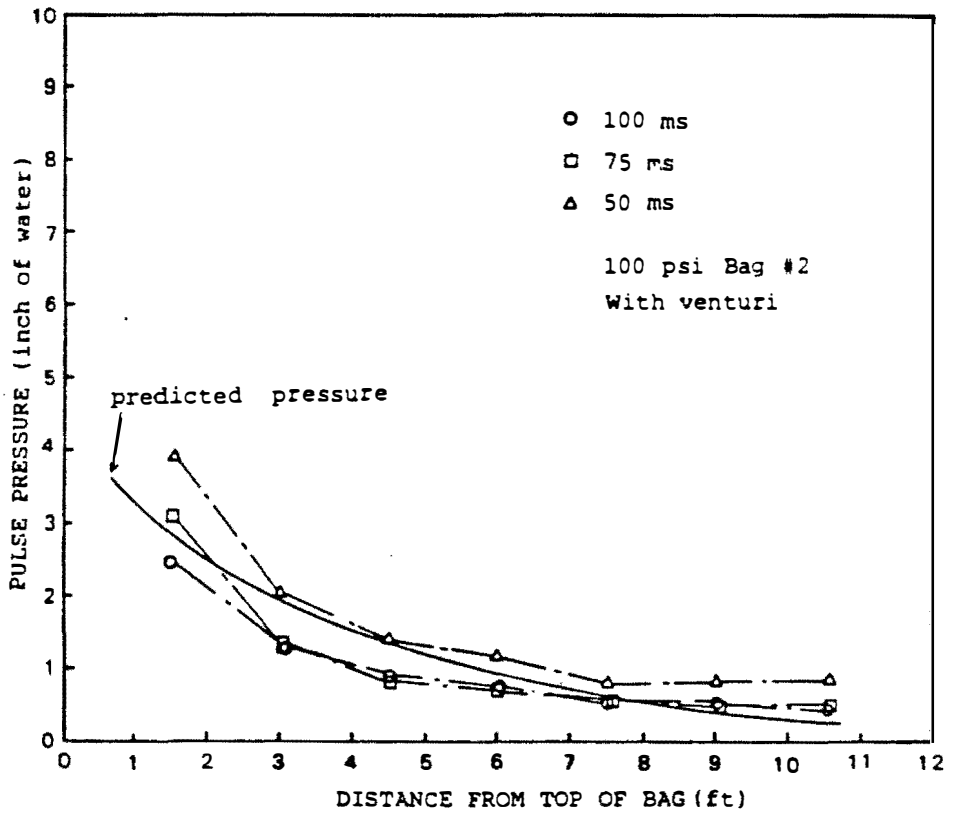

Figure 4.26. Pulse pressure developed in the bag versus the distance from the top of the bag (clean bag with venturi, bag #2, 100 psi).

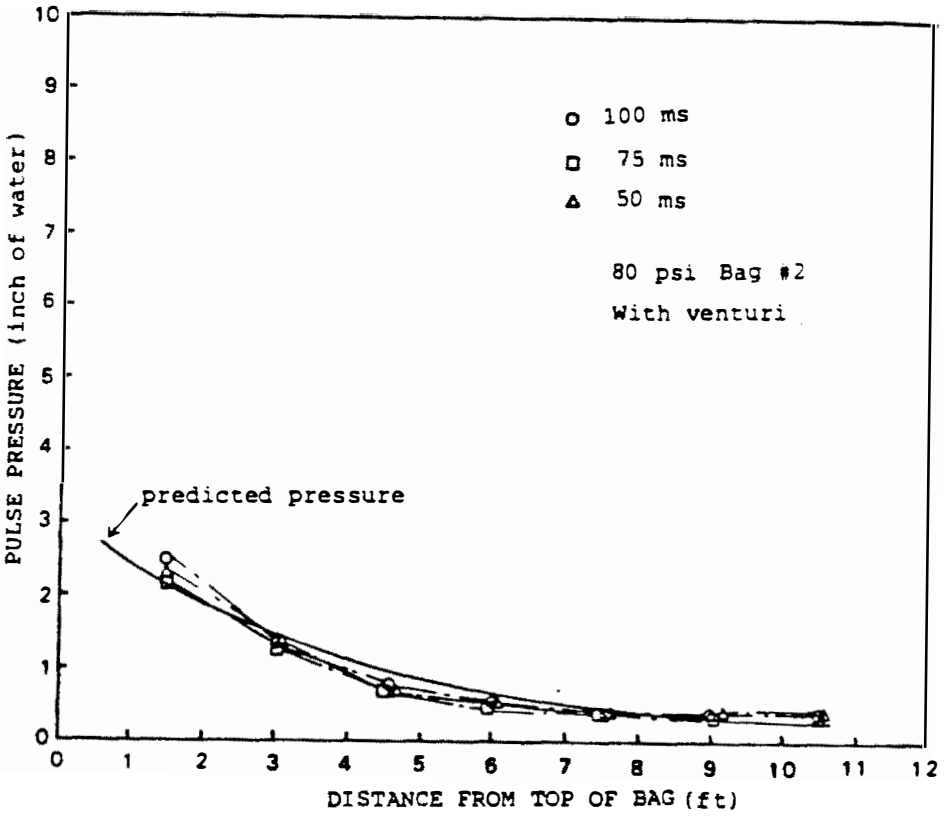

Figure 4.27. Pulse pressure developed in the bag versus the distance from the top of the bag (clean bag, with venturi, bag #2, 80 psi).

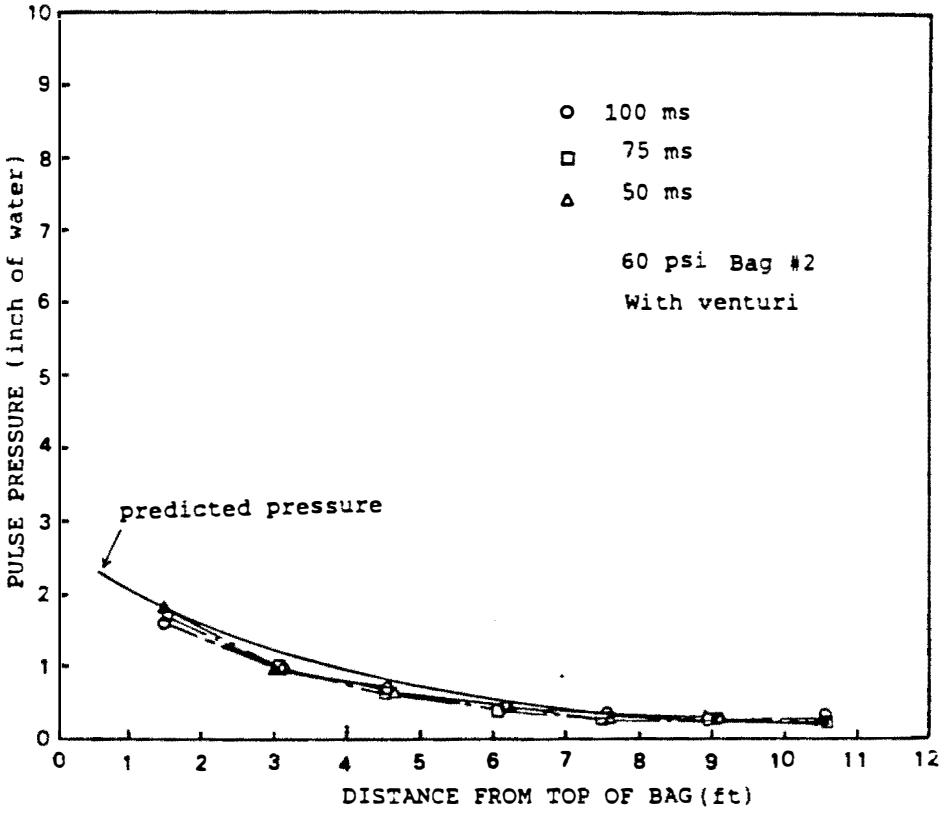

Figure 4.28. Pulse pressure developed in the bag versus the distance from top of the bag (clean bag with venturi, bag #2, 60 psi).

data is acquired from standard system configuration with venturi at 60 psig reservoir pressure. The solid lines show the ADM (equation 4-36) predicted pressure (Pg=0.0067 ft/sec/inch w.g., d=0.5 ft, entry loss = 64%).

Figure 4.29 shows the pulse pressure exerted along the bag for a dirty system (short lateral = 21", housing 4 bags). It should be noted that the system configuration is different from the standard system and direct comparison will not be made. The ADM is applied for the data of 4" lateral/bag spacing, 100 psi reservoir pressure. The predicted value is shown in solid line (Pg=0.0067 ft/sec/inch w.g, entry loss = 43%).

As a reference, a comparison is also made of the model to Humphries and Madden's data(1981). This is shown in Figure 4.30 The pulse pressures were measured for three values (120, 80, and 40 psig) of reservoir pressure. The model is applied for the reservoir pressure of 80 psi(Pg = 0.0067 ft/sec/inch w.g., entry loss = 43%, D = 4.3")

Figure 4.31 shows the calculated versus measured pressure developed in the bag (R^2 =0.68, N=83). Since the reflected pressure at the bottom of the bag was not considered in the model, the predicted pressures are always lower than the measured value in the region of the bottom half of the bag.

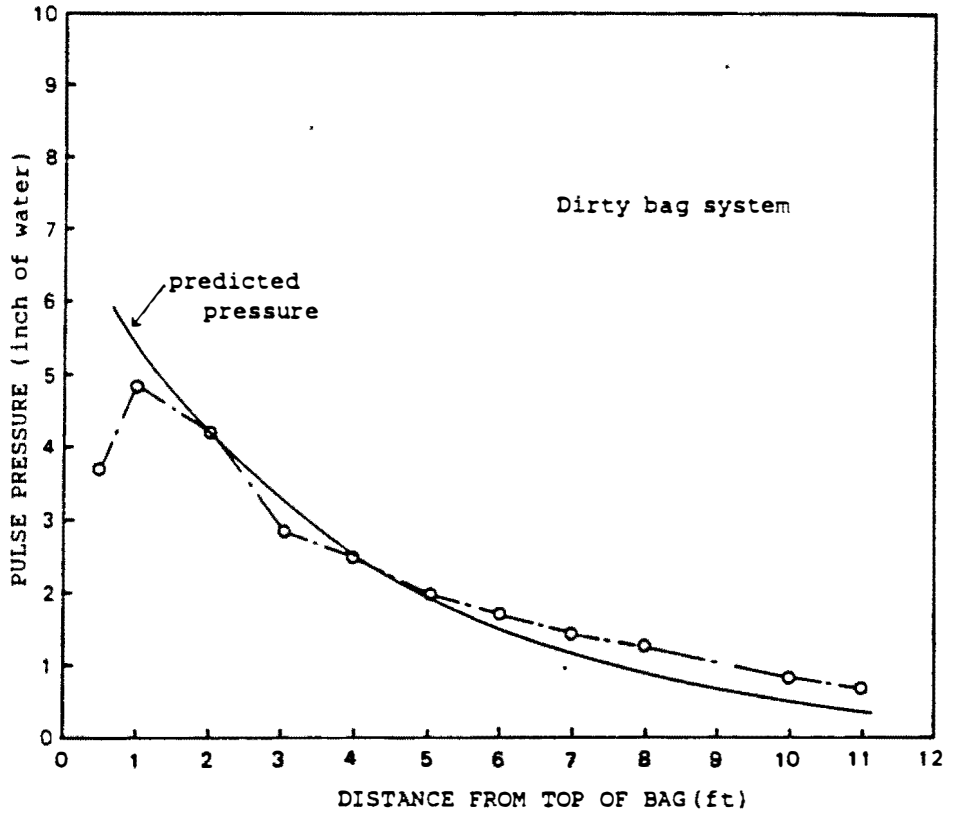

Figure 4.29. Pulse pressure developed in the bag versus the distance from the top of the bag (dirty bag system, 100 psi).

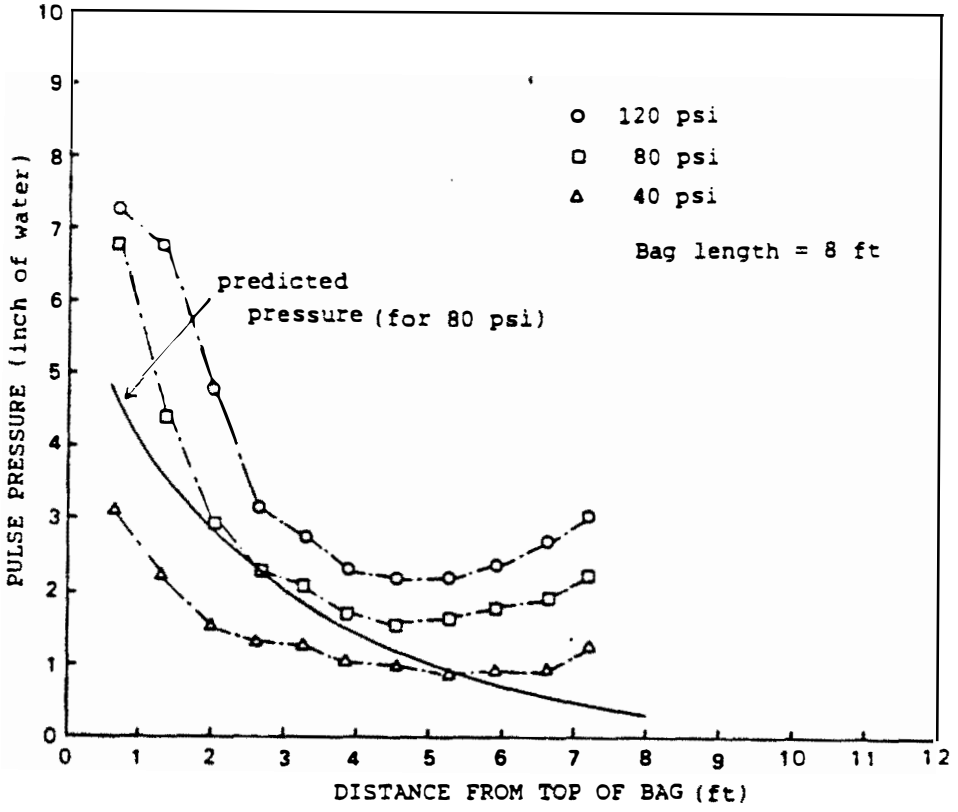

Figure 4.30. Pulse pressure developed in the bag versus the distance from the top of the bag (Humphries and Madden,1981).

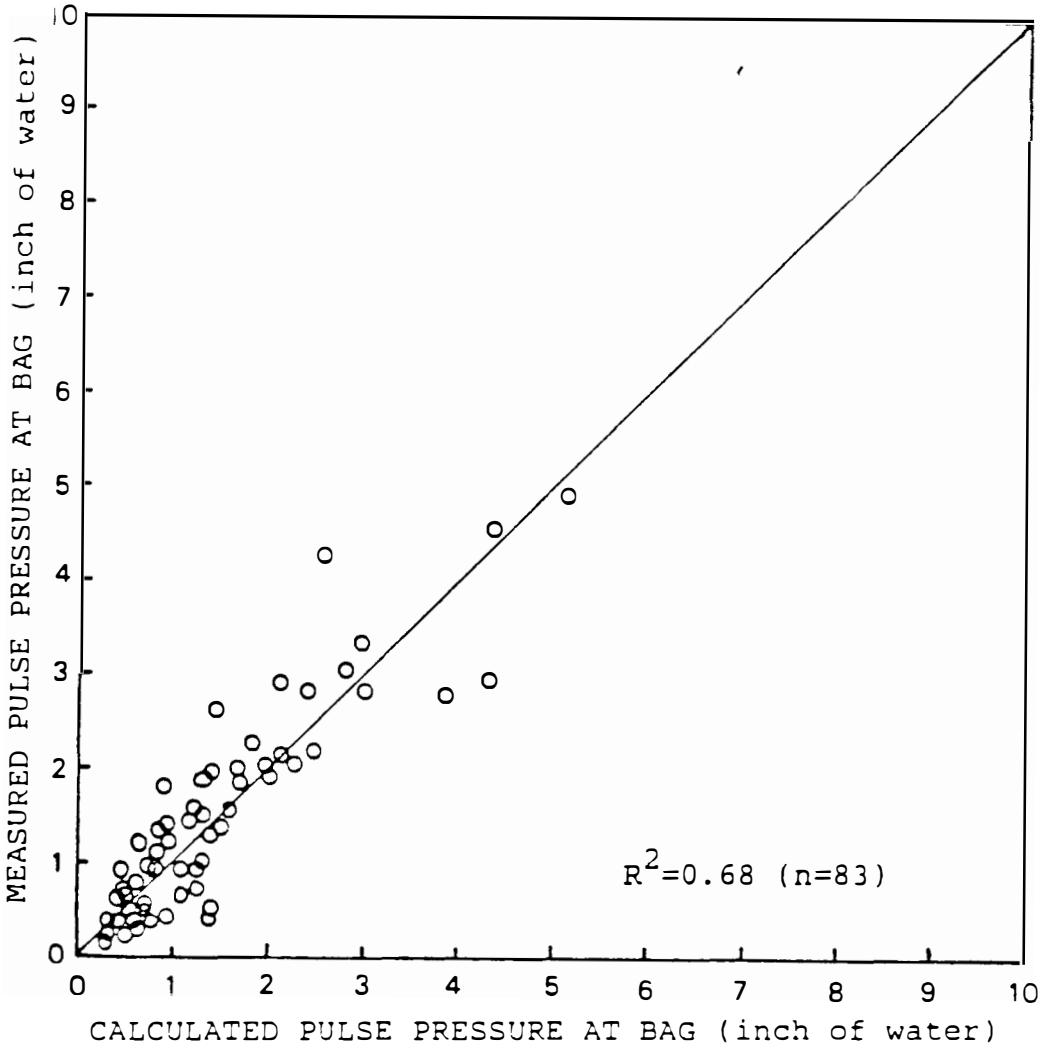

Figure 4.31. A comparison of calculated versus measured bag pressure.

It can be concluded that the model(ADM) is able to predict the exponential nature of the pressure dissipation mechanism and the pressure developed at the top portion of the bag.

CHAPTER V

CONCLUSIONS

A predictive model for the pulse pressure in a pulse-jet fabric filter has been developed. Two types of models are presented: Simplified Static Model and Dynamic Model.

The Simplified Static Model treats the system as a series of spherical tanks in which the pressure develops uniformly throughout each tank. Each tank in series is connected by a valve. Then, the mass balance equation is applied for the system and solved numerically. The predicted pressure and the pressure wave pattern agrees well with the pressure trace observed at the lateral and the bag. Sensitivity analysis has been conducted to evaluate the effect of configurations and operating parameters.

The dynamic model is developed to predict the local pressure developed in the system. The reservoir/lateral system is considered as a simple shock tube and the theory of a simple shock tube is applied to the system to predict the maximum pressure developed in the lateral. Then, the maximum pressure developed at the entry of the bag is predicted based on the velocity of the injected air. The pressure developed at the top of the bag dissipates along the bag due to the permeation of air mass through the bag surface. The mass balance equation is applied to the mass of air traveling along the bag. Empirical corrections are

applied to the dynamic model due to the complexity of the theoretical treatment. The empirical correction factors introduced are the friction coefficient in the lateral pipe, pressure losses at the bag entrance, and the permeability of the bags. The model (ADM) clearly explains the mechanism of the local pressure development in the lateral and the exponential decay of the pulse pressure along the bag.

The proposed models provide valuable information to the designer and user of pulse-jet fabric filters. The models can be employed to assist in the design of the pulse-jet fabric filter, to understand the behavior of the system, and to predict the performance due to the change of an operating condition within the constraints imposed by the assumptions and/or empirical corrections contained in the models.

Also preliminary conclusions have been drawn regarding the effect of the venturi. The venturi, as employed in pulse-jet fabric filters, was originally intended to provide 1) pressure recovery of the air jet, 2) entrainment of additional air and 3) redirection of the air flow in cases where there may have been a slight misalignment of the lateral/bag. However, it was found in this study that the venturi causes adverse effects on the bag pressure. Experimental results indicated that the maximum pressures for the system with a venturi were lower than the maximum pressures observed for the system without a venturi. When the venturi is not applied or designed properly, the venturi

may act as a resistance rather than as originally intended. Therefore, some caution must be taken to utilize the venturi effectively. Although the venturi produced a lower pressure in the bag, it would be premature to conclude that the venturi should be eliminated, since it also functions to re-align the direction of a poorly aligned lateral pipe. Further study is needed to determine the long-term effectiveness of the venturi.

Limitations of the Proposed Models and Recommendation for Their Improvement.

The proposed models are able to predict the pulse pressure developed in the pulse-jet fabric filter and are able to describe the behavior of the pulse-jet system. The models are particularly useful for the preliminary design of the system and prediction of performance changes due a change in design parameters and operating conditions. The proposed models provide sufficient information to satisfy the needs in the practical engineering field. However, there are some cases in which more accurate information may be required. In such cases, a more complex model may still be needed.

The proposed models have some limitations as a result of the assumptions made in the course of model development. Assumptions introduced are:

(1) Friction force and loss of mass can be ignored for the flow in the lateral.

(2) Properties of flow at the entry of the bag can be determined based on mass balance equations. No air entrainment is considered.

(3) Pressure loss at the entry of the bag is proportional to the magnitude of pressure developed at the entry of the bag. An empirical correction has been determined for the lateral-pipe/bag configuration used in this study. This correction may not be the same for different configurations and requires further investigation.

(4) Maximum pressure is developed at 10 inches (Kirshner and Katz, 1975) from the lateral for this configuration. While this can be calculated for any configuration, it has not been incorporated into the present model.

(5) Pressure drop due to friction is negligible compared to the pressure loss due to loss of mass associated with the permeability of the bag. (6) Momentum and energy equations are ignored for the prediction of the pulse pressure dissipation along the bag (i.e. effect of velocity change was not considered).

These assumptions are introduced because of the complexity of the theoretical treatment and experimental approach in order to simplify the solution method . Therefore, further effort should be made in these areas to improve the models.

Future Research Needs

Application of a more reliable theory. The flow mechanism between the lateral pipe and the bag is very complex involving several different flow processes. The high pressure air in the lateral pipe is expanded to the atmospheric pressure entraining surrounding air; the pressure of the air jet is then recovered by the venturi at the entrance of the bag. Also, a small difference in entry configuration such as bag alignment and/or installation of a venturi will affect the magnitude of the pressure developed at the entry of the bag. Therefore, it is very difficult to obtain the flow properties and energy losses at the entrance of the bag.

A more rigorous theory should be developed to determine the flow properties and the pressure loss incurred at the entrance of the bag. Until such theory has been developed, an empirical loss coefficient must be used.

Improvement of solution method. In order to improve the accuracy of the model, the governing equations for unsteady flow must be solved without introducing assumptions. A system of non-homogeneous quasi-linear partial differential equations may be solved numerically by employing finite element and finite difference methods. These numerical methods require information for the initial

and the boundary conditions. For example, the loss of mass through the orifice, the bag surface, and the friction coefficient must be described as a function of flow properties.

Experimental data. Experiments should be conducted to provide the data for developing the theory and solution method. Particularly, data on (a) flow properties (u, P) at time t in the lateral and bag, (b) pressure losses for various bag entry configurations, (c) friction coefficients, and (d) permeability.

REFERENCES

REFERENCES

Bakke, Even, "Optimizing Filtration Parameters," J. Air Poll. Control Assoc., vol 24, No.12 pp.1150-1154,1974.

Barrer, R. M., Diffusion in and through solids, The Macmillan Company, New York, 1941.

Billings C.E. and J.E. Wilder, Handbook of Fabric Filter Technology, Volume I, Fbaric Filter Systems Study, EPA No. APTD0690 (NTIS No. PB-200-648), Dec. 1970.

Cunningham R.E. and R.J.J. Williams, Diffusion in Gases and Porous Media, Plenum Press, New York, 1980.

Dennis, R. and L. Silverman,"Fabric Filter Cleaning by Intermittent Reverse Air Pulse," ASHRAE J., 4(3):43, 1962.

Dennis, R. and J. E. Wilder, Fabric Filter Cleaning Studies. EPA 650 12-75-009 (NTIS No. PB-240-372) Jan., 1975.

Dennis, R., Cass, R.W., Cooper, D.W., Hall,R.R., Hampl, V., Klemm, H.A., Langley, J.E., and stern, R.W., Filtration Model for Coal Fly Ash with Glass Fabrics, EPA-600/7-77-084, August 1977.

Dennis, R. and H.A. Klemm, "Modeling concepts for pulse-jet filtration," J. Air Poll. Control Assoc., 30 (1):38, 1980.

Dennis, R., J.E. Wilder and D.L. Harmon, "Predicting Pressure loss for Pulse Jet Filters," J. Air Poll. control Assoc., 31 (9):987, 1981

Ellenbecker, M.J. and D. Leith, "Dust Removal from Non-Woven Fabrics--Cleaning Methods Need to be Improved," Filtration & Separation, 18 (4) 316, 1981.

Humphries W. and J.J. Madden, "Fabric Filtration for Coal-Fired Boilers:Nature of Fabric Failers in Pulse-Jet Filters," Filtration & Separation, pp. 503-509, 1981.

Humphries W. and J.J. Madden, "Fabric Filtration for Coal-Fired Boilers: DustdislodgementinPulse-jet Filters," Filtration & Separation, pp. 40-44, 1983.

John, James E.A., Gas Dynamics, Boston: Allyn and Bacon, Inc.,1969.

Kirshner, J.M. and S. Katz, Design Theory of Fluidic Components, New York: Academic Press, Inc., 1975.

Klingel R. and F. Loffler, "Stdies on Dust Collection and Cleaning Efficiency of a pulse jet fabric Filter," World Filtration Congress III, pp35-42, 1983.

Leith, D. and M. W. First, "Pressure Drop in a Pulse-Jet Fabric Filter," Filtration and Separation, 14 (5) 473, 1977.

Leith, D, First M.W. and Gibson D.D., "Effect of Modified Cleaning Pulses on Pulse Jet Filter Performance," Filtration & Separation, pp. 400-406, 1978.

Leith, D. and M.J. Ellenbecker, "Theory for Pressure Drop in a Pulse-Jet Cleaned Fabric Filter," Atmospheric Environment, 14: 845-852, 1980.

Leith, D. and M.W. First, "Performance of a Pulse-Jet Filter at High Filtration Velocity, I. Particle Collection," J. Air Poll. Control Assoc., Vol.27,No. 6, PP. 534-539, June, 1977.

Leith, D., and M.J. Ellenbecker, "Theory for Penetration in a Pulse-Jet Cleaned Fabric Filter," J. Air Poll. Control Assoc., Vol. 30, No. 8, pp. 877-881, August, 1980.

Owczarek, J. A., Fundamentals of Gas Dynamics, International Textbook Co., Scranton, Pa., 1964.

Shapiro, A. H., The Dynamics and Thermodynamics of Compressible Fluid Flow, Ronald Press, New York, 1953.

Strauss, W., Industrial Gas Cleaning, Pargamon Press, New York, 1966.

Zucrow, J.M. and J.D. Hoffman, Gas Dynamics, John Wiley and Sons, New York, 1977.

APPENDIXES

Appendix A

Data matrix of the experiment and example photographs of pulse-pressure wave.

Experimental Data

The experimental data consists of two kinds of data sets: clean bag and dirty bag test data.

The data of the clean bag test was utilized to characterize the pulse pressure exerted along the bag under various design and operating conditions. Also, the predictive model for the pulse pressure exerted inside of the bag was developed based on this data. The data matrixes of the experiments are shown in Tables B.1, B.2, and B.3. The measured parameter was the pulse pressure at various locations along the bag and the lateral pipe.

The data of the dirty bag test was utilized to examine the effect of pulse characteristics, which was identified by the clean bag test, on the system efficiency and pressure drop. The measured parameters are the system efficiency and pressure drop in addition to the pulse pressure exerted inside of the bag. The data matrix of the experiment is shown in Table B.4.

The photographs of the pressure wave for run No. 01 of test (A) were included in this section as an example.

Table A.1. Clean bag test (A)

Run No.	01	02	03	04	05	06	07	08	09	10
Permeable bag	X	X			X	X	X		X	
Impermeable bag			X	X				X		X
Open-ended bag		X		X						
Closed-ended bag	X		X		X	X	X	X	X	X
Reservoir Pressure 100 psi	X	X	X	X			X	X	X	X
80 psi					X					
60 psi						X				
Bag length 12 ft	X	X	X	X	X	X				
9 ft							X	X		
6 ft									X	X

Table A.2 Lateral pipe test

Run No.	1	2	3	4
Tank Pressure 100 psi	X			
80 psi		X		
60 psi			X	X
Closed-ended lateral pipe	X	X		
Open-ended lateral pipe				X

Table A.3 Clean Bag Test (B)

Run No.	01	02	03	04	05	06	07	08	09	10	11	12	13	14
With venturi		X	X	X	X	X	X	X	X	X			X	
Without venturi	X										X	X		
lateral pipe/bag spacing 4"	X	X	X	X	X	X	X	X	X	X			X	X
8"											X			
12"												X		
The lateral pipe diameter 1 1/2"	X	X	X	X	X	X	X	X	X	X	X	X		
2"													X	X
Reservoir pressure 100 psi	X	X	X	X							X	X	X	X
80 psi					X	X	X							
60 psi								X	X	X				
Pulse duration 50 ms	X	X			X			X			X	X	X	X
75 ms			X			X			X					
100 ms				X			X			X				

Note: Special tests were also conducted. For example, various types of the bag entrance configurations were tested.

Table A.4 Dirty Bag Test (C)

Run No.	01	02	03	04	05	06	07	08	09	10	11	12
Air to cloth ratio 3.0	X	X	X				X	X	X	X		X
6.0				X	X	X					X	
Dust size (mmd) 9.0	X	X	X	X	X	X	X	X	X			
5.0										X		X
Lateral pipe/bag spacing 4"	X			X			X			X	X	X
12"		X			X			X				
20"			X			X			X			
Type of fabrics Felt	X	X	X	X	X	X				X	X	
Fiberglass					X	X	X			X		
With venturi	X	X	X	X	X	X	X	X	X			X
Without venturi										X	X	

Data Description

- .standard system configuration
- .operating conditions:
  - reservoir pressure =100 psi
  - pulse time = 50 ms
- .conversion factors:
  - 4.8 psi/v for the lateral pressure
  - 9.8" H_2O/v for the bag pressure
- .bag dimensions:
  - 6"dia. x 12'L
- .pressure port:
  - 7 port @ 1.5 ft

- ·time = 50 ms/div.
- ·pulse pressure = 5 v/div.
- ·bag pressure = 0.1 v/div.

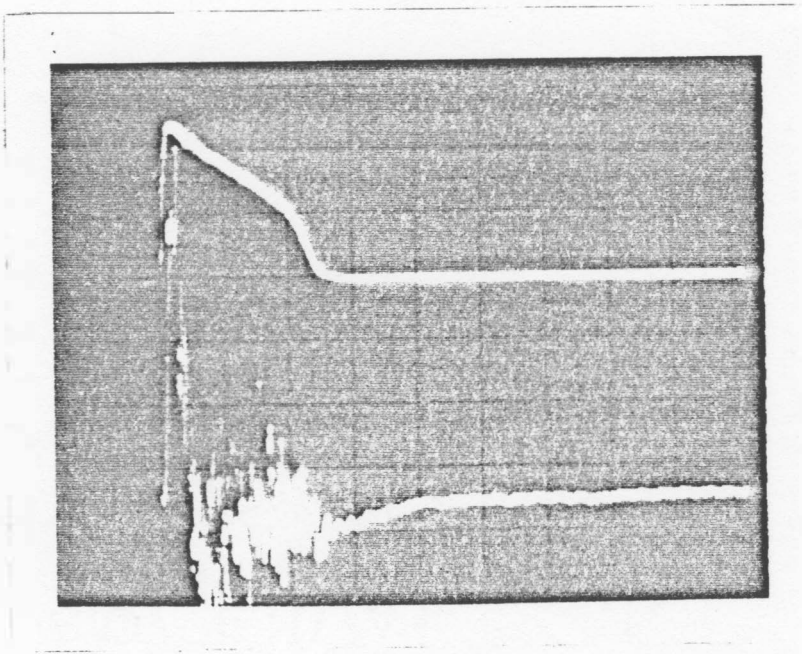

port #1

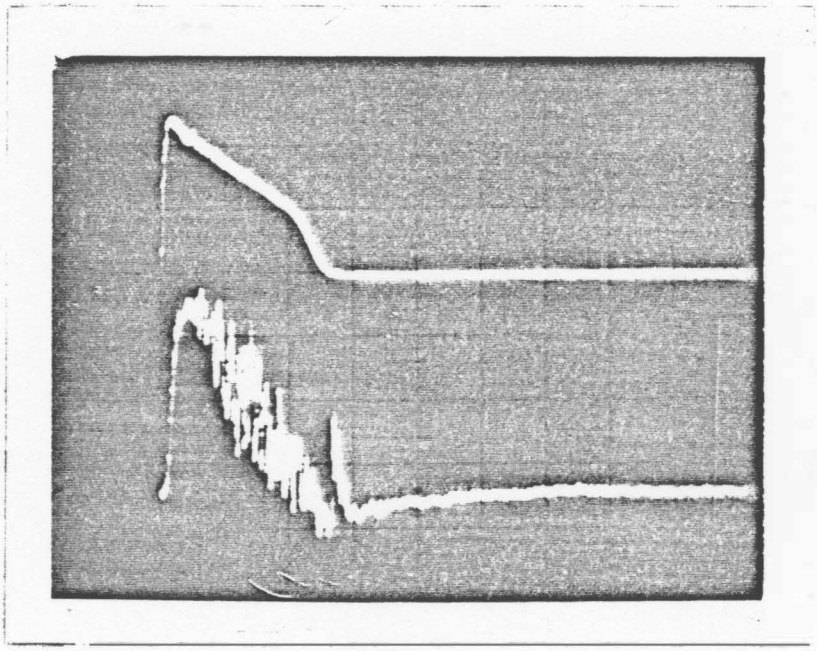

port #2

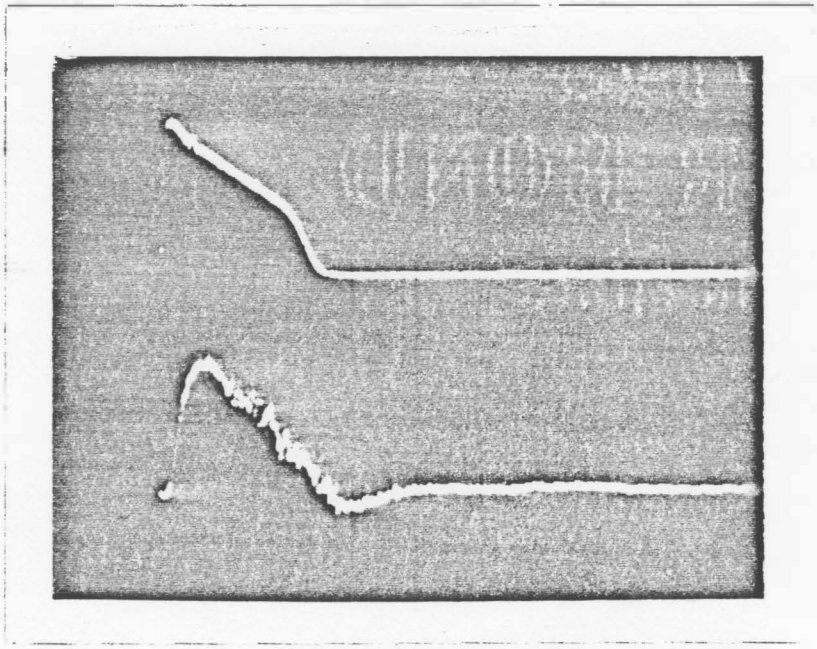

port #3

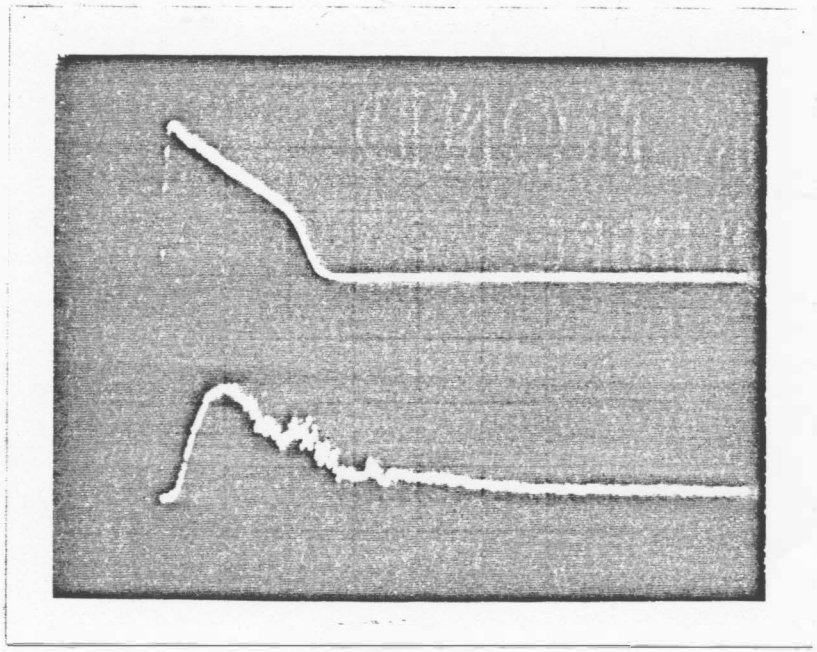

port #4

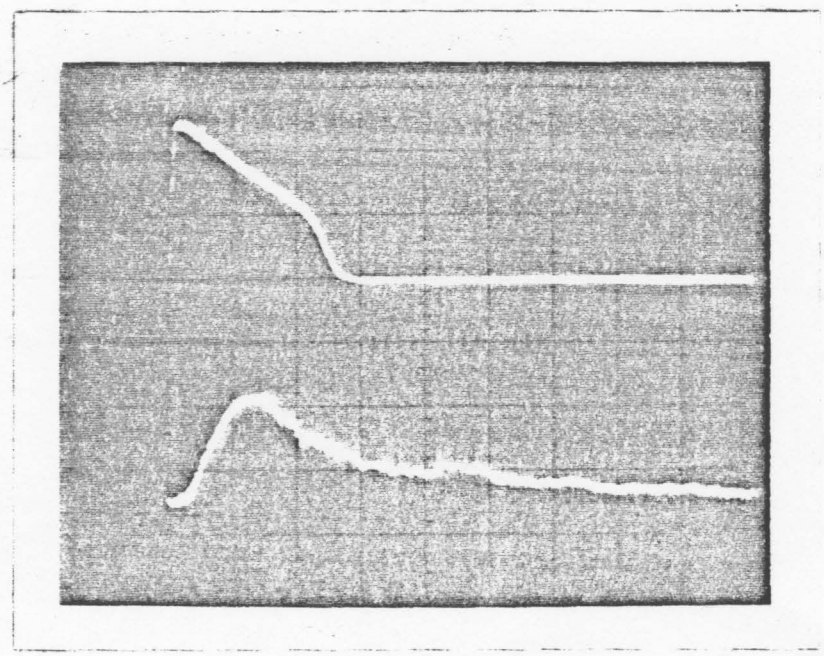

port #5

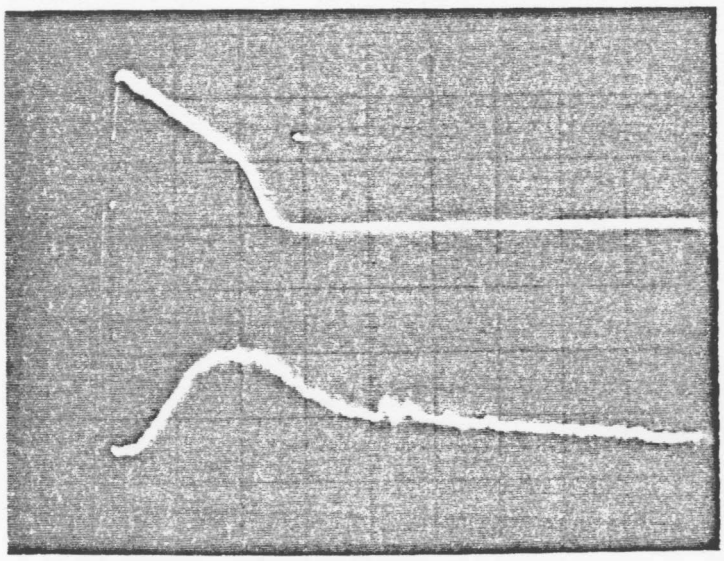

port #6

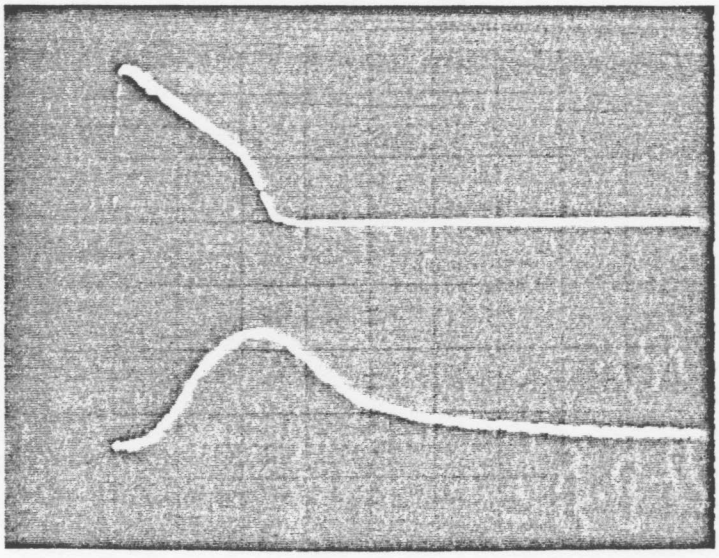

port #7

Appendix B

Computer program

```
5 REM program name :PMPP
10 REM The Predictive Model for the pulse pressure
20 REM in a pulse-jet Fabric Filter
30 REM by S. Mitsutomi,     May 1986
40 KEY OFF:SCREEN 0,1:COLOR 15,0,0:WIDTH 40:CLS
60 COLOR 10,0:LOCATE 4,3,0:PRINT CHR$(213)+STRING$(30,205)+CHR$(184)
70 LOCATE 5,3,0:PRINT CHR$(179)+"        Predictive Model        "+CHR$(179)
80 LOCATE 6,3,0:PRINT CHR$(179)+STRING$(30,32)+CHR$(179)
90 LOCATE 7,3,0:PRINT CHR$(179)+"    for the Pulse Pressure    "+CHR$(179)
95 LOCATE 8,3,0:PRINT CHR$(179)+STRING$(30,32)+CHR$(179)
100 LOCATE 9,3,0:PRINT CHR$(179)+" in a Pulse-Jet Fabric Filter "+CHR$(179)
105 LOCATE 10,3,0:PRINT CHR$(212)+STRING$(30,205)+CHR$(190)
130 REM
200 COLOR 14,0
280 LOCATE 14,3,0:PRINT "Model Selections: "
290 LOCATE 16,3,0:PRINT "1- Simplified Static Model"
295 LOCATE 18,3,0:PRINT "2- Dynamic Model"
300 LOCATE 24,3,0:PRINT "ESC KEY - EXIT"
310 LOCATE 25,3,0:PRINT "ENTER NUMBER OF THE PROGRAM"
340 REM
350 K$ = INKEY$:IF K$ <> "" THEN GOTO 340
360 K$ = INKEY$:IF K$ = "" THEN GOTO 360
380 IF MID$(K$,1,1) = "1" THEN CHAIN "ssm"
390 IF MID$(K$,1,1) = "2" THEN CHAIN "adm"
550 IF MID$(K$,1,1) = CHR$(27) THEN GOTO 570
560 GOTO 10
570 SCREEN 0,1:COLOR 7,0:CLS:END
1000 GOTO 10
-x-x-x-x-x-x-x-x-x-x-x-x-x-x-x-x-x-x-x-x-x-x-x-x-x-x-x-x-x-x-x-x-x-x-x-x-x-x-x
5 REM program name: ssm
6 REM ...simplified static model
7 WIDTH 80: KEY OFF
10 REM notations
20 REM          1..reservoir
21 REM          2..lateral
22 REM          3..bag
23 REM          4..valve
24 REM          5..orifice
25 REM          6..bag surface
26 REM          9..bag inlet
99 HC=0
100 REM   constants
110 G=1.4
115 C=32.2
120 R=53.3
125 F=27.6756
130 G1=2/(G-1)
135 G2=-(G-1)/G
139 REM   volume
140 V1=.92
145 V2=.1209
150 V3=2.3562*14
154 REM   pressure
155 P0=14.7
160 P1=P0+100
165 P2=P0
170 P3=P0
174 REM   temperature
175 T0=530
180 T1=T0
185 T2=T0
190 T3=T0
194 REM ...area of the valve (1.5" dia.)
195 A1=1.767/144
199 REM ...area of the orifices (3/8" x 14 holes)
200 A2=1.546/144
204 REM   area of a bag surface
205 A3=2714.3*14/144
207 REM   area of a bag inlet
208 A9=28.274*14
209 REM   permeability
210 K=.5/35/60
214 REM   time increment
215 D=.0005
```

```
216 REM ... valve opening time (ms)
217 TM=100
220 REM ....display input data
221 COLOR 14,0:CLS
225 PRINT " Input Data:"
226 PRINT " ________________ "
227 PRINT
230 PRINT " 1-constants : g=";G;" c=";C;" R=";R;" f=";F
231 PRINT
235 PRINT " 2-volumes : V1=";V1;" V2=";V2;" V3=";V3
236 PRINT
240 PRINT " 3-prtessurs : P0=";P0;" P1=";P1;" P2=";P2;" P3=";P3
241 PRINT
245 PRINT " 4- temperatures : T1=";T1;" T2=";T2;" T3=;T3
246 PRINT
250 PRINT " 5-areas : A1=";A1;" A2=";A2;" A3="; A3;" A9=";A9
251 PRINT
255 PRINT " 6- permeability : K=";K
256 PRINT
260 PRINT " 7- program parmeters: d=";D;" tm= ";TM;" hc= ";HC
261 PRINT " ____________________________________________________"
262 PRINT
263 PRINT " Any change? enter number of the data record. "
264 INPUT " no change = [enter] ";K$
265 IF K$ <> "" THEN GOSUB 4000
299 REM   loop for time
300 REM .....RESERVOIR \ LATERAL
400 R1=P2/P1
460 LPRINT "     time   tank(psi) lateral(psi) bag-inlet(inch h2o)"
465 REM * * *  excution
470 REM   loop for time
480 REM .....RESERVOIR \ LATERAL
490 R1=P2/P1
500 IF R1<.528 GOTO 800
510 REM  non critical
520 P4=P2
530 S4=SQR(G1*(R1^G2-1))
535 IF X1>TM THEN S4=0
540 GOTO 1000
700 REM.....CRITICAL
800 P4=.528*P1
810 S4=1
815 IF X1>TM THEN S4=0
1000 T4=T1/(1+S4^2/G1)
1010 S4=S4*SQR(G*C*R*T4)
1020 M1=A1*S4*P4/(R*T4)
1030 D1=(-1)*M1*R*T1/V1
1040 P1=P1+D1*D
1100 REM ....LATERAL\ATMOSPHE E
1200 R2=P0/P2
1205 IF R2<.528 GOTO 1800
1210 REM non-critical
1215 P5=P0
1218 IF R2>1 GOTO 3010
1220 S5=SQR(G1*(R2^G2-1))
1225 GOTO 2000
1800 P5=.528*P2
1805 S5=1
1900 REM
2000 T5=T2/(1+S5^2/G1)
2005 S5=S5*SQR(G*C*R*T5)
2010 M2=A2*S5*P5/(R*T5)
2015 D2=(M1-M2)*R*T2/V2
2020 P2=P2+D2*D
2021 REM .....BAG
2022 P9=M2*S5/(C*A9)*F*144
2025 S6=K*(P3-P0)*F
2030 M3=A3*S6*P3/(R*T3)
2035 D3=(M2-M3)*R*T3/V3
2040 P3=P3+D3*D
2050 P8=(P3-P0)*F
2055 REM if bag pressure > the pressure of the air jet
2056 REM then bag pressure = pressure of the air jet
2057 BAGP=P8
2058 IF P9<P8 THEN BAGP=P9
2059 IF P8<P9 THEN BAGP=P8
2060 Y1=Y*1000
```

```
2065 IF P2MAX < P2 THEN P2MAX=P2
2066 IF BPMAX < BAGP THEN BPMAX=BAGP
2070 IF HC=1 THEN LPRINT USING "######.##"; X1,P1,P2,P9,P8,BAGP
2080 X=X+D
2999 REM   loop end
3000 GOTO 490
3010 PRINT " the maximum pressure developed in the lateral pipe"
3015 PRINT "                . . .";P2MAX; "psia"
3020 PRINT " the maximum pressre developed in the bag"
3030 PRINT "                . . .";BPMAX; "inch of water"
3040 INPUT "enter 1 to continue";K$
3042 IF K$="1" THEN CHAIN "pmpp"
3044 IF K$ <> "1" GOTO 3040
3050 END
4000 REM ..... data input
4010 IF K$="1" THEN INPUT " enter g,c,r,f";  G,C,R,F
4020 IF K$="2" THEN INPUT " enter v1,v2,v3"; V1,V2,V3
4030 IF K$="3" THEN INPUT " enter p0,p1,p2,p3"; P0,P1,P2,P3,P4
4040 IF K$="4" THEN INPUT " enter t1,t2,t3"; T1,T2,T3
4050 IF K$="5" THEN INPUT " enter a1,a2,a3,a4,a9"; A1,A2,A3,A4,A9
4060 IF K$="6" THEN INPUT " enter k";K
4070 IF K$="7" THEN INPUT " enter d,tm";D,TM,HC
4100 RETURN 220
-x-x-x-x-x-x-x-x-x-x-x-x-x-x-x-x-x-x-x-x-x-x-x-x-x-x-x-x-x-x-x-x-x-x-
5 REM Dynamic Model
6 REM prog. name: adm
10 REM constants:
13 C0=27.6756
15 E=.0001
20 G1=1.4
25 G4=1.4
30 T1=530
35 T4=530
40 R1=53.3
45 R4=53.3
50 REM ..data input
55 GOSUB 9000
60 REM ..
65 Q=P4/P1
71 A1=G1*R1*T1
75 A4=G4*R4*T4
80 A0=A4/A1
85 J1=(G1+1)/(2*G1)
90 J2=2*G4/(G4-1)
95 J3=(G1+1)/(G1-1)
100 REM ...the pressure in the lateral pipe
110 GOSUB 1000
200 REM ... the velocity of air jet
210 GOSUB 2000
300 REM ... calculate pressure developed by the injected
305 REM ... air jet
310 GOSUB 3000
400 REM ...consider the pressure loss at the entrance of the bag
410 IF TP=1 THEN DP0=DP2*PLC1
415 IF TP=2 THEN DP0=DP2*PLC2
500 REM calculate the pressure dissipated along the bag
510 REM ...if u, pg, f is not known, use eq.4-36
520 IF INFB=0 THEN GOSUB 5000
530 REM ...if u, pg, f is known,use eq.4-29
540 IF INFB=1 THEN GOSUB 6000
600 REM ...calculate reflected pressure at the bottom of the
605 REM ...bag (eq. 2-20)
610 GOSUB 7000
700 REM ...consider the effect of reflected pressure at the bottom
705 XBPR=RRR*EXP(-DRC*(BL-XBG)/DOJ)
710 IF XBP < XBPR THEN XBP=XBPR
800 REM ... display the results and data generation for
805 REM ... graphics
810 GOSUB 9800
890 INPUT "enter 1 to continue";K$
891 IF K$="1" THEN CHAIN "pmpp"
892 IF K$ <> "1" GOTO 890
900 END
```

```
999 REM *** subroutines
1000 REM .....calculate the pressure in the lateral pipe
1096 REM trial and error determination of m3 for p4
1097 REM initial m3 ------------------------
1098 M3=.1
1099 I=.1
1100 F=1+(G4-1)*M3/2
1110 C=(G1*M3/F)^2
1120 R2=1+.5*A0*C*(J1+SQR(J1^2+4/A0/C))
1130 R4=R2*F^J2
1140 D=Q-R4
1150 IF D<0 THEN GOTO 1180 ELSE IF D>0 GOTO 1160 ELSE GOTO 1500
1160 M3=M3+I
1170 GOTO 1100
1180 IF(I-E) <= 0 THEN GOTO 1500 ELSE GOTO 1190
1190 M3=M3-I
1200 I=I/10
1210 GOTO 1160
1500 REM m3 has been determind
1510 M2=2/((G1*(G1-1))*(R2+1/R2-2)/(J3+R2)
1520 M2=SQR(M2)
1600 M0=1+J1*(R2-1)
1610 M0=SQR(M0)
1800 REM ...The pressure behind the reflected shock wave
1810 J4=(3*G1-1)/(G1+1)
1820 R5=(J4*R2-1/J3)/(R2/J3+1)
1905 REM ...consider the friction loss in the lateral pipe
1906 P2=R2*P1
1910 U2=M2*SQR(A1*32.2)
1920 L=P2*144/(53.3*T1)
1930 YF=LPF
1940 Y0=(L*U2^2/2)*(4*LLP/LPD)
1950 Y1=Y0/(32.2*144)
1960 Y=Y1*YF
1970 R2C=R2-Y/P1
1972 R5C = (J4*R2C-1/J3)/(R2C/J3+1)
1975 P5C=R5C*(R2*P1-Y)
1999 RETURN
2000 REM ...jet velocity
2005 REM .....CALCULATE THE LATERAL PRESSURE AT THE BAG LOCATION
2010 LW=P5C*144/(53.3*T1)
2020 XY0=(LW*U2^2/2)*(4*XLP/LPD)
2030 XY=YF*XY0/(32.2*144)
2035 PRINT "Y0";Y0;"xy0";XY0;"y=";Y;"xy";XY
2040 XP5C=P5C-XY
2050 REM .....calculate the jet velocity
2051 PRINT XY0,LW,XY
2052 PRINT U2,XY0,Y0
2060 CTA=P1/XP5C
2070 IF CTA < .528 THEN GO O 2300
2080 XP0=XP5C
2090 XM0=SQR(G1*(CTA^G2-1)
2100 GOTO 2400
2300 XP0=.528*P5C
2310 XM0=1
2400 XT0=T1/(1+XM0^2/G1)
2410 XV0=XM0*SQR(G1*C0*R1*XT0)
2500 REM
2510 XVJ=(XP5C/P1)*(T1/XT0)*(DOR/DOJ)^2*XV0
2520 U2=XVJ
2530 IF INFB=1 THEN U2=INF1
2550 RETURN
3000 REM ....jet pressure
3090 A1=SQR(A1*32.2)
3100 M2=U2/A1
3110 REM trial and error
3120 MS=1!
3125 I=.1
3130 M2C=(2/(G1+1))*(MS-1/MS)
3140 D=M2-M2C
3155 IF D<0 THEN GOTO 3180 ELSE IF D>0 GOTO 3160 ELSE GOTO 3500
3160 MS=MS+I
3170 GOTO 3130
3180 IF(I-E) <= 0 THEN GOTO 3500 ELSE GOTO 3190
3190 MS=MS-I
3200 I=I/10
3210 GOTO 3160
3500 REM ms has been determined
3510 R21=1+(2*G1/(G1+1))*(MS^2-1)
3520 P2=R21*P1
3530 DP2=(P2-P1)*C0
```

```
3600 RETURN
5000 REM ...pressure dissipated along the bag
5001 REM ...eq. (4-36)
5010 DPI=DP2
5020 XBP=DPI*EXP(-DRC*XBG/DOJ)
5100 RETURN
6000 REM ...if jet velocity,bag permeability,friction coefficient
6001 REM ...are known,use this subroutine.
6005 REM prog. name: bpm
6010 REM calculation of dissipating pressure along the bag
6015 REM ...if all effect should be considered, set eff=1
6016 EFF=1
6020 REM constants:
6030 R=53.3
6040 T=530
6050 PA=14.7
6055 PI=3.14
6060 C=27.6756
6065 C0=32.2
6070 REM ...data input
6075 REM .. VELOCITY OF THE INJECTED AIR (V)
6080 V=INF1
6085 REM .. PRESSURE DEVELOPED AT THE TOP OF THE BAG
6090 DP0=DP2
6095 REM .. PERMEABILITY OF THE BAG
6100 K=INF3
6105 REM .. FRICTION COEFFICIENT OF THE BAG
6110 F=INF2
6115 REM .. BAG CONFIGURATION
6120 D=DOJ/12
6125 BL=BL
6130 A=PI*D^2/4
6135 REM .. PARAMETERS
6140 DT=.001
6145 TIME=0
6150 REM .....
6155 PB0=PA+DP0/C
6160 PB=PB0
6180 RA=PA*144/(R*T)
6200 REM  excution
6201 DX=DT*V
6202 TIME=TIME+DT
6205 REM pressure drop due to loss of mass
6210 RB=PB*144/(R*T)
6220 DP=(PB-PA)*C
6225 K2=(PB+PA)/(2*PA)
6230 U=K2*K*DP
6240 DML=4*U*RA/D
6250 ML=DT*DML
6260 PML=ML*R*T/144*C
6290 REM pressure drop due to friction
6300 DPF=(RB*V^2)*4*F/(2*D)/C0/144*DX*C
6390 REM pressure drop due to loss of momentum
6400 DPM=U*ML/C0/144*C
6490 REM accumulation of the pressure loss along the bag
6500 X=X+DX
6510 PBG=PB
6520 RB=RB-ML
6530 PB=RB*R*T/144
6550 PF=PF+DPF
6560 PM=PM+DPM
6570 PL=PL+PML
6580 PFML=PL+PF+PM
6581 REM ...effect of all the parameters
6582 IF EFF=1 THEN PB=PBG-(DPF+DPM+PML)/C
6585 XI=ABS(X-INT(X))
6590 IF XI >.01 THEN IF XI < .99 GOTO 6690
6690 IF X >= BL GOTO 6800
6700 GOTO 6200
6705 C0=C
6800 RETURN
7000 REM ...reflected pressure at the battom of the bag
7010 XBPR0=DPI*EXP(-DRC*BL/DOJ)
7015 XBPR0=XBPR0/C0
7020 RR0=1+J2/(J3*(P1/(XBPR0+P1))+1)
7030 RRR=XBPR0*RR0
7100 RETURN
9000 REM ...system configuration and operating parameters
9005 P1=14.7
9010 P4=100+14.7
```

```
9015 PLC1=.43
9020 PLC2=.64
9025 REM ...friction ccefficient in the lateral pipe
9030 LPF=.001
9035 REM ...location of the bag from the closed end
9036 REM ...of the lateral
9040 XLP=40
9050 LPD=1.5
9060 LLP=93.95
9070 DOR=3/8
9080 DOJ=6
9085 REM ...bag length(ft)
9086 BL=12
9090 REM ... location along the bag
9091 XBG=4
9100 REM ...pressure dissipation rate
9105 REM ...based on experimental data
9110 REM ...(drc=k*pg/d)
9115 DRC=.26*6
9200 REM ...type of bag entrance
9210 TP=1
9220 INFB=0
9230 REM ...if infb=1 then enter jet velocity(inf1)
9231 REM ...friction coefficient(inf2),permeability of the bag(inf3)
9233 INF1=100
9235 INF2=.004
9238 INF3=50*.5/35/60
9300 RETURN
9800 REM ...print results
9810 WIDTH 80:CLS
9815 PRINT "-------operating parameters and system configuration------"
9820 PRINT " reservoir pressure=";P4;"psi"
9830 PRINT " bag diamter x length=";DOJ;" x ";BL
9840 PRINT "lateral pipe diameter x length=";LPD;" x ";LLP
9845 PRINT "friction coefficient of the lateral=";LPF
9850 PRINT "pressure loss at the entrance of the bag"
9855 PRINT "            type1=";PLC1
9856 PRINT "            type2=";PLC2
9860 PRINT "-------results----------------"
9865 PRINT "incident pressure=";P2;"psi"
9870 PRINT "reflected pressure=";P5C;"psi"
9875 PRINT "lateral pressure at bag location";XP5C;" psi "
9880 PRINT "at ";XLP;"inches from closed end of the lateral"
9885 PRINT "pressure at the top of the bag";DPI;" in. w.g."
9890 PRINT "pressure at";XBG;" ft from the top of the bag ";XBP;"in. w.g."
9900 RETURN
-x-x-x-x-x-end-x-x-x-x-x-x-end-x-x-x-x-x-x-end-x-x-x-x-x-x-
```

VITA

Satoru Mitsutomi was born in Otakuma, Saga, Japan on April 22, 1949. He attended elementary school in that city and was graduated from Saga Nishi High School, Saga, in March 1968. The following April he entered the National Defence Academy, Yokosuka, and in March 1972 he received a diploma in Aeronautics.

After a three year tour of duty with Japan Air Self Defence Force, he entered The Graduate School of the Ritsumeikan University, Kyoto, in April 1975. He received the Master of Engineering degree with a major in Civil Engineering in 1977.

In January 1978 he accepted a research assistantship at the Illinois Institute of Technology, Chicago and began study toward a Master's degree in Environmental Engineering. He received this degree in December 1979.

In the fall of 1980 he accepted a research assistantship at the University of Tennessee, Knoxville. He received the Doctor of Philosophy degree with a major in Civil Engineering in June 1986.

He is a member of the Air Pollution Control Association, American Meteorological Society, and The Society of Powder Technology, Japan.